

INFORMATION TO USERS

This manuscript has been reproduced from the microfilm master. UMI films the text directly from the original or copy submitted. Thus, some thesis and dissertation copies are in typewriter face, while others may be from any type of computer printer.

The quality of this reproduction is dependent upon the quality of the copy submitted. Broken or indistinct print, colored or poor quality illustrations and photographs, print bleedthrough, substandard margins, and improper alignment can adversely affect reproduction.

In the unlikely event that the author did not send UMI a complete manuscript and there are missing pages, these will be noted. Also, if unauthorized copyright material had to be removed, a note will indicate the deletion.

Oversize materials (e.g., maps, drawings, charts) are reproduced by sectioning the original, beginning at the upper left-hand corner and continuing from left to right in equal sections with small overlaps. Each original is also photographed in one exposure and is included in reduced form at the back of the book.

Photographs included in the original manuscript have been reproduced xerographically in this copy. Higher quality 6" x 9" black and white photographic prints are available for any photographs or illustrations appearing in this copy for an additional charge. Contact UMI directly to order.

UMI

A Bell & Howell Information Company
300 North Zeeb Road, Ann Arbor MI 48106-1346 USA
313/761-4700 800/521-0600

NOTE TO USERS

The original manuscript received by UMI contains pages with slanted print. Pages were microfilmed as received.

This reproduction is the best copy available

UMI

**TO MY LORD.
TO THE LOVE OF MY LIFE, MY WIFE CRISTY,
AND OUR CHILDREN LUIS, LAURA AND ANDRES.
TO MY PARENTS FRANCISCO AND ALBERTINA,
MY BROTHERS GUILLERMO AND FRANCISCO,
AND SISTERS JENNY AND ALMA.**

University of Alberta

**Modelling Electrostatic Propensity of
Protective Clothing Systems**

by

Jose Alberto Gonzalez



**A thesis submitted to the Faculty of Graduate Studies and Research in partial fulfilment
of the requirements for the degree of**

Doctor in Philosophy

in

Textiles & Clothing

Department of Human Ecology

Edmonton, Alberta

Spring 1998



National Library
of Canada

Acquisitions and
Bibliographic Services

395 Wellington Street
Ottawa ON K1A 0N4
Canada

Bibliothèque nationale
du Canada

Acquisitions et
services bibliographiques

395, rue Wellington
Ottawa ON K1A 0N4
Canada

Your file *Votre référence*

Our file *Notre référence*

The author has granted a non-exclusive licence allowing the National Library of Canada to reproduce, loan, distribute or sell copies of this thesis in microform, paper or electronic formats.

The author retains ownership of the copyright in this thesis. Neither the thesis nor substantial extracts from it may be printed or otherwise reproduced without the author's permission.

L'auteur a accordé une licence non exclusive permettant à la Bibliothèque nationale du Canada de reproduire, prêter, distribuer ou vendre des copies de cette thèse sous la forme de microfiche/film, de reproduction sur papier ou sur format électronique.


L'auteur conserve la propriété du droit d'auteur qui protège cette thèse. Ni la thèse ni des extraits substantiels de celle-ci ne doivent être imprimés ou autrement reproduits sans son autorisation.

0-612-29040-9

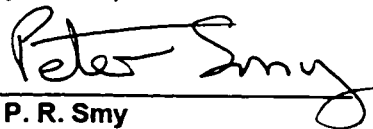
University of Alberta

Faculty of Graduate Studies and Research


The undersigned certify that they have read, and recommended to the Faculty of Graduate Studies and Research for acceptance, a thesis entitled **Modeling the Electrostatic Propensity of Protective Clothing Systems** submitted by **Jose Alberto Gonzalez** in partial fulfilment of the requirements for the degree of **Doctor in Philosophy in Textiles and Clothing**.



Dr. E. M. Crown
(Supervisor)



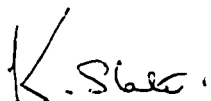
Dr. P. R. Smy
(Co-Supervisor)



Dr. N. Kerr



Dr. C. E. Capjack



Dr. K. Slater

Date: 1998.04.13

Abstract

At the present time, there are no mathematical models to explain the electrostatic phenomenon on protective clothing systems or to predict their static behavior when worn by workers under hazardous environments. The current research was planned to develop mathematical models of the static behavior of textile systems under different environmental conditions, and to establish numerical techniques to accurately and reliably assess the static propensity of clothing systems.

Mathematical equations of the form $V_p = f(V_S, V_H, V_T)$ have been developed considering peak potential as a function of fabric system, humidity and temperature. Results correlate well with data from tests based on the proposed ASTM Method. Additional equations derived to predict peak discharge potential from a capacitor such as a clothed human body produced good agreement with data from tests following the modified ASTM Method. Also, equations of the form $V = f(t, \tau)$ were developed considering charge decay as a function of time and time constant. Charge decay data for two-layer systems from tests following the proposed ASTM Method (draft F23.20.05) fit well ($R^2 > .90$) the exponential model. To predict the electrostatic propensity of protective clothing systems, numerical techniques were developed based on both empirical and theoretical models. According to previous research, a linear model was utilized to establish a relationship between small-scale and human-body data. Results from calculations using this model were in agreement with values obtained from regression analyses on empirical data.

Industry can benefit from the use of these mathematical models and numerical techniques as they can help in predicting the electrostatic behavior of different garment systems under any relative humidity level and temperature. The use of data from single-layer measurements, tested at standard conditions, in combination with established data and/or constants is also an advantage for a quick and low-cost assessment. With the use of the models, it is possible to determine the combination of fabrics that offers the best protection not only for the primary hazard but also in terms of the lowest electrostatic propensity at specific environmental and working conditions.

Acknowledgements

The author wishes to express a very special gratefulness to Dr. Elizabeth M. Crown for her generosity, guidance, patience and friendship throughout all these years at the University of Alberta.

Special thanks are also extended to Dr. Nancy Kerr who opened the door at the university and for generous and invaluable help that made this work possible. Also, special thanks are extended to Dr. Peter Smy and Dr. Syed Rizvi, Department of Electrical and Computer Engineering for providing professional assistance, expert advice and, principally, friendship.

Special appreciation is expressed to the Staff of the Department of Human Ecology, specially Linda McKay, Elaine Bitner, Crystal Dawley-Tate and Diana Parsons for easing the work of this research. To Tannis Grant for her valuable work during long hours of testing at the lab.

Last but not least, the author would like to thank the Natural Sciences and Engineering Research Council of Canada (NSERC), and E.I. DuPont de Nemours for funding this research. Without their financial assistance this project would have been impossible.

Table of Contents

	PAGE No.
CHAPTER 1.- Introduction	1
Background	1
Statement of the Problem and Purpose	3
Specific Objectives	5
Delimitation and Limitations of the Study	5
Overview of Dissertation	6
Definition of Terms	8
References	11
CHAPTER 2.- Review of Literature	13
Basic Principles of Electrostatics	13
Charge Generation	12
Maximum Charge Density	15
Charge Dissipation	15
Hazards from Electrostatics	16
Evaluation of Hazards Created by Electrostatic Discharges	17
Minimum Ignition Energy	18
Environmental Conditions and Electrostatic Propensity	19
Sorptive Properties of Textile Fibres	19
Effect of Moisture and Temperature on Electrostatic Characteristics of Textile Materials	21
Measurements of Static Electricity of Textiles	23
Human Body Experiments	23
Small Scale Tests	24
Modelling in Electrostatics	26
Summary	27
References	28
CHAPTER 3.- A Modified Version of Proposed ASTM F23.20.05 Method on	
Static Propensity	34
Preamble	34
Introduction	34
Method	36
Fabrics	36
Procedures	37

	PAGE No.
Data Analyses	38
Results and Discussion	39
Conclusions	42
References	43
CHAPTER 4.- Modelling of Surface Charge Dissipation on Thermal Protective Fabrics	45
Preamble	45
Introduction	45
Modelling Charge Decay	46
Comparison Between Calculated and Observed Charge Decay Results	49
Discussion and Conclusions	50
References	52
CHAPTER 5.- Modelling the Static Charge Transfer on, and Discharge From Thermal Protective Fabric Systems During Small-scale Testing	54
Preamble	54
Introduction	54
Modelling Electrostatic Propensity	56
Systems Component: Mathematical Model for a Two-Layer System Following ASTM Draft Method F23.20.03	57
System Component: Mathematical Model for a Two-Layer System Following a Modified ASTM Method	61
Humidity Component	64
Temperature Component	67
Combined Effect of Humidity and Temperature on Peak Potential	69
Complete Mathematical Model	70
Discussion and Conclusions	70
References	72
CHAPTER 6.- Development of Mathematical Models to Predict the Static Propensity of Thermal Protective Clothing Systems	74
Preamble	74
Introduction	74
Method in Empirical Modelling	78
Results and Discussion in Empirical Modelling	78

	PAGE No.
Theoretical Modelling	80
Discussion and Conclusions	83
References	84
CHAPTER 7.- Summary, Conclusions, Implications and Recommendations	86
Summary	86
Limitations	88
Conclusions	89
Implications and Recommendations	94
Implications and Recommendations for Industry	94
Implications and Recommendations for Further Research	94
References	95
Appendix 1: Some characteristics of textile fibers which make up the fabric systems	97
Appendix 2A: Electrostatic characteristics of thermal protective garments at low humidity	98
Appendix 2B: Electrostatic characteristics of thermal protective garment systems at various low humidities	118
Appendix 3: Method to determine the dielectric constant	133
Appendix 4: Method to determine the coefficient of static friction	134
Appendix 5: Mean electrical resistance and surface resistivity of various fabrics	135
Appendix 6: Results of testing following the proposed and modified ASTM methods with vinyl rubbing wheel at various humidities and temperatures	136
Appendix 7a: Modelling the humidity and temperature effect on 100% cotton	141
Appendix 7b: Modelling the humidity and temperature effect on FR cotton	144
Appendix 7c: Modelling the humidity and temperature effect on aramid/carbon	147
Appendix 7d: Modelling the humidity and temperature effect on aramid/PBI	150
Appendix 7e: Modelling the humidity and temperature effect on aramid/FR viscose	153
Appendix 8: Developed triboelectric series	156
Curriculum Vitae	158

LIST OF TABLES

		PAGE No.
Table 3.1	Characteristics of fabrics used in the experiment	37
Table 3.2	Analysis of variance: Potentials, energies, and charge decay for two-layer specimens at 0 and 20% RH and 20 °C	41
Table 4.1	Peak potentials, charge decays, time constants and regression coefficients (R^2) following proposed ASTM Method F23.20.05 at 0 and 20% RH	47
Table 4.2	Calculated time constants for various fabric systems at 0 and 20% RH	50
Table 5.1	Results of calculations using theoretical model of the system component following proposed ASTM Method, F23.20.05 at 0% RH	61
Table 5.2	Results of calculations using theoretical model of the system component following a modified ASTM Method at 0% RH	63
Table 5.3	Values of constant "b" and R^2 for proposed ASTM Method, F23.20.05 between 0 and 30% RH	66
Table 5.4	Values of constant "b" and R^2 for modified ASTM Method between 0 and 30% RH	66
Table 5.5	Values of temperature constant "c" for proposed ASTM method	68
Table 5.6	Comparison between calculated and observed results following proposed ASTM method F23.20.05 at 22 °C	69
Table 5.7	Results of calculations using complete theoretical model following proposed ASTM method F23.20.05 at 20 and 30% RH and 22 °C	71
Table 6.1	Correlations (R) between human-body discharge potentials and energies, and both small-scale peak potentials, and charge decays	78
Table 6.2	Correlation coefficients (R) and regression coefficients (R^2) among small-scale parameters and human-body data at 0 and 20% RH	79
Table 6.3	Values of variables for small-scale and human-body experiments	81
Table 6.4	Results from calculations of constant "m"	82

LIST OF FIGURES

		PAGE No.
Figure 1.1	A clothed body model in a human-ecological perspective	4
Figure 1.2	Modelling the electrostatic phenomenon and prediction of static propensity of protective clothing systems	7
Figure 3.1	Diagram of modified ASTM Method tribo-electric test device	38
Figure 3.2	Mean peak potential from fabric surface	40
Figure 3.3	Mean discharge potentials from capacitor	40
Figure 3.4	Mean charge decay at 5 seconds for proposed ASTM method	42
Figure 4.1	Charge decay curves for different fabric systems at 20% RH	48
Figure 5.1	Triboelectric charging process	57
Figure 5.2	Measuring charge from a uniformly charged insulator	58
Figure 5.3	Diagram of a modified ASTM method	62
Figure 6.1	Linear relationship between test battery 1 and body data at 20% RH	80

Chapter 1.- Introduction

Background

A concern regarding safety and health of workers in various areas of industry has generated research and development in the area of personal protective equipment (PPE). Personal protective equipment includes personal protective clothing and gear such as respirators, face masks, and other controls. This research was focused on thermal protective clothing which is designed to extend people's physical and physiological limitations in response to environmental conditions. However, such personal protective clothing may generate hazard rather than protection; for example, it can cause electrostatic discharges (sparks) at low humidity and temperature which can lead to an explosion in the presence of flammable gases, and to the loss of human life. Moreover, workers in the oil and gas industries have expressed opinions that some thermal protective clothing they are required to wear may be hazardous due to its static propensity. Many still hold a traditional belief that 100% cotton garments are less prone to static electricity than are garments of more thermally stable fibres such as aramid. This belief is based on measurements of certain electrical properties taken under conditions of relatively high humidity and may be misleading for low humidity environments.

These facts and other ones cause general concern about the electrostatic phenomenon on textile materials and/or human bodies. Some well known undesirable effects include clinging of charged clothing together or to the body as well as dust attraction to charged materials, thereby causing soiling of clothing in places like stores. Often people experience shocks when, after walking over a carpet, they touch a metal knob or a light switch; or when after sliding off a car seat, they touch the car body. The resulting shock is caused by the discharge of several thousand volts in the form of a spark (Roth, 1990).

The everyday manifestations of static electricity mentioned above are minor irritants compared with the problems caused by the same effects in industry. In the electronic and other high-technology industries, there can be damage to or malfunctioning of equipment when a static-sensitive component comes into contact with a person or a material with a static build up. But the most serious effect of an electrostatic discharge (ESD) is its ability to ignite flammable gases, vapours, or powders, resulting in fires and explosions and the possible loss of human life. Human spark ignition of flammable materials is a significant concern in the oil, military, chemical, electronic, and other industries.

Key considerations in the analysis of a process to determine the degree of hazard associated with human spark scenarios are the mechanisms by which the electrostatic energy is generated, stored, and discharged. The amount of energy which can be generated is usually a

function of the charge generation characteristics of the clothing and footwear on the person involved (Berkey, Pratt and Williams, 1988). Wilson (1987) found that the major determinants of sparking potential are relative humidity, the fabrics/ substances involved, and the degree of friction involved. Energy storage is dependent on the capacitance of the body while the discharge energy is controlled largely by the body resistance and the configuration of the point of discharge (Wilson, 1977/1978). In cold regions like Alberta, the absolute humidity level declines extremely with very cold temperature, so the electrostatic hazard can be more significant than in warmer regions. People who work outdoors in extreme cold conditions may be required to wear thermal protective clothing when working in unsafe circumstances. It has been shown that clothing made of thermal protective materials such as aramid or flame retardant cotton may generate enough energy to ignite a fuel vapour-air mixture when worn under low humidity conditions (Rizvi, Crown, Osei-Ntiri, Smy and Gonzalez, 1995). By walking over non-conducting floor covering, the body potential can be raised to over 10 kV (Wilson, 1982), but the charge involved is only approximately 1 micro coulomb (μC) (Greason, 1992). On discharge, less than 10 millijoules (mJ) is released, which is only a thousandth of the amount regarded as harmful (Wandel, Gutschik & Carl, 1972).

A considerable amount of research has been done on the charge generation characteristics of various types of textiles used in clothing and carpeting as well as the materials used in footwear. A clothed human body can be modelled as a conductor, which may be charged by tribo-electrification or induction (Tolson, 1980; Rizvi et al, 1995). Electrostatic charge will accumulate on the outer surface of the conducting body and on the fabric. Research has also been focused on the charge storage capacity of the human body and its subsequent discharge. These efforts have included measurement and modelling of the capacitance of the body, and the voltage and associated energies which can be stored on the body. On the other hand, research at the small-scale level also has been carried out and has included evaluation of electrostatic characteristics of materials (e.g., dielectric constant, surface resistivity) and charge generation, analysis of consequences of ESD, and modelling the effect of single variables (e.g., humidity, temperature, and friction) on static propensity of textile surfaces, or a combination of them.

Most research on static propensity of textiles has been done on single fabric layers. Evaluation of electrostatic discharges becomes more complex for multiple layers of clothing than for single layers. Multiple layers with blends of different fibres are even more difficult to evaluate. Also, since high-performance textile materials used in personal protective equipment have been in the market for only a few years, most of the research reported to date, both human-body and small-scale, was done on regular natural and synthetic textile materials.

Statement of the Problem and Purpose

There are no mathematical models to explain the electrostatic phenomenon or predict the static behaviour of protective clothing systems. The present research was planned to develop mathematical models for explaining the static phenomenon of textiles under different environmental and clothing conditions, and to establish numerical techniques for accurately assessing the electrostatic propensity of protective clothing systems. The investigation addressed the following problems:

- 1.- How and why the charge dissipation process is affected by tribo-electrification, and does it vary from single- to multiple-layer fabric systems? Specifically, which elements or variables are involved and affect charge decay? and how can charge dissipation modelling help in decreasing the static hazard?
- 2.- What is the process of charge transfer between layers of fabrics during a small-scale test? What are the determinants of peak potential from either a surface or a capacitor? Can mathematical models discriminate measurements following different test methods?
- 3.- How can the relationship between human-body model and a small-scale tester be improved? Can a mathematical model be developed to be used to predict the static behaviour of clothing systems from small-scale test data?
- 4.- Is there any small-scale test protocol which can reliably and accurately measure electrostatic characteristics of textile systems?, and can measurements taken by the method be meaningful for prediction of static hazard from a clothed person?

In establishing the mathematical relationships peak potential was considered a function of fabric system, humidity, and temperature, and charge decay a function of time and time constant ($\tau = RC$, resistance x capacitance) according to the following mathematical expressions:

For peak potential,

$$VP = f (Vs, VH, VT) \quad \text{Eq. 1.1}$$

Where:

VP = predicted peak potential for a two-layer fabric system,

Vs = fabric system effect on peak potential,

VH = humidity effect on peak potential, and

VT = temperature effect on peak potential

For charge decay,

$$V = f (t, \tau) \quad \text{Eq. 1.2}$$

Where:

V = predicted potential (V) at time t

t = decay time, and

τ = time constant, where $\tau = RC$

A human-ecological perspective provided a framework for a holistic, multi-disciplined approach to the study of complex interactions between human beings, their nearest environment, namely clothing, and the surrounding physical environments -both atmospheric conditions and built physical ones, allowing a clothed human-body model to be developed. Figure 1.1 shows a modified model, originally proposed by Kilsdonk (1983), of a clothed person (H) and, through a micro-environment generated between the clothing and the person, its interactions with non-human, human-built and social-behavioural environments. Thus, the static phenomenon is understood as the interaction among those different elements present during an electrostatic discharge event, and not as the effect of a single variable. Variations of those parameters and their effect on the static propensity were initially and individually studied. Then, these elements were incorporated as a whole into different models where their combined effect was taken into account in explaining the process during a static-charge/discharge event, and predicting the electrostatic propensity of protective clothing systems. As a result, it was possible to determine the combined effect of all parameters and its consequences on static charge generation and/or dissipation when those variables were varied, and the static tendency of protective garment systems could be assessed.

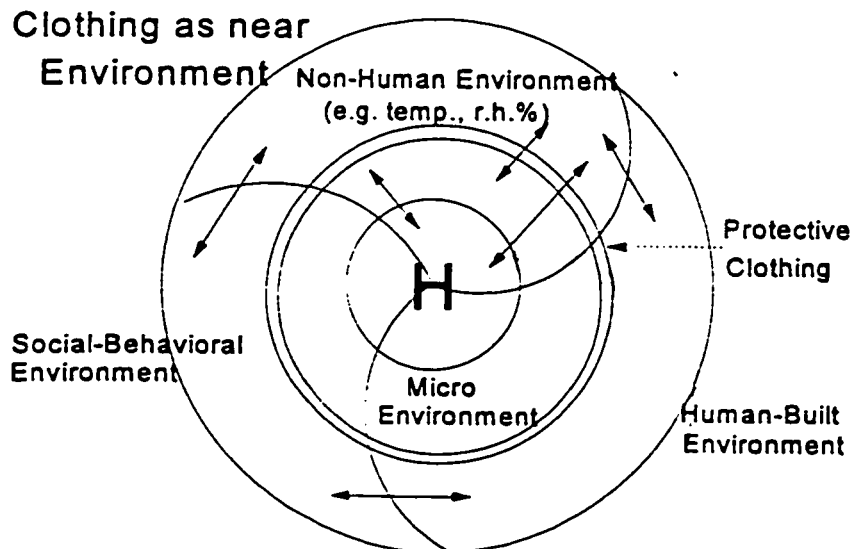


Figure 1.1. A clothed body model in a human-ecological perspective
(Adapted from Kilsdonk, 1983)

Specific Objectives

The objectives of the study were to:

1. develop mathematical equations based on known theory to explain electrostatic phenomena in real-life conditions, and models to establish relationships between small-scale and human-body data;
2. measure some physical characteristics of the fabrics used during the investigation, and use these parameters in testing the models:
 - a) dielectric constants ($K = \epsilon/\epsilon_0$) of fabrics at 0% RH;
 - b) friction constants between two textile surfaces at different relative humidity levels and temperatures;
 - c) surface resistivity of fabrics at different relative humidity levels.
3. measure peak potential of static discharges from fabric systems and capacitor at different relative humidity levels and temperatures;
4. measure charge decay time for the surface charge on fabric systems at different relative humidity levels and temperatures;
5. determine mathematical relationships between peak potentials and charge decay and relative humidity, temperature, or fabric system; including interaction effects;
6. verify the developed theoretical mathematical models with observed data.
7. establish numerical techniques for the prediction of the static propensity of protective clothing systems by using:
 - 7.1. Observed data from small-scale and human-body testing and,
 - 7.2. Calculated data from mathematical equations developed in Objective 1.

Delimitation and Limitations of the Study

The delimitations during the research were:

1. The composition of fabric systems was restricted to protective fabrics made of aramid/carbon core, FR cotton, aramid/PBI, and aramid/FR viscose fibers. See Appendix 1 for detailed information of these fibers.
2. Levels of relative humidity for testing were limited to 0, 20, and 30% relative humidity.
3. Testing temperatures were limited to 4, 22, and 30° C.
4. The methods followed in measuring the dependent variables were the draft ASTM standard test method for evaluating tribo-electric (static) charge generation on protective clothing materials, No. F23.20.05 and a modification of this method.

5. Only one human activity, a clothed human body sliding off a car seat, was considered for analysis and comparison¹.

A limitation that affected the present study is the availability of only limited data from human-body experiments at low relative humidity levels and room temperature obtained during another phase of the larger project.

Overview of Dissertation

Significant research in the fields of static electricity and textiles conducted in the last 50 years is reported in Chapter 2, ranging from basic principles of electrostatics, the hazards caused by ESD, through the different methods and techniques to measure the static propensity of textile materials, to the modelling in electrostatics. It is shown that most of the published research has been carried out based on the evaluation of static charges from textile surfaces or human bodies in combination with single variables affecting their propensity. No research was found that incorporated a human-ecological perspective as this present study did.

In Chapter 3, a modification to the proposed ASTM Test Method for Evaluating Triboelectric (Static) Charge Generation on Protective Clothing Materials (F23.20.05) procedure is reported. The modification was developed to measure peak potentials and energies from a capacitor, as well as peak potentials and decay rates from specimen surfaces charged by tribo-electrification. The test system simulates a clothed human body rubbing an insulated surface and touching a grounded object, generating a spark of several thousand volts. A revised version of this chapter was presented at the Sixth International Symposium on Performance of Protective Clothing: Emerging Protection Technologies, sponsored by ASTM Committee F23 on Protective Clothing in Orlando, FL., and published as Gonzalez, Rizvi, Crown and Smy (1997).

Chapters 4, 5, and 6 describe the modelling process shown in detail in Figure 1.2, and which includes several steps to complete all models. The purpose of the small-scale testing theoretical models is to determine the static propensity of two-layer fabric systems by using data from small-scale tests on single layer specimens (considered the outer layer of a fabric system when combined with different fabrics as the inner layer of the system). With the use of those mathematical models, it is possible to explain the process involved in the charge generation, its transfer through fabric layers, and its consequent dissipation and/or discharge. Also, it is possible to explain how and why temperature and humidity affect the static phenomenon.

¹During the human-body experiments (Rizvi et al, 1995), it was found that results and trends in body-discharge potential varied when two human activities -sliding off a car seat and removing an outer garment- were studied. See Appendices 2A and 2B for a detailed explanation of the method used during human-body experiments.

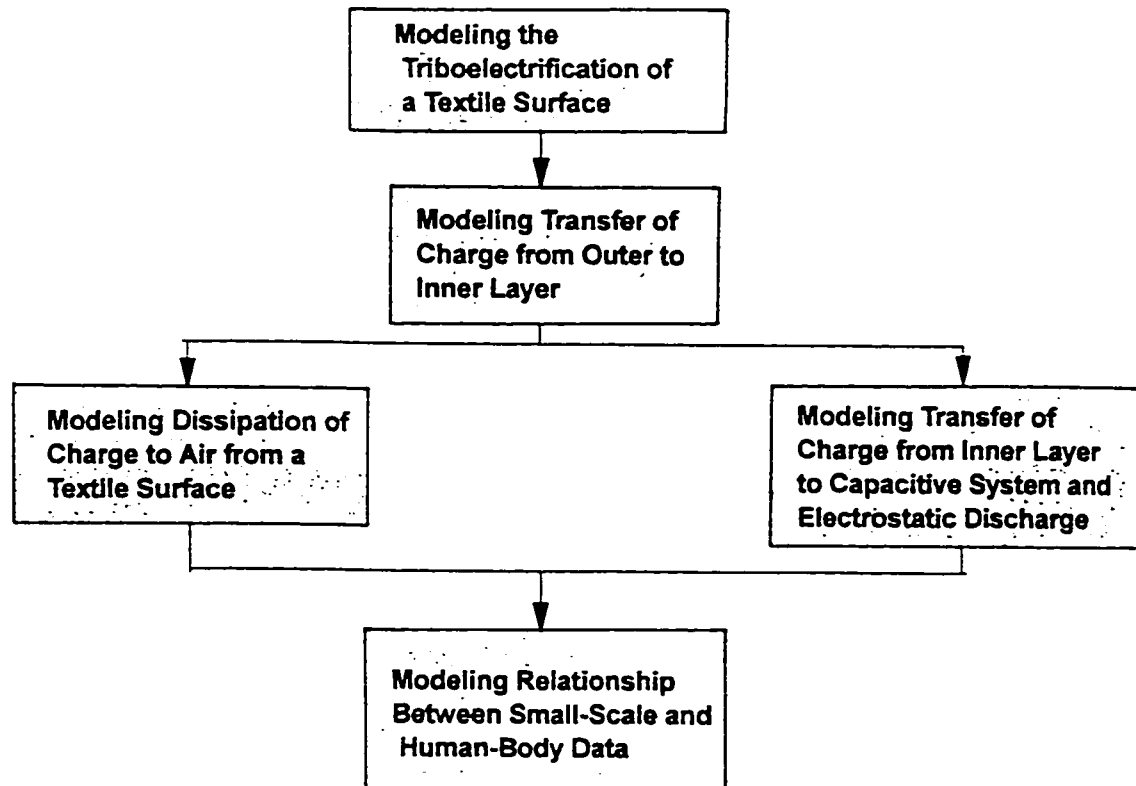


Figure 1.2. Modelling the electrostatic phenomenon and prediction of static propensity of protective clothing systems

Mathematical models for decay of surface charges on thermal protective fabric surfaces are reported. The models are used to determine the effect of surface characteristics on the static propensity of fabric systems, for example: time constant, capacitance of fabric surface, and other parameters of interest. These models could help us to understand better the static phenomenon of surface charges generated by tribo-electrification, and why and how the decay of those charges differs from other types of surface electrification, induction-conduction and corona charging, as well as the suppression effect of multiple layers on charge dissipation.

Different mathematical models to explain charge transfer between layers of fabric, measurement of charge from a textile surface, and electrostatic discharge from a capacitor, and the corresponding effects of humidity and temperature on fabric systems are developed and reported. Calculations made using these models and single-layer data are compared to results obtained during small-scale tests of two-layer fabric systems.

The development of mathematical models to predict the static propensity of thermal protective clothing systems was carried out in two steps: a) empirical modelling based on small-scale and human-body experiments, and b) theoretical modelling. Empirical models were used for determining the best relationship between those from small-scale testing and from human-

body experiments. The determined relationship is the basis for mathematical equations and numerical techniques to assess the electrostatic propensity of thermal protective clothing systems in real-life conditions.

It was found empirically that small-scale and human-body data fit the linear model well. Therefore, the theoretical model was based on a linear model, where the most influential variables on static charge were incorporated. Different equations were determined for correlating either proposed or modified ASTM method data and human-body results.

Conclusions, implications, and recommendations drawn from this research are presented in Chapter 7. An understanding of the static phenomenon from both physics and textile science points of view is one of the most important results of the present work. Implications of the resultant models are discussed in detail from industrial and academic perspectives. Also, the advantages of a human-ecological framework for studying the electrostatic phenomenon on the human-body are discussed. Recommendations are established for industry, for further research of the models and numerical techniques, for research required for more comprehensive understanding of the static generation on textile surfaces, and for the extension of the models to any type of textile material.

Definition of Terms

For the purpose of the present research, the following definitions apply:

Static Electricity: Static electricity connotes the phenomena of attraction and repulsion observed between electrical charges on insulators (non-conductors), and it differs from "dynamic electricity" which is utilised in the generation of power or energy when it passes through a conducting system (Crugnola and Robinson, 1959, p.2).

Electrostatic Propensity: The capacity of a non-conducting material to acquire and hold an electrical charge by induction (via corona discharge) or tribo-electrification (ASTM D4238-90, p.399).

Electrostatic Discharge (ESD): ESD is a transfer of static charges between bodies at different potentials caused by direct contact or induced by an electrostatic field (Taylor and Secker, 1994, p.232).

Tribo-Electrification: Generation of static charge caused by the repeated contact and separation between two materials brought about by rubbing.

Static Charge (q): If an object exerts an electrical force on another object, it is said to be charged. The force exerted is dependent on the amount of the charge; that is, a static charge is considered an amount or quantity of electricity. If a body is electrically neutral, the resultant charge is zero. The unit of static charge, Coulomb [C]², corresponds to a charge of 6.25×10^{18} electrons (Taylor and Secker, 1994, p.17).

Potential (V): The potential difference dV between two points in a dielectric field is defined as: $dV = V_f - V_i = -W_{if} / q_0$, where q_0 is a test charge on which work (W_{if}) is done by the field, V_f is the final potential, and V_i is the initial potential. The SI unit of potential is the Volt [V] where 1 Volt = 1 Joule/Coulomb (Halliday-Resnick, 1988, p.608).

Capacitance (C): The ratio of the charge on one electrode to the potential difference between the electrodes. The SI unit of capacitance is the Farad [F]. Generally, the capacitance of a capacitor is evaluated by (1) finding the electric field E due to this charge, (2) evaluating the potential difference V , and (3) calculating C from equation: $C [F] = q [C] / V [V]$ (Halliday-Resnick, 1988, p.632).

Potential Energy (U): The potential energy of a charged capacitor, given by $U = 1/2 VQ$ is the work required to charge it. This energy is conveniently thought of as stored in the electric field E associated with the capacitor. By extension, stored energy can be associated with an electric field generally, no matter what is its origin. The SI unit of potential energy is the Joule [J] (Halliday-Resnick, 1988, p.632).

Charge Decay Rate: The rate at which an initial charge generated and/or induced on a textile surface is dissipated by some decay mechanisms (e.g., conduction and ionization of the air).

Permittivity: The capacity of a material to hold a charge, expressed in capacitance per unit length [F/m]. It may be defined either in terms of the capacitance, C , of a condenser with the material between parallel plates of area A and separation d , or in terms of the force F between two charges Q_1 and Q_2 at a distance r in the material (Morton and Hearle, 1975, p.481).

Dielectric Constant: The ratio between the permittivity of a material and the permittivity of free space ($\epsilon_0 = 8.854 \times 10^{-12}$ F/m). It is also called relative permittivity (Morton and Hearle, 1975, p.481).

²The symbols for units of different physical parameters are shown in square brackets (e.g., [C]).

Surface Resistivity: The surface resistance multiplied by that ratio of specimen surface dimensions (width of electrodes defining the current path divided by the distance between electrodes) which transforms the measured resistance to that obtained if the electrodes had formed the opposite sides of a square. The unit of surface resistivity is ohm/square. (ASTM D 257-93).

Volume Resistivity: The volume resistance multiplied by that ratio of specimen volume dimensions (cross-sectional area of the electrodes divided by the distance between electrodes) which transforms the measured resistance to that resistance obtained if the electrodes had formed the opposite sides of a unit cube (ASTM D 257-93).

Human Ecology: Defined as the scientific and holistic study of humans as social, physical, and biological beings in interaction with each other, their physical, socio-cultural, aesthetic, and biological environments, and with the material and human resources of these environments (Sontag & Bubolz, 1988).

Personal Protective Clothing (PPC): Any garment or group of garments for the purpose of isolating a body or parts of the body from a potential hazard, extending people's physical and physiological limitations in response to those hazardous conditions (ASTM F23.20.05-94).

Human-Body Model (HBM) ESD: An ESD event meeting the waveform criteria specified in a standard, and approximating the discharge from the fingertip of a typical human body (EOS/ESD-S5.1-1993).

HBM-ESD Tester: Equipment that applies human-body model ESD to a component (EOS/ESD-S5.1-1993).

References

ASTM. (1990). ASTM Committee D-13 on Textiles. Standard Test Method for Electrostatic Propensity of Textiles (D 4238 - 90). Philadelphia, PA: American Society for Testing and Materials.

ASTM. (1993). ASTM Committee D-9 on Electrical and Electronic Insulating Materials. Standard Test Method for DC Resistance or Conductance of Insulating Materials (D 257 - 93). Philadelphia, PA: American Society for Testing and Materials.

ASTM. (1994). ASTM Committee F-23 on Protective Clothing. Test Method for Evaluating Triboelectric (Static) Charge Generation on Protective Clothing Materials (Draft F23.20.05). Philadelphia, PA: American Society for Testing and Materials.

Berkey, B. D., Pratt, T. H., & Williams, G. M. (1988). Review of literature related to human spark scenarios. Plant/Operations Progress, 7(1), 32-36.

Crugnola, A. M., & Robinson, H. M. (1959). Measuring and predicting the generation of static electricity in military clothing (Textile series, Report No. 110). Natick, MA: Quartermaster Research & Engineering Command, US Army.

Gonzalez, J. A., Rizvi, S. A., Crown, E. M., & Smy, P. R. (1997). A modified version of proposed ASTM F23.20.05: Correlation with human body experiments on static propensity. In J. O. Stull & A. D. Schwope, Performance of Protective Clothing (pp. 47-61) Vol. 6, ASTM STP 1273. Philadelphia, PA: American Society for Testing and Materials.

Greason, W. D. (1992). Electrostatic discharge: A charge driven phenomenon. Journal of Electrostatics, 28, 199-218.

Halliday, & Resnick (1988). Physics (3rd. ed.). New York: Macmillan.

Kilsdonk, A. G. (1983). Human Ecology: Meaning and usage. East Lansing, MI: College of Human Ecology, Michigan State University.

Morton, W. E., & Hearle, J. W. S. (1975). Dielectric properties. In W. E. Morton, & J. W. S. Hearle, Physical Properties of Textile Fibres (2nd ed.) (pp. 481-501). London: William Heinemann Ltd and The Textile Institute.

Rizvi, S. A. H., Crown, E. M., Osei-Ntiri, K., Smy, P. R., & Gonzalez, J. A. (1995). Electrostatic characteristics of thermal-protective garments at low humidity. Journal of The Textile Institute, 86, 549-558.

Roth, R. (1990). Simulation of electrostatic discharges. Journal of Electrostatics, 24, 207-220.

Sontag, M. S., & Bubolz, M. M. (1988). A human ecological perspective for integration in home economics. In M. Doherty-Poirier (Creator), Perspectives of Human Ecology/Home Economics: Collected Readings, Fall 1995 (pp. 9-14). Edmonton: University of Alberta.

Taylor, D. M., & Secker, P. E. (1994). Industrial Electrostatics: Fundamentals and Measurements. Somerset, England: Research Studies Press Ltd.

Tolson, P. (1980). The stored energy needed to ignite methane by discharges from a charged person. Journal of Electrostatics, 8, 289-293.

Wandel, M., Gutschik, E., & Dormagen, W. C. (1972). Moderne Teppichfasern - Probleme und Möglichkeiten. Antistatik, anschmutz - und brennverhalten. Chemiefasern/Textilindustrie, (5), 397-401.

Wilson, N. (1977). The risk of fire or explosion due to static charges on textile clothing. Journal of Electrostatics, 4, 67-84.

Wilson, N. (1982). Incendiary spark discharge due to static on clothing. Protective Clothing. Manchester, England: Shirley Institute, 97-113.

Wilson, N. (1987). Effects of static electricity on clothing and furnishing. Textiles, 16(1), 18-23.

Chapter 2. Review of Literature

Basic Principles of Electrostatics

Charging that occurs when two solids come into contact has been referred to as contact charging, frictional charging, tribo-electric charging and tribo-electrification. Usually, but by no means exclusively, contact charging is used to describe simple contacts between surfaces (i.e., contacts in which no sliding or rubbing occurs between the contacting surfaces). When any of the other terms is used it is implied that when the contact is made, relative movement of the contacting surfaces occurs in a direction tangential to the contact interface.

An electrostatic system may be represented by a simple electrical equivalent circuit. It consists of four elements only: a current generator, I , to represent the charge generating mechanism, a capacitor, C , on which charge is stored, a resistance, R , which represents the charge relaxation mechanism in the electrically stressed insulator, and a **spark gap** which limits the maximum voltage that can be attained in the system.

Charge storage occurs on the system capacitance while the resistance of the system allows the charge to dissipate. The capacitor may be an insulating material or a person not properly grounded. The magnitudes of the capacitance and resistance determine the decay time (or relaxation time) of charge in the system, i.e., $\tau = RC$ (Taylor and Secker, 1994).

Electrostatic charges are invariably produced at the interface between two dissimilar materials when they are brought into firm contact with each other. These charges may comprise electrons, ions, and charged particles of the bulk materials, or any combination of these (Taylor and Secker, 1994). Henry (1953) reported that when the two surfaces are separated, either with or without obvious rubbing, charged particles are found to have crossed the boundary, with the usual result that the two surfaces have gained equal and opposite charges. For materials which are poor conductors of electricity (insulators), as are most textiles and polymers, the causes of charging are very complex. In good conductors, the charging is largely electronic in nature, but the surface of textiles is usually contaminated with additives, finishes, dirt and moisture, in all of which resides an abundance of ions (Wilson, 1987). Because there is little information on the ionic population of surfaces before contact is made, it is not possible to predict the magnitude of the transferred charge (Taylor and Secker, 1994).

Charge Generation

Static electricity is generated when almost any pair of surfaces is separated, unbalancing the molecular configuration in the case of relatively non-conductive materials (Sello and Stevens, 1983). Unless the electrical states of the two materials are extremely well balanced,

there will be a large transfer of charge when their surfaces are brought into contact (Morton and Hearle, 1975). But materials differ in their propensity to lose some of their electrons when in contact with another material (Crow, 1991). The energy required to cause the removal of an electron from a metal is called the **work function** (ϕ_w). When two bodies make contact, that which has the lower work function loses electrons to that with the higher work function.

Work function is the minimum energy required to extract the weakest bound electron from its maximum excursion distance from the surface to infinity (Gallo and Lama, 1976). Also, **work function** is defined as the difference in energy between the Fermi level and the zero of potential energy, and represents the minimum energy required at absolute zero to enable an electron to escape from the potential box (Arthur, 1955). A solid may be represented energetically as a potential well, where zero potential energy represents the space outside the solid (vacuum level). **A** is zero of kinetic energy, so that an electron of kinetic energy **AB** has total energy **OB** and is confined to the potential well. An electron in level **C** has total energy **OC** and is a free electron. A metal may be represented in this manner, the continuous spectrum of levels being filled up to energy **A** and empty above that (Harper, 1967; Taylor and Secker, 1994).

When the solid is an insulator, the energy spectrum is discontinuous, and energy levels are divided into two bands separated by a forbidden band of width E_1 . The lower or valance band is full and the upper or conduction band is empty under normal conditions. Since the valance band is full and an electron at the top of the valance has no higher energy level available, no acceleration in an electric field is possible (Arthur, 1955). These models are used to explain contact charging in terms of electron transfer, resulting in three main types of contact: metal-metal, metal-insulator, and insulator-insulator. The last two are important to the phenomenon of charge generation on textiles.

The transfer of electrons to an insulator is somewhat complex. Electrons can only move and carry current if they have sufficient energy to jump out of the filled band, through the forbidden band, into the conduction band. The chance of their acquiring this excess of energy is small, and any electron transferred to an insulator must be transferred into the conduction band (Morton and Hearle, 1975). This would lead to conductivity in charged insulators, which is not true. Gonsalves (1953) has suggested that there may be additional energy levels on the surface of an insulator called **surface states (Tamm levels)**, which enable an electron to remain localized on the insulator surface in an energy state within the range of energies of the forbidden band.

Although rubbing is not necessary for charge generation, it usually increases the amount of charge produced. **Tribo-electrification, frictional charging, or tribo-electric charging** are the terms that apply when an electrostatic charge is generated on a body by frictional forces,

which is probably the major mechanism for the generation of electrostatic charge in textile materials (Harper, 1967; Wilson and Cavanaugh, 1972, Taylor and Secker, 1994). Experiment shows that, when an insulating surface is rubbed either by a conductor or another insulator, charge transfer may be several orders of magnitude greater than in a simple touching contact. This may be rationalized by noting that rubbing increases the intimacy of the contacting surfaces. Hersh and Montgomery (1955) found that the manner of rubbing, the length of material rubbed, the normal force, and rubbing velocity (in some cases) affected the amount of charge generated. Haenan (1976) showed that charge transfer increased with rubbing pressure, and Coste and Pechery (1981) showed that charge transfer was greatest when surface roughness was small. Some researchers (Montgomery, Smith and Wintermute, 1961; Zimmer, 1970; and Ohara, 1979) have shown some instances where the charging goes through a maximum value. Such effect has been related to local temperature gradients appearing across the contact, resulting in the enhanced diffusion of electrons from the hotter to the cooler surface (Taylor and Secker, 1994).

Maximum Charge Density

The factors which determine the maximum density of charge that can remain on a surface without discharging into the surrounding medium are complicated. They are nevertheless important because discharge into the surrounding medium can set a limit to the charge obtained by friction charging. In the case of ambient air, when the electric breakdown field (EBD) of 2.7 MV/m is exceeded, a corona, brush or even a spark discharge will occur which will dissipate the excess surface charge (Gibson and Loyd, 1965).

In insulating sheets, an extended charge of uniform density σ on the surface gives a field just outside the charged surface of magnitude $\sigma/2\epsilon_0$. The maximum charge density, σ_{max} , that can be tolerated before this field exceeds the breakdown strength, EBD, of the ambient medium is given by

$$\sigma_{max} = 2\epsilon_0 EBD \quad \text{Eq. 2.1}$$

When one surface of an initially uncharged sheet is tribo-charged, the limiting charge density will be half this value because, as the contacting surfaces separate, all the flux lines, i.e., the electric field, will be bounded by the two separating surfaces. Thus

$$\sigma_{max} = \epsilon_0 EBD \quad \text{Eq. 2.2}$$

which for air yields, $\sigma_{max} = \pm 24 \mu\text{C}/\text{m}^2$ (Ji, Takahashi, Komai and Kobayashi, 1989).

Charge Dissipation

There are substantial differences in the ways a charge is dissipated, depending on whether it is located on an insulated conductor or on an intrinsically insulative material. In both cases, there are also differences that depend on whether the dissipation is carried out by charge

carriers already present or if these carriers are created by the process itself. All neutralization processes deal with the movement of charges under the action of electric fields (established by the charges to be dissipated) spreading the charges or re-combining opposite charges, and making the fields decay or at least decrease (Chubb, 1988).

The transport of charge in a decay process is described by the basic relation (Ohm's law):

$$j = \lambda E = (1/\rho)E \quad \text{Eq. 2.3}$$

where E is the field strength in a given point from the charge to be dissipated, j is the current density in the direction of E around the point, and λ and ρ are the conductivity and resistivity, respectively. Although the decay is always described by this basic equation, it is convenient to distinguish between three different types of decay processes: a) charge decay of a capacitive system, b) charge decay of a non-conducting system, and c) charge decay through the air.

An insulated conductor may be characterized electrically by its capacitance C and leakage resistance R , both with respect to ground, and this arrangement is called a capacitive system. It is a special characteristic for the decay of charge on a conducting system that the contact between the conductor and the resistive path only needs to be established at a single point. The capacitance C is an integral measure of the distribution of the electric field from a given charge on the conductor, between the conductor and ground. The capacitance will thus depend upon the location of the conductor and may change somewhat if the conductor itself or other neighbouring conductors are moved (Jonassen, 1991).

In the case of a non-conducting system (insulator or semi-insulator), the charge decay may depend, in a rather complex way, on the geometrical, and dielectric and resistive conditions of the environment (Baumgartner, 1987). If a charge is located on an insulator there is in principle no way by which the charge may ever dissipate. If, however, the charged insulator is surrounded by a conducting fluid in contact with the surface, the charge or the field from the charge may dissipate by oppositely charged ions being attracted to the insulator. This is not so simple when air is the current carrying medium because atmospheric air is normally neutral, but it may be ionized, that is made to contain mobile charge carriers. The dissipation effect depends upon the air containing ions of opposite polarity to the charge on the insulator (Jonassen, 1991).

Hazards from Electrostatics

Static electricity has long been cited by investigators as a possible cause of accidental ignition of flammable or explosive liquids, gases, dust, and solids. Many cases have been documented (Scott, 1981; Crow, 1991) where charges generated on an object reach the level at

which the resistance of the air-gap between the object and a conductor at a lower potential breaks down, producing a spark.

Evaluation of Hazards Created by ESD

Static electricity manifests its destructive nature through ESD. The electrostatic build-up on people or materials, particularly non-conductive materials such as textiles, can be significant in the dry conditions of Canada's winter. In cold regions like Alberta, the absolute humidity level declines sharply at very cold temperatures, so the electrostatic hazard can be more significant than in warmer regions, and even natural fibres like wool and cotton, when completely dry, are very poor conductors.

Workers in the oil and gas industries have expressed opinions that some thermal protective clothing they are required to wear may not be safe due to its static propensity. Many still hold a traditional belief that 100% cotton garments are less prone to static electricity than are garments of more thermally stable fibres such as aramid. This belief is based on measurements of certain electrical properties taken under conditions of relatively high humidity and may be misleading for low humidity environments. The ability of many fabrics to hold on to a static charge is a function of the relative humidity and their anti-static nature or finish.

The average individual walking across a non-conductive floor or sliding off a car seat can generate discharge potentials up to 15 kV, depending on the environment, for example in low relative humidity (Matisoff, 1986; Rizvi et al., 1995). The main hazard of ESD, or sparks, is their incendiary properties. They usually pose no electrical danger to human beings because the charges generated are too small. Depending on the individual, the human body has a threshold for shock of over 3 kV (Sclater, 1990). However, a spark of just less than 50 V can damage ESD-sensitive electronic devices (McAteer, 1987). Spark discharge occurs when the electric field strength exceeds the air breakdown value of 2.7 MV/m at atmospheric pressure, which means that the maximum charge density that can exist on a plane surface is about $24\mu\text{C}/\text{m}^2$ (Taylor and Secker, 1994).

Tolson (1980) reported that the incendiarity of a discharge can be estimated once the circumstances of charge accumulation are known. Charge accumulation on an ungrounded conductor (human body or discrete conductive fabric) and charge accumulation on an insulator (synthetic fabrics and plastics) are two very different situations. The former represents by far the greatest risk because it can discharge all the electrostatic energy instantaneously in the form of a spark. In the case of electrically insulating materials (e.g. fabric), however, their high surface and volume resistivity impede the flow of charge to the point of discharge and only a fraction of the total charge on the surface is released in the discharge. The equation to calculate potential energy can not therefore be used to calculate the energy of the discharge because the charged

insulator is not intrinsically an equipotential surface (Löbel, 1987). The character of a discharge from an insulator may be described in terms of the total charge transferred in the discharge and its distribution with space and time. Thus, the incendivity of a discharge depends not only upon the total amount of energy or charge released, but also upon the time distribution of the energy (Glor, 1988). A corona discharge extended in time is less incendive than a short-lived spark of the same total energy (Gibson and Lloyd, 1965).

Minimum Ignition Energy (MIE)

The ignition energy of a gas, vapour or dust depends strongly on the percentage of flammable material present. At low concentrations the ignition energy is high but decreases to a minimum at some critical concentration before rising again on further increasing the concentration. The lowest energy required to cause ignition of the material, or a mixture of it in critical concentration with air, is known as the minimum ignition energy (MIE).

There is no standard method to measure the energy required to ignite flammable gases. Typically, a known mixture of gas and air is placed in a grounded plexiglas box which contains an electrode. A charge is discharged through the electrode, either from a charged person or from a capacitor. Wilson (1982) reported that the critical voltage at which ignition occurs decreases with the size of the electrode down to 1 mm and then increases again with the smallest electrode because of corona discharging, and that the lowest voltage for an ignition is independent of body capacitance.

Assessment of the ignition risk from an electrostatically charged body essentially requires comparison of the igniting power of any discharge from the body with the minimum ignition energy of the flammable atmosphere (Glor, 1988; Owens, 1984). Wilson (1977/1978) showed that the minimum ignition energy of coal gas and air is 0.03 mJ, of natural gas and air is 0.3 mJ. The MIE required to ignite methane and air in a closed chamber by a spark between a finger and an earthed electrode has been evaluated as 18.6 mJ (Wilson, 1977/78), 5.9 mJ (Movilliat and Monomakhoff, 1977), 1.1 mJ (Tolson, 1980), and as low as 0.5 mJ (Crugnola and Robinson, 1959). These experiments were performed under different conditions -gas mixtures, electrode sizes, and body capacitance. Rizvi and Smy (1992) found that the minimum energy density thresholds for incendive and non-incendive sparks were 10 J/m^2 and 0.25 J/m^2 , respectively.

Environmental Conditions and Electrostatic Propensity

Sorptive Properties of Fibres

Fibres vary significantly in quantity of water vapour they absorb. Most textile fibres absorb moisture (water vapour) from the air. As the relative humidity (RH) of the air increases, the amount of moisture absorbed generally increases. The amount of moisture a fibre contains has a profound effect on the mechanical and electrical properties of the fibre. The rate of absorption depends on a variety of factors: temperature, air humidity, wind velocity, surrounding space, thickness and density of material, nature of the fibre, etc. (Morton and Hearle, 1975).

The amount of moisture the fibre contains when placed in an environment at a certain temperature and relative humidity is called its **moisture regain** which is determined as a percent of the dry weight of the fibre, or **moisture content** which is determined as a percent of conditioned weight.

When regain is related to relative humidity, a phenomenon called hysteresis is observed. The **absorption isotherm** is a plot of equilibrium regains at successively higher humidities of a specimen initially bone-dry; the **desorption isotherm** is a plot for a specimen initially wet, at successively lower humidities (Taylor, 1952). The regain curves for different fibres are **S**-shaped; the **S** becoming more distinct as the hydrophilicity of the fibres increases. In general, the amount of moisture absorbed increases rapidly as relative humidity increases from 0% to 10%, more slowly from 10% to 80%, and then more rapidly from 80% to 100%.

Within a fibre, the material accessible to moisture will be either the surfaces of crystalline regions or the non-crystalline regions. In crystalline regions, the fibre molecules are closely packed together in a regular pattern. Thus, it will not be easy for water molecules to penetrate into a crystalline region, and, for absorption to take place, the active groups would have to be freed by the breaking of some bonds or cross-links. The moisture at any particular relative humidity would be proportional to the amount of effectively non-crystalline material (Hearle and Peters, 1963).

The extent to which fibres absorb moisture depends largely on the presence of polar groups, their availability in the amorphous areas and on the strength of hydrogen bonding. At 0 to 10% RH, moisture is absorbed by freely available polar groups in the amorphous areas. Between 10 and 80% RH, a slower spreading apart of the polar groups in the amorphous areas occurs because saturation of all available polar groups is nearly complete. The greatest reduction in the rigidity of the fibre occurs in this region (Morton and Hearle, 1975). The sharp increase in absorption that occurs over 80% RH results predominantly from moisture accumulation being held by the forces of surface tension in capillary spaces between fibres or in

crevices in the fibre surface. This unbound moisture is held only loosely by the fibre (Morton and Hearle, 1975).

When a fibre absorbs water, heat is developed. It results from the attractive forces between the fibre molecules and water molecules. The greater the moisture absorption of the fibre, the greater will be the amount of heat evolved (Taylor, 1952). The evolution of heat raises the temperature of the fibres and increases their water vapour pressure, slowing down the rate of absorption. This process will continue until the vapour pressure of the fibres has become almost equal to that outside. This is a state of "transient equilibrium" in which further absorption is impossible until heat has been lost by the specimen. As heat is lost to the surrounding atmosphere, the temperature decreases, which allows a further increase in regain to occur and maintains the vapour pressure close to that of the atmosphere. This continues until "final equilibrium" is reached with both temperature and vapour pressure equal in fibre and atmosphere (Mackay and Downes, 1969).

The evolution of heat also has a considerable effect on the rate of conditioning of textile materials. Textile materials take a long time to come into equilibrium with their surroundings. The most obvious way of explaining the slowness of conditioning is to assume that it is due to the slowness with which water molecules diffuse through the fibre, and through the air to the fibre. If the concentration of water molecules varies from place to place in a given medium, the molecules will diffuse from regions of high concentration to regions of low concentration until their distribution becomes uniform (McMahon and Watt, 1965).

In considering absorption, one must take into account the interaction between the water molecules and the molecules of the fibre substance. All natural animal and vegetable fibres have reactive groups in their molecules that attract water. The first water molecules must be absorbed directly onto the hydrophilic groups, but, for those absorbed after the first, there is a choice. They may be attracted to other hydrophilic groups, or they may form further layers on top of the water molecules already absorbed. The directly attached water molecules will be firmly fixed, fitting closely to the structure of the molecules. They will be limited in their movement. The indirectly attached water molecules will be more loosely held (Hearle and Peters, 1963).

Calculation of the division between directly and indirectly attached water, and its relation to relative humidity, has been the subject of much theoretical speculation. Peirce (cited in Morton and Hearle, 1975) developed a model for calculating this division. It is the directly attached water that changes the forces between molecules and breaks cross-links, so that it should have a greater effect than the indirectly attached water on the physical properties of the fibre. On the other hand, it will be the indirectly attached water molecules that will be the first to evaporate, so these would be expected to have the greatest effect on the vapour pressure.

Peirce assumes that only a fraction of the sites is effective in indirect absorption and that when these are filled there is saturation. The reason given for assuming that not all sites are effective is that one indirectly attached water molecule can seal off a number of sites.

Brunauer, Emmett, and Teller (cited in Morton and Hearle, 1975) derived an equation (the BET equation) for gases and vapour adsorbed in multi-layer materials. This equation gives a sigmoidal isotherm which shows a good fit with several practical examples of absorption. The analysis is based on the equilibrium between the rate of evaporation and the rate of condensation on the surface, but it does not take account of effects due to swelling. Windle (cited in Morton and Hearle, 1975) presented a model in an application to wool which incorporated the swelling effect and he assumed the absorbed water molecules could be divided into three types: localized water, directly absorbed onto absorption sites and limited to one per site; intermediate water, absorbed onto localized water molecules and limited to one on each localized water molecules; and mobile water, absorbed on intermediate water molecule, with no restriction on numbers.

Hailwood and Horrobin (cited in Morton and Hearle, 1975) combined an attachment of the first water molecules onto particular sites in the polymer molecule with a solution theory for the further absorption of water by the material. They consider that some of the water is present as hydrates formed with definite units of the polymer molecule and that the remainder forms an ideal solid solution in the polymer. By consideration of the chemical equilibrium, they derive an equation relating the amount of water absorbed to the relative humidity.

Quite a different approach to moisture sorption was developed by Barkas (cited in Morton and Hearle, 1975), starting from the analogy between swelling and osmotic phenomena. He considered that water passes into the region of high polymer concentration from a low concentration region, causing the polymer to swell. This continues until the stresses generated by the deformation of the polymer are sufficient to prevent more water from flowing in.

The absorption of water by fibres is an example of a process that encompasses not only the relation between regain and humidity but also associated phenomena, such as hysteresis, heat effects, the variation of regain with temperature, the influence of moisture on physical properties, and all the complicated factors arising from the interaction of moisture and mechanical effects owing to the limited swelling of fibres.

Effect of Moisture and Temperature on Electrostatic Characteristics of Textile Materials

Several researchers have reported the great effect environmental conditions have on electrical characteristics of textile materials. Hearle (1953) found that the moisture content of a textile fibre is the most important factor in determining its electrical resistance. Hearle and others (King and Medley, 1947; Medley, 1950; Sereda and Feldman, 1964) have shown that the

resistivity of yarns and other textile materials increases exponentially with decrease in the relative humidity of the environment with which they are in equilibrium.

Not only the electrical resistivity of a fibre is affected by changes in its moisture content. Rizvi, Crown, Gonzalez and Smy (in press) reported that mean discharge potentials and energies from clothed humans decreased to about 50% with some garment systems when the relative humidity increased from 0 to 20%. Crugnola and Robinson (1959) evaluated several garment systems at different relative humidity levels. They found that below 20% RH all garment systems generated high voltages considered dangerous by the U.S. National Bureau of Standards (N.B.S.), but none of the garment combinations produced potentials required for the detonation of the most active materials studied by the N.B.S.

Sereda and Feldman (1964) explained that the rapid decrease in charge generation at high humidity is due to an increase in conductivity and/or charge dissipation along a surface-water film. A change in relative humidity produces a change in the equilibrium moisture content of most textile materials, and hence alters their chemical nature (Hersh and Montgomery, 1956). Also, the moisture content of the ambient air plays a role in the generation and dissipation of charges. Onogi, Sugiura and Nakaoka (1996) found atmospheric charge dissipation into the air by water molecules through evaporation of water droplets from textile surfaces, resulting in static charge reduction. Furthermore, they reported that the rate constant for the atmospheric charge dissipation depends on the water content of the textile material.

The effect of temperature has not been addressed as thoroughly as the influence of moisture. Hearle (1953) reported that the resistance of limited number of textile fibres decreased as the ambient temperature increased, and that relationship fit to some extent a logarithmic model. Also, significant increase in body potentials was found when the temperature was decreased from room temperature to -40°C (Crugnola and Robinson, 1959). Sharman, Hersh and Montgomery (1953) reported a decrease in conductivity in both drawn and undrawn nylon filaments as the temperature decreased from 45 to 15°C , but they found that at none of the temperatures studied could the temperature dependence be accounted for as a simple rate process.

Onogi, Sugiura and Matsuda (1997) reported interaction effects of temperature and moisture content in either fibre or ambient air, and their combined influence on static dissipation from textile surfaces. They reported variation in the critical water content of different fibres at various temperatures. Critical water content is a characteristic of the structure of the polymer molecule and also the bulk structure of the fibre. Absorbed water in a sample with less than this critical water content could not carry charge into the air. They also evaluated the slopes of the line relating the rate constant of charge dissipation for various fabrics and the free water, and found that at all temperatures the slopes for each fabric were quite different. Thus, they

concluded that the rate constant for charge dissipation into the air does not generally depend on only the amount of free water in the textile fabric, but also on the vapour pressure of water (absolute humidity).

Measurements of Static Electricity in Textiles

There have been two main approaches to assessing the electrostatic propensity of textile materials. One is to measure the charge built up on a clothed person or the electrical capacitance of a body (human-body model); the second is to measure some electrostatic characteristics of textiles (e.g., surface resistivity, charge decay rate, peak potential, etc.) in small-scale tests.

Human Body Experiments

There is no standard method for measuring the static charge built up on a person. The generally accepted method is for a person to walk in a controlled fashion on a controlled surface into a Faraday cage. This is a wire cage onto which is induced an equal but opposite charge to that on the person entering it. This induced charge is recorded to give a measure of the static electricity on the person.

Most human-body experiments have been conducted in the United States, Canada and in the United Kingdom. Measurements of the charges generated between different materials agree somewhat with rankings in existing tribo-electric series, where materials placed close to each other develop less static charge than those ranked further apart. Some conclusions are that the static propensity of clothing depends on such factors as temperature, humidity, the type of textile, the type of charge mechanism, and the nature of the footwear worn (Crow, 1991).

Experiments at The Arctic Aeromedical Laboratory (Veghte & Millard, 1963) were conducted specifically on the accumulation of static electricity on Arctic clothing. In the experiment, three different Arctic clothing outfits made mainly from nylon were worn by fifteen different subjects. The electrostatic charges on the clothing systems and the capacitance of the subjects were measured. The experiments were conducted at ambient temperature ranging from 5 to -43° C and relative humidity at between 50% and 74%. The research pointed out the dangers of personnel working outside, coming indoors and removing exterior clothing in a dry environment, a situation which tends to produce very high electrostatic charges.

Wilson's study (1977/1978) was intended to investigate the charge generation characteristics of clothing in normal use by workers. The objective of this project was to assist in developing a specification which could be used to identify safe fabrics for use when handling flammable materials. The garments were the type worn by military personnel and were made of

fabrics such as polyester and linen/polyester coveralls, aramid and cotton flying suits, and polyurethane coated nylon weather suits. The subject wearing a garment and a pair of rubber-soled shoes, sat down on a covered chair and slid off it into a standing position. The chair cover materials were lambswool, PVC-coated cotton, leather, and cotton canvas. In all cases, the body voltages were discharged to ground via the fingers to produce sparks which were measured. This work was done at relative humidities in the range of 15 to 80%, at 21° C. The result showed that cotton as well as synthetic fabrics are static prone at low humidity.

Scott (1981) noted that the majority of work on the incendivity of spark discharges from the human body had concentrated on surface resistivity of fabrics and the voltages generated on the body. He found that the capacitance of the human body varies according to size, the footwear being worn and stance, that larger bodies have greater capacitance, and that insulated footwear raises the electrical insulation of the body and lowers the body capacitance.

De Santis and Hickey (1984) measured the static build-up on an Extended Cold Wet Clothing System (ECWCS) before and after laundering. They measured the potential accumulated with a Faraday cage enclosing a test participant wearing various ECWCS items. The dressing and removing of garments took place outside the cage at a test temperature of -40° C. The authors concluded that the donning and doffing of the outer Gor-Tex jacket created very little static electricity. The polyester pile shirt showed evidence of static charge which resulted from the shirt brushing against a static-generating material.

Researchers at the University of Alberta (Rizvi et al., 1995; Crown, Smy, Rizvi & Gonzalez, 1995; Rizvi, Crown, Gonzalez and Smy, in press) developed a method in which a clothed person performs a physical activity, and then touches a grounded electrode. The discharge potential of the resulting spark is measured and monitored by a digital oscilloscope. From the discharge-voltage waveform, other parameters of interest, for example: transferred charge, discharge energy, peak current, duration of event, etc., were calculated. They reported the characteristics of ESD from humans wearing protective garment systems and doing two activities: sliding off a car seat, and walking and removing a garment. The experiments were done under very low humidity, at room temperature. It was found that garments made of antistatic fibres (aramid/carbon and aramid/stainless steel) generated static charges of less energy than those made of non-antistatic fibres (aramid and FR cotton), but those charges were still bigger than the MIE of different gases, vapours and mixtures.

Small-Scale Tests

Several standard methods to measure different static characteristics are utilized, but there is generally a lack of correlation between small-scale and human-body data. Small-scale

tests normally measure the electrostatic characteristics of an insulator and do not represent the real phenomenon of a charged clothed human body being discharged through a grounded object.

Measurements in small-scale tests are different from measurements in human-body experiments as their physical quantities are different in value and order of magnitude. Several conditions are involved in real-life sparks: electrostatic discharges are the result of the typical charge generation processes (tribo-electrification, induction and conduction charging), charge accumulation, type of materials involved, capacitance of the system, atmospheric conditions, etc. In order to understand better and control the various parameters which are related to ESD, the use of appropriate instrumentation, measurements, and standardized test methods is necessary.

Measurement of electrical resistivity is a frequently used method for the evaluation of static propensity of textiles (Coelho, 1985, Löbel, 1987). One of the most accepted small-scale methods used is surface resistivity [e.g., AATCC Test Method for Electrical Resistivity of Fabrics (76-1987), and ASTM Standard Test Methods for d-c Resistance or Conductance of Insulating Materials (D257-93)]. The advantages of this kind of measurement over the determination of surface potentials are many. Measurement of electrical resistivity is described as simple and reproducible, and commercial equipment is widely available (Ramer and Richards, 1968). Teixeira and Edelstein (1954) discussed the fundamental principles of resistivity, giving definitions and explaining how charges are developed and how they are dissipated. Wilson (1963) showed experimentally that resistance along and through a fabric was a main factor in determining the rate of leakage of charge from the charged surface and through the structure, respectively, provided that the capacitance was maintained constant.

Measurement of charge decay rate on fabrics is another well known and industry-wide method (e.g. ASTM Standard Test Method for Electrostatic Propensity of Textiles (D4238-90), Federal Test Standard 101C Method 4046 Electrostatic Properties of Materials, and Federal Test Standard 191A Method 5931 Determination of Electrostatic Decay of Fabrics). In using a charge decay meter to measure the dissipation rate, decay time indicates the ability of the surface to transfer the electrons from a charged body through the work surface to ground. Thus, the greater the resistance, the slower the charge decay rate (Matisoff, 1986).

Taylor and Elias (1987) discussed the problem of measuring the static dissipative properties of materials and proposed a new charge decay meter capable of measuring decay times from 100 ms to 10,000 s. They showed that for many materials surface resistivity did not correctly specify the ability of the material to dissipate static charge. Chubb (1990) described a new approach for the measurement of charge decay on insulating and semi-insulating materials. Charge was deposited on the material and a fast response electrostatic field meter was used to measure the rate of charge decay. Chubb and Malinverni (1993) reported the results of

comparative studies on the charge decay characteristics of a variety of materials as observed by Federal Test Standard 101C Method 4046 and by the method developed by Chubb. They concluded that measurements by FTS 101C relate to charge decay by the fastest charge migration component of the materials whereas the method developed by Chubb gives times determined by charge decay on the outermost surface of the material. Chubb and Malinverni stated that since the ability of materials to dissipate static charge depends upon charges generated by tribo-charging the outermost surface it is such decay times which are of practical relevance.

To overcome some shortcomings of the standard test methods mentioned above, ASTM Standard Test Method for Evaluating Triboelectric (Static) Charge Generation on Protective Clothing Materials (F23.20.05) has been proposed. This draft method may be used to evaluate the static electrical charge generated by tribo-electrification and the rate of discharge on protective clothing. The system has been in use since the late 1960's by the National Aeronautics and Space Administration (NASA) (Gompf, 1984). Although the method incorporates controlled frictional charging, and reliable measurements of potentials have been obtained in experiments carried out at the University of Alberta, the charge decay results obtained in those experiments have given very low correlation with either triboelectric charge obtained by the method or human-body discharge potentials. Stull (1994) reported that "... although this method may not appraise the hazard under actual use conditions, it does permit the ranking of material performance and identification of potential material problems for a given set of conditions. It seems particularly suited for chemical protective applications" (p.26).

Modelling in Electrostatics

There have been many investigations in the field of electrostatics aimed to develop mathematical models that could explain the electrostatic phenomenon. Most of the research has been carried out for the electronics industry because it is in this industry where electrostatic discharges most easily show their destructive effect.

Hearle's (1953) investigation of the electrical resistance of fibres led him to determine several mathematical expressions relating resistance to the characteristics of a fabric and environmental conditions. He found that resistance of textile materials and either temperature or moisture fit logarithmic models well, which was also found by other researchers (Cusick and Hearle, 1955; Clark and Preston, 1955).

Hersh and Montgomery (1955) carried out a very comprehensive investigation of static electrification of filaments. They built special equipment for testing tribo-electrification on fibres, and a tribo-electric series was determined with the help of this device. They found that the

magnitude of the charge generated was directly proportional to the length of material rubbed and to the normal force between the fibres, and that charge transfer was independent of velocity when insulators were rubbed together.

Berta and Gastanek (1979) presented physical and mathematical models to simulate discharge between a charged insulating surface and a grounded sphere. Boxleitner (1990) reported the results of a computer simulation of the effect of ESD on printed circuit board mounted integrated circuits caused by charged boards and personnel. It was concluded that the ESD threat to integrated circuits (ICs) on personal computer boards (PCBs) may vary by a factor of 100, depending on the ESD source, the discharge point, and the structure and design of the PCB. Greason (1990) presented a preliminary model to study ESD induced potentials in electronic systems. A spherical geometry was used and results were presented for ESD to various sized electronic systems, which are either floating or grounded. Wilson and Ma (1991) examined ESD fields both analytically and experimentally; a simple dipole model of an ESD spark was developed and used to predict the radiated fields. Measurements indicated that electric fields can be quite significant (> 150 V/m at 1.5 m) for short periods of time in nanoseconds, particularly for relatively low-voltage events (< 6 kV).

Jonassen (1991) reported different equations based on the exponential model for three different types of charge decay schemes: a) for charge decay of a capacitive system, b) for charge decay of a non-conducting system, and c) for charge decay through the air. Wilson (1963) found a strong linear correlation between electrical resistance and electrostatic charge decay, and that charge decay followed well the exponential model of the form $Q = Q_0 \exp(-t/\tau)$. Onogi et al (1996) assumed that if the charge decay into the air is linearly proportional to the charge density on the surface (the same as the first-order reaction), the static charge (Q) at t time after rubbing can be expressed by the exponential model.

Greason (1995) analyzed human-body electrostatic discharges using a capacitance model. He found that when a human body with multiple charged sources (clothing and shoes) assumes a seated position at a work station, a body potential is developed which depends on both the present environment and the previous history of grounding of the human body, and that the nature of the coupling factors in effect at the initial grounding determines the amount of charge transferred to the body.

Summary

Almost five decades have passed since textile researchers first began seriously addressing the effects of static electricity on clothing and people. Since that time, volumes have been written explaining the detrimental effects of this natural phenomenon. The need for in-

depth understanding of the fundamentals of electrostatics in several industries has been growing fuelled by the proliferation of synthetic fibres, and the use of atmospherically controlled environments, high speed manufacturing, and static-sensitive devices.

The major concern with static electricity is that electrostatic discharges (ESD) have proven to be significant ignition sources for flammable gases, vapours, or powders which may be present in certain industrial environments, resulting in fires and explosions and the possible loss of human life. Sources of ESD are as numerous and varied as the processes and material combinations in industry.

Considerable research has been done on the charge generation and dissipation characteristics of textiles used in clothing. However, several issues remain unanswered, and many data from past investigations have not been updated using new digital and computerized equipment available today. Also, the electrostatic characteristics of many new high-performance fibres used in personal protective equipment have not been thoroughly investigated. Furthermore, the industry is still in need of test methods which strongly correlate with real-life conditions.

Although several researchers have carried out investigations in the field, mainly in the 1950's, which led them to develop mathematical equations for explaining the static phenomenon in textiles, further research is required to determine theoretical models that fully explain the charge generation and dissipation on textiles and clothing, and predict the static propensity of protective clothing systems. Most of the mathematical equations developed have been based on empirical data obtained with the use of early technologies and on limited conditions of old fabric structures, which limit their use in modern industrial applications.

References

AATCC. (1989). AATCC Committee RA32. Electrical Resistivity of Fabrics (76-1989). Research Triangle Park, NC: American Association of Textile Chemists and Colourists.

Arthur, D. F. (1955). A review of static electrification. Journal of The Textile Institute, **46**, 721-734.

ASTM. (1990). ASTM Committee D-13 on Textiles. Standard Test Method for Electrostatic Propensity of Textiles (D 4238 - 90). Philadelphia, PA: American Society for Testing and Materials.

ASTM. (1993). ASTM Committee D-9 on Electrical and Electronic Insulating Materials. Standard Test Methods for DC Resistance or Conductance of Insulating Materials (D 257 - 93). Philadelphia, PA: American Society for Testing and Materials.

Baumgartner, G. (1987). A method to improve measurements of ESD dissipative materials. In EOS/ESD Symposium Proceedings Vol. EOS-9 (pp. 18-27). Rome, NY: The EOS/ESD Association and IIT Research Institute.

Berta, I., & Gastanek, N. (1979). The energy of electrostatic discharges. In J. Lowell (Ed), Electrostatics Vol. 48, (pp. 67-72). Bristol, UK: IOP Publishing Ltd.

Chubb, J. N. (1988). Measurement of static charge dissipation. In J. L. Sproston (Ed.), Electrostatic Charge Migration (pp. 73-81). Bristol, UK: IOP Publishing Ltd.

Chubb, J. N. (1990). Instrumentation and standards for testing static control materials. IEEE Transactions on Industry Applications, 26, 1182-1187.

Chubb, J. N., & Malinverni, P. (1993). Comparative studies on methods of charge decay measurement. Journal of Electrostatics, 30, 273-284.

Clark, J. F., & Preston, J. M. (1955). Electrical resistance of viscose rayon at low temperatures. Textile Research Journal, 25, 797-798.

Coelho, R. (1985). The electrostatic characterization of insulating materials. Journal of Electrostatics, 17, 1327.

Coste, J., & Pechery, P. (1981). Influence of surface profile in polymer-metal contact charging. Journal of Electrostatics, 10, 129-136.

Crow, R. M. (1991). Static electricity: A literature review (U) (Technical Note 91-28). Ottawa. ON: Defence Research Establishment Ottawa.

Crown, E. M., Smy, P. R., Rizvi, S. A., & Gonzalez, J. A. (1995, June 30). Ignition hazards due to electrostatic discharges from protective fabrics under dry conditions. In Final Report Presented to Alberta Occupational Health and Safety, Heritage Grant Program. Edmonton, AB: University of Alberta.

Crugnola, A. M., & Robinson, H. M. (1959). Measuring and predicting the generation of static electricity in military clothing (Textile series, Report No. 110). Natick, MA: Quartermaster Research & Engineering Command, US Army.

Cusick, G. E., & Hearle, J. W. S. (1955). The electrical resistance of two protein fibres. Journal of The Textile Institute, 46, 369-370.

De Santis, J. A., & Hickey, S. L. (1984). Investigation of electrostatic potential of extended cold wet clothing system (ECWS) (APG-MT-6018). Aberdeen, MD: Aberdeen Proving Ground.

Gallo, C. F., & Lama, W. L. (1976). Some charge exchange phenomena explained by a classical model of the work function. Journal of Electrostatics, 2, 145-150.

Gibson, N., & Lloyd, F. C. (1965). Incendivity of discharges from electrostatically charged plastics. British Journal of Applied Physics, 16, 1619-1631.

Glor, M. (1988). Electrostatic Hazards in Powder Handling. Letchworth, England: Research Studies Press.

Gompf, R. H. (1984). Triboelectric testing for electrostatic charges on materials at Kennedy Space Center. In EOS/ESD Symposium Proceedings Vol. EOS-6 (pp. 58-63). Rome, NY: The EOS/ESD Association and IIT Research Institute.

Gonsalves, V. E. (1953). Some fundamental questions concerning the static electrification of textile yarns: Part I. Textile Research Journal, 23, 711-718.

Gonzalez, J. A., Rizvi, S. A., Crown, E. M., & Smy, P. R. (1997). A modified version of proposed ASTM F23.20.05: Correlation with human body experiments on static propensity. In J. O. Stull & A. D. Schwobe (Ed), Performance of Protective Clothing (pp. 47-61) Vol. 6, ASTM STP 1273. Philadelphia, PA: American Society for Testing and Materials.

Greason, W. D. (1990). Modelling ESD induced potentials in electronic systems. In EOS/ESD Symposium Proceedings Vol. EOS-12 (pp. 74-81). Rome, NY: The EOS/ESD Association and IIT Research Institute.

Greason, W. D. (1995). Quasi-static analysis of electrostatic discharge (ESD) and the human body using a capacitance model. Journal of Electrostatics, 35, 349-371.

Haenen, H. T. M. (1976). Experimental investigation of the relationship between generation and decay of charges on dielectrics. Journal of Electrostatics, 2, 151-173.

Harper, W. R. (1967). Contact and frictional electrification. London, UK: Oxford University Press.

Hatch, K. L. (1993). Textile Science. Minneapolis-St. Paul, MN: West Publishing.

Hearle, J. W. S. (1953). The electrical resistance of textile materials: Parts I to IV. Journal of The Textile Institute, 44, 117-198.

Hearle, J. W. S., & Peters, R. H. (1963). Fibre structure. Manchester, England: The Textile Institute.

Henry, P. S. H. (1953). Survey of generation and dissipation of static electricity. The British Journal of Applied Physics, 4(2), 6-11.

Hersh, S. P., & Montgomery, D. J. (1955). Static electricity of filaments. Experimental techniques and results. Textile Research Journal, 25, 279-295.

Hersh, S. P., & Montgomery, D. J. (1956). Static electrification of filaments. Theoretical Aspects. Textile Research Journal, 26, 903-913.

Ji, X., Takahashi, Y., Komai, Y., & Kobayashi, S. (1989). Separating discharges on electrified insulating sheet. Journal of Electrostatics, 23, 381-390.

Jonassen, N. (1991). Electrostatic decay and discharge. In EOS/ESD Symposium Proceedings Vol. EOS-13 (pp. 31-37). Rome, NY: The EOS/ESD Association and IIT Research Institute.

Löbel, W. (1987). Antistatic mechanism of internally modified synthetics and quality requirements for clothing textiles. In B. C. O'Neill (Ed), Electrostatics'87 Vol. 85 (pp. 183-186). Bristol, UK: IOP Publishing Ltd.

Mackay, B. H., & Downess, J. G. (1969). The kinetic of water-vapour sorption in wool. Part II: Results obtained with an improved sorption vibroscope. Journal of The Textile Institute, 60, 378-394.

Matisoff, B. S. (1986). Handbook of electrostatic discharge controls. New York: Van Nostrand Reinhold Co.

McAteer, O. J. (1987). An overview of the ESD problem. In B. C. O'Neill (Ed), Electrostatics'87 Vol. 85 (pp. 155-164). Bristol, UK: IOP Publishing Ltd.

McMahon, G. B., & Watt, I. C. (1965). Temperature changes in sorption systems due to heat of sorption. Textile Research Journal, 35, 37-44.

Montgomery, D. J., Smith, A. E., & Wintermute, E. H. (1961). Static electrification of filaments: Effect of filament diameter. Textile Research Journal, 31, 25-31.

Morton, W. E., & Hearle, J. W. S. (1975). Physical properties of textile fibres. London, UK: The Textile Institute & William Heinemann Ltd.

Movilliat, P., & Monomakhoff, H. (1977). Ignition of gas mixtures by discharge of a person with static electricity. In Proceedings of International Conference on Safety in Mines (pp. 230-242). Varna, Bulgaria.

Ohara, K. (1979). Contribution of molecular motion of polymers to frictional electrification. In J. Powell (Ed), Electrostatics'79 Vol. 48 (pp. 257-264). Bristol, UK: IOP Publishing Ltd.

Onogi, Y., Sugiura, N., & Nakaoka, Y. (1996). Dissipation of triboelectric charge into air from textile surfaces. Textile Research Journal, 66, 337-342.

Onogi, Y., Sugiura, N., & Matsuda, C. (1997). Temperature effect on dissipation of triboelectric charge into air from textile surfaces. Textile Research Journal, 67(1), 45-49.

Owens, J. E. (1984). Hazards of personnel electrification: Nomex vs. NoMoStat. Wilmington, DE: E. I. DuPont de Nemours & Co.

Ramer, E. M., & Richards, H. R. (1968). Correlation of the electrical resistivities of fabrics with their ability to develop and to hold electrostatic charges. Textile Research Journal, 38, 28-35.

Rizvi, S. A. H., Crown, E. M., Gonzalez, J. A., & Smy, P. R. (in press). Electrostatic characteristics of thermal-protective garment systems at various low humidities. Journal of The Textile Institute

Rizvi, S. A. H., Crown, E. M., Osei-Ntiri, K., Smy, P. R., & Gonzalez, J. A. (1995). Electrostatic characteristics of thermal-protective garments at low humidity. Journal of The Textile Institute, 86, 549-558

Rizvi, S. A. H., & Smy, P. R. (1992). Characteristics of incendive and non-incendive spark discharges from the surface of a charged insulator. Journal of Electrostatics, 27, 267-282.

Sclater, N. (1990). Electrostatic discharge protection for electronics. Blue Ridge, PA: Tab Books.

Scott, R. A. (1981). Static electricity in clothing and textiles. Thirteenth Commonwealth Defence Conference on Operational Clothing and Combat Equipment (Malaysia). Colchester, UK: Stores and Clothing Research and Development Establishment.

Sello, S. B., & Stevens, C. V. (1983). Antistatic treatments. In M. Lewin & E. M. Pearce (Ed), Handbook of Fiber Science and Technology: Volume II, Part B (pp. 291-315). New York, NY: Marcel Dekker, Inc.

Sereda, P. J., & Feldman, R. F. (1964). Electrostatic charging on fabrics at various humidities. Journal of The Textile Institute, 55, 288-298.

Sharman, E. P., Hersh, S. P., & Montgomery, D. J. (1953). The effect of draw ratio and temperature on electrical conduction in nylon filaments. Textile Research Journal, 23, 793-798.

Stull, J. (1994). Measuring static charge generation on PC materials. Safety & Protective Fabrics, 2 (8), 24-26.

Superintendent of Documents. (1990). Determination of electrostatic decay of fabrics (Federal Test Method Standard 191A, Method 5931). Washington, DC: Government Printing Office.

Superintendent of Documents. (1969). Electrostatic properties of materials (Federal Test Method Standard 101B, Method 4046). Washington, DC: Government Printing Office.

Taylor, D. M., & Elias, J. (1987). A versatile charge decay meter for assessing antistatic materials. In B. C. O'Neill (Ed), Electrostatics'87 Vol. 85 (pp. 177-181). Bristol, UK: IOP Publishing Ltd.

Taylor, D. M., & Secker, P. E. (1994). Industrial electrostatics: Fundamentals and measurements. Somerset, England: Research Studies Press Ltd.

Taylor, J. B. (1952). Sorption of water by viscose rayon at low humidities. Journal of The Textile Institute, 43, T489-T515.

Teixeira, N. A., & Edelstein, S. M. (1954). Resistivity: One clue to the electrostatic behaviour of fabric. American Dyestuff Reporter, 43, 195-208.

Tolson, P. (1980). The stored energy needed to ignite methane by discharges from a charged person. Journal of Electrostatics, 8, 289-293.

Veghte, J. H., & Millard, W. W. (1963). Accumulation of static electricity on arctic clothing (Technical Report AAL-TDR-63-12). Fort Wainwright, AK: Arctic Aeromedical Laboratory, Aerospace Medical Division.

Wilson, D. (1963). The electrical resistance of textile materials as a measure of their anti-static properties. Journal of The Textile Institute, 54, 97-105.

Wilson, L. G., & Cavanaugh, P. (1972). Electrostatic hazards due to clothing (Report No. 665). Ottawa, ON: Defence Research Establishment Ottawa.

Wilson, N. (1982). Incendiary spark discharge due to static on clothing. Protective Clothing. Manchester, England: Shirley Institute, 97-113.

Wilson, N. (1987). Effects of static electricity on clothing and furnishing. Textiles, 16(1), 18-23.

Wilson, N. (1979). The nature and incendiary behaviour of spark discharges from the body. In B. C. O'Neill (Ed), Electrostatics'79 Vol. 48 (pp. 73-83). Bristol, UK: IOP Publishing Ltd.

Wilson, N. (1985). The nature and incendiary behaviour of spark discharges from textile surfaces. Journal of Electrostatics, 16, 231-245.

Wilson, N. (1977). The risk of fire or explosion due to static charges on textile clothing. Journal of Electrostatics, 4, 67-84.

Wilson, P. F., & Ma, M. T. (1991). Fields radiated by electrostatic discharges. IEEE Transactions EMC, 33, 10-18.

Zimmer, E. (1970). Electrostatic charging of high-polymer insulating materials. Kunststoffe, 60, 456-468.

Chapter 3. A Modified Version of Proposed ASTM F23.20.05 Method on Static Propensity¹

Preamble

A modification of the proposed ASTM Test Method for Evaluating Tribo-electric (Static) Charge Generation on Protective Clothing Materials (F23.20.05) procedure has been developed to measure peak potentials and energies from a capacitor, as well as peak potentials and decay rates from specimen surfaces charged by tribo-electrification. The test system simulates a clothed human body rubbing an insulated surface and touching a grounded object, generating a spark of several thousand volts.

Experiments following both the proposed ASTM method and its modification were conducted at both 0% and 20% relative humidity (RH) and room temperature. Several one- and two-layer fabric systems were tested, including combinations of aramid/PBI, aramid/carbon, aramid/FR viscose, non-FR cotton and FR cotton. Both test methods seem to have good reliability, and showed a trend where anti-static fabrics could be charged to lower discharge potential than cellulose based fabrics.

Introduction

This chapter deals with the use of test methods based on peak potential and charge decay measurements of textile systems charged by tribo-electrification. Previous research on electrostatic propensity of textiles has been carried out on single-layer fabrics, but the evaluation of electrostatic discharges becomes more complex for multiple layers of clothing than for single layers. Multiple layers with blends of different fibres are even more difficult to evaluate. A clothed human body can be modelled as a conductor, covered with a fabric or fabrics, which is charged by tribo-electrification or induction (Rizvi et al, 1995). Electrostatic charge will accumulate on the outer surface of the conducting body and on the garments. This stored energy in the body would be discharged upon contact with a grounded conductive object. The small-scale test methods utilized in this study are aimed at simulating both instances, the charge on the textile surface and on the body and its subsequent dissipation or discharge.

Much has been written about methods to evaluate electrostatic properties, but there seems to be little consensus. Some believe that build-up of static charge depends upon the

¹The paper: Gonzalez, J. A., Rizvi, S. A., Crown, E. M., & Smy, P. R. (1997). A modified version of proposed ASTM F23.20.05: Correlation with human body experiments on static propensity. In J. O. Stull & A. D. Schwoppe, Performance of Protective Clothing Vol. 6, ASTM STP 1273 (pp. 47-61). Philadelphia, PA: American Society for Testing and Materials, was mainly based on this chapter

electrical resistance of the material (Ballou, 1954; Wilson, 1963). Others (Crugnola and Robinson, 1959; McLean, 1955; Teixeira and Edelstein, 1954) list the limitations of this assumption, as follows: (a) it is inaccurate for a textile fabric; (b) it ignores the effect of a second surface; (c) it ignores the effect of a blend; and (d) resistivity can at best furnish only a clue to one mechanism of charge dissipation, namely conduction.

Current test methods have not been completely satisfactory, as reported by Crow (1991). In AATCC Test Method 76-1987 Electrical Resistivity of Fabrics, ASTM Standard Test Methods D257-93 for d-c Resistance or Conductance of Insulating Materials, and similar methods, the surface resistivity is determined by means of an electrical resistance meter. For the AATCC method it is recommended that measurements be done at various levels of humidity. The ASTM methods are not suitable for use in measuring the electrical resistivity/conductivity of moderately conductive materials, as in the case of fabrics with conductive fibres such as carbon and stainless steel. Also, Scott (1981) explained that methods which measure the resistivity of fabrics are inadequate as a means of testing the effectiveness of chemical anti-static finishes, and that body voltage or charge measurements are essential to determine the real effects of these additives.

ASTM Standard Test Method D4238-90 for Electrostatic Propensity of Textiles measures the charge induced onto a rotating specimen by a d-c current and its subsequent rate of decay. Federal Test Standard 101C Method 4046, Electrostatic Properties of Materials is used to determine the electrostatic properties of materials in film and sheet form, by measuring the time required to induce a charge on the surface of the material, the intensity and polarity of the charge, and the time required for complete dissipation of the induced charge. In Federal Test Standard 191A Method 5931, Determination of Electrostatic Decay of Fabrics the time it takes for an induced charge on a fabric surface to decay to 10% of the initial level is determined. A number of comments have been made about the interpretation of observations by these methods. FTS 101C Method 4046 is restricted to "homogeneous" and sheet materials and is not applicable to installed surfaces and "non-homogeneous" materials like textiles (Chubb and Malinverni, 1993). When the decay test is applied to non-homogeneous materials with different resistivity layers, a field suppression effect can cause ambiguous measurements (Baumgartner, 1987). Also, a method which requires the flow of charge across the surface from an electrode is not appropriate because this only provides charge flow via the conducting features and does not ensure reliable charging of any relatively insulating features, which is where the charge is likely to be retained (Chubb, 1988). Some fabrics that "pass" a surface resistivity test and/or the charge decay test may still develop high values of tribo-electrification (Owens and Klein, 1990). These comments which were directed at FTS 101C, Method 4046 are also valid for the FTS 191A, Method 5931.

ASTM Standard Test Method for Evaluating Tribo-electric (Static) Charge Generation on Protective Clothing Materials (Draft F23.20.05) has been proposed to overcome the shortcomings of those test methods mentioned above. This method may be used to evaluate the static electrical charge generated by tribo-electrification and the rate of discharge on protective clothing. The National Aeronautics and Space Administration (NASA) has used the system since the late 1960's (Gompf, 1984). Although the method incorporates controlled frictional charging, and we have obtained high reliability in our tests, the charge decay results have given very low correlation with either tribo-electric charge obtained by the method or human-body discharge potentials. Stull (1994) reported that the method is suitable for chemical protective applications, and is aimed for ranking materials rather than predicting electrostatic propensity.

A simple modification of the proposed ASTM method was therefore developed to measure potentials and energies from the discharge of a capacitor which has been previously charged from the tribo-electrification of a fabric system. The system was designed to simulate the phenomenon experienced by a clothed human body which rubs an insulated surface and touches a grounded object generating a spark. It is intended for both single- and multiple-layer fabric systems, and for any humidity level. As a result, the electrostatic propensity of protective clothing systems can be assessed, and standards can be established according to the known minimum ignition energy (MIE) of incendive sparks for different gas mixtures.

Method

This experimental research was conducted under low humidity conditions on multiple-layer specimens of thermal protective fabrics. The independent variables were relative humidity and fabric system, and the dependent variables were peak discharge potential and discharge energy from a resistor/capacitor unit, as well as peak potential on the textile surface and percentage of initial charge decayed at five seconds.

Fabrics

Fabric characteristics are detailed in Table 3.1. The two-layer fabric systems used in the experiment were: 1) FR cotton - 100% non-FR cotton, 2) meta-aramid/carbon - 100% non-FR cotton, 3) meta-aramid/PBI - 100% non-FR cotton, 4) aramid/FR viscose - 100% non-FR cotton, 5) FR cotton - FR cotton, 6) meta-aramid/carbon - meta-aramid/carbon, 7) meta-aramid/PBI - meta-aramid/carbon, and 8) aramid/FR viscose - meta-aramid/carbon. See Appendix 1 for detailed technical information on these fibers. The size of each specimen was 200 x 200 mm, as specified by the proposed ASTM method. Five two-layer specimens were obtained for each

sample, according to standard sampling procedures. Each fabric specimen was washed following CAN/CGSB 4.2 No.58 M90 Colourfastness and Dimensional Change in Domestic Laundering of Textiles, procedure III. Then, all specimens were conditioned according to CAN/CGSB 4.2 No.2 M88 Conditioning Textile Material for Testing inside a 4.12 m x 3.23 m x 3.81 m environmental chamber where the humidity was carefully controlled and monitored at 0% and 20% relative humidity.

TABLE 3.1--Characteristics of fabrics used in the experiment

Fabric	Weave	Count (w x F) (yarns/cm)	Mass (g/m²)
100% (non-FR) cotton	3/1 Twill	37 x 22	210
100% FR cotton	Satin	35 x 19	320
meta-aramid/carbon	Plain	23 x 21	205
meta-aramid/PBI ^a	Plain	26 x 22	145
aramid/FR viscose	Twill	32 x 21	265

^a This non-commercial meta-aramid/PBI fabric has a topical anti-static treatment

Procedures

The modification to the proposed ASTM procedure involves placing a 12 mm conducting aluminium plate ("E" in Figure 3.1), which is connected to a 220 pF capacitor ("J" in Figure 3.1), on the opposite side of the specimen to the rubbing wheel. The value of the capacitor is the average human-body capacitance reported elsewhere (Wilson, 1977/78). A static eliminator² is used at the beginning of the test to eliminate any initial charge in the specimens. During the rubbing process, the charge is accumulated in the capacitor. At the end of the charging process, the conducting plate is disconnected from the specimen, the specimen holder is lowered and an electrometer³ and digital oscilloscope⁴ are activated to measure and record peak potential and charge decay from the fabric surface as in the proposed ASTM method. Then a manual switch

²Simco model 300

³Electro-Tech System model 105

⁴Tektronix model 2430A

is pressed and the resulting discharge through the capacitor is measured through a probe⁵ and recorded by a second digital oscilloscope⁶.

Parts of the Apparatus

- A) Slide for conducting plate
- B) DC motor
- C) Chuck
- D) Rubbing wheel
- E) Conducting plate and wire
- F) Slide for DC motor
- G) Static detecting head
- H) Specimen holder
- I) Switch
- J) RC unit
- K) 3 Lb (1.36 kg) weight stack
- L) Opening
- M) Frame

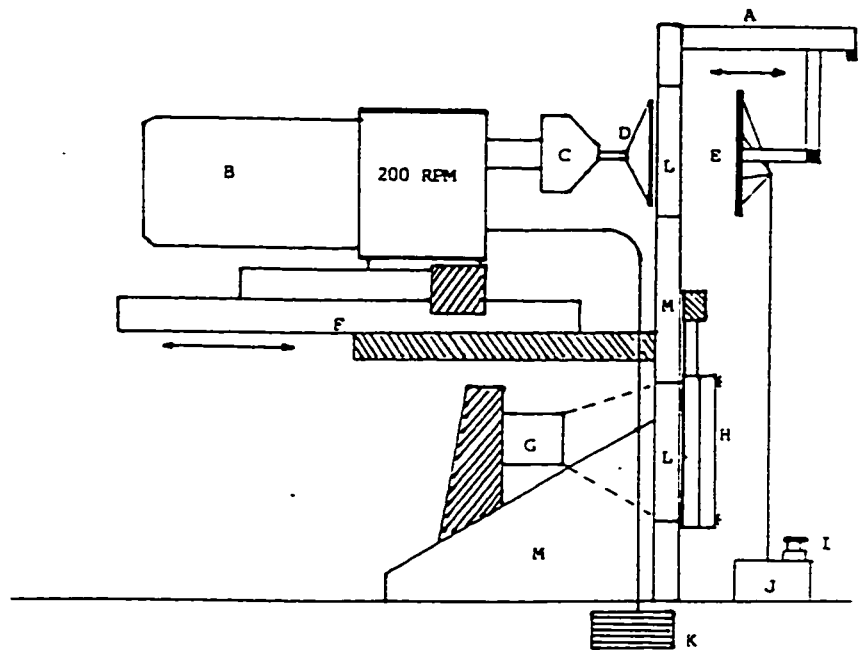


Figure 3.1. Diagram of modified ASTM Method Tribo-electric Test Device

From the recorded waveforms the peak potential is measured and the transferred charge, discharge energy, peak current, duration of the event, and other parameters of interest are calculated. The total charge flow (transferred) Q is calculated by integrating the potential V waveform and dividing this by the grounding resistance:

$$Q = \int idt = (1 / R) \int Vdt \quad \text{Eq. 3.1}$$

The total energy is then determined by calculating half the product of the total charge from Eq. 3.1 and the potential:

$$U = (1/2) QV \quad \text{Eq. 3.2}$$

Data Analyses

Using commercially available, SPSS version 6.1 software, the following statistical analyses were performed, with the level of significance for testing hypotheses set at $p < .05$.

⁵ 10x passive Tektronix model P6109B, impedance 10M Ω

⁶ Tektronix model 320

- 1) Descriptive statistics, to characterize each fabric group with respect to the dependent variables.
- 2) Two-way analysis of variance (ANOVA), to test the null hypothesis that there are no significant differences in peak potential among the different fabric combinations at different humidity levels.
- 3) One-way ANOVA and Duncan's multiple range tests, to determine which fabric groups differ significantly from each other.

Results and Discussion

Two-way ANOVA found significant main effects of fabric system and relative humidity as well as two-way interaction effects on **peak discharge potential and discharge energy** (discharge from capacitor), and on **peak potential and charge decay** (from textile surface), indicating that there are significant differences in these parameters among fabric systems, but that those differences are affected by relative humidity. Thus, the null hypothesis that there are no significant differences among fabric systems at different humidity levels is rejected.

Mean peak potentials from the textile surface and peak discharge potentials from the capacitor for each fabric system at 0 and 20% relative humidity (RH) are plotted in Figures 3.2 and 3.3, respectively, and with very few exceptions show similar trends (i.e. anti-static fabrics yielded lower peak potentials than non-antistatic fabrics), although the magnitude differed and there were slight differences in individual system rankings between the two tests. This trend was also in agreement with that observed in human-body experiments (Crown et al, 1995; Rizvi et al, in press). Results of the one-way ANOVA and Duncan's multiple range test (Table 3.2) generally suggest that for peak discharge potentials from a capacitor and peak potentials from a textile surface, fabric systems differ significantly ($p < .05$) from each other, although there are some homogeneous subsets. Also, results for these parameters suggest that fabric systems can generally be grouped according to the outer layer; therefore, they have been grouped in that way in Table 3.2, and in Figures 3.2 and 3.3.

The fabric systems with the highest peak potentials from the capacitor also showed the lowest percent decay at 5 seconds following the proposed ASTM test at 0% RH (Table 3.2 and Figure 3.4). These results suggest that fabric systems producing low peak potentials may yield fast charge decay, and those systems producing high peak potentials may yield slow charge decay. However, this tendency is not observed at 20% RH, and some researchers have found no correlation between tribo-electric charge and charge decay (Fowler, 1988; Owens and Klein, 1990).

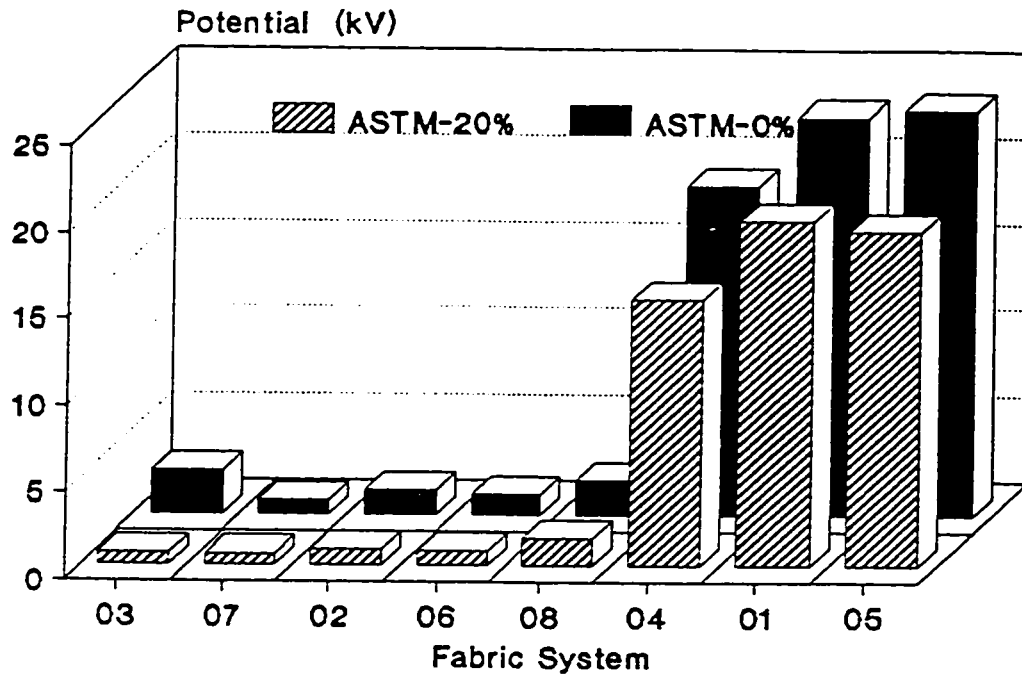


Figure 3.2. Mean peak potential from fabric surface

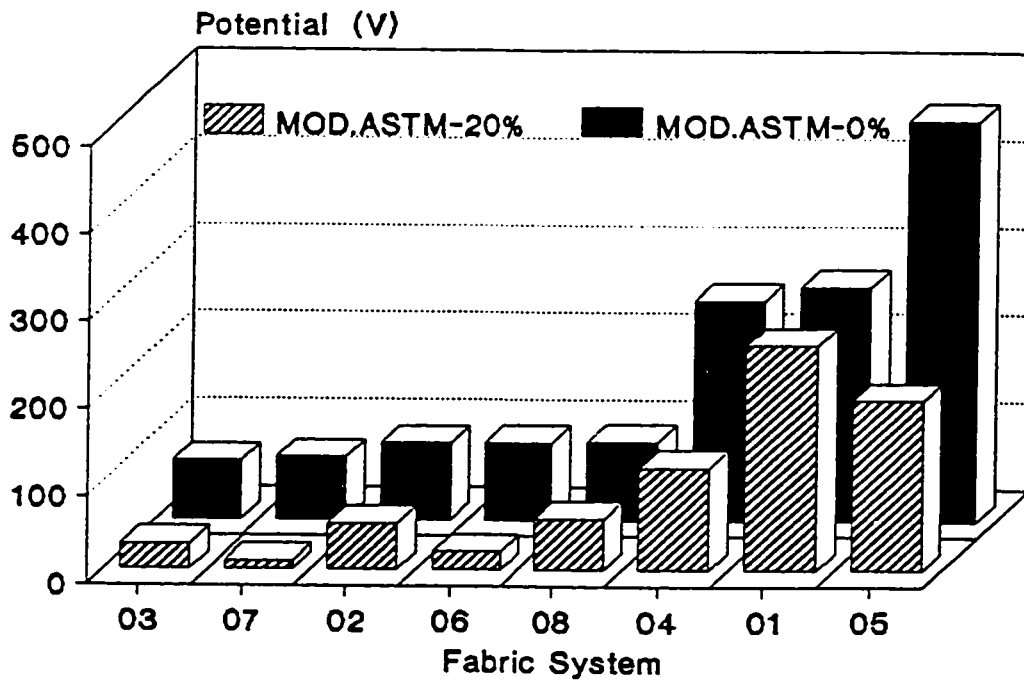


Figure 3.3. Mean discharge potentials from a capacitor

Table 3.2. Analysis of variance: Potentials, energies, and charge decay for two-layer specimens at 0 and 20% RH and 20° C

Code	Fabric System (Outer - Inner)	Modified ASTM						Proposed ASTM						
		Peak Potential (V)		Disch. Energy (nJ)		Peak Potential (kV)		% Decay at 5 s.		Peak Potential (kV)		% Decay at 5 s.		
		Mean	Std. Dev.	Mean	Std. Dev.	Mean	Std. Dev.	Mean	Std. Dev.	Mean	Std. Dev.	Mean	Std. Dev.	
0% RH														
03	aramid /PBI - 100% cotton	67.40 ^a	18.35	2.97 ^a	1.49	2.49 ^c	0.33	8.83 ^c	3.12					
06	aramid/carbon - aramid/carbon	88.80 ^a	24.38	5.15 ^a	2.70	1.17 ^{a,b}	0.12	3.41 ^b	1.00					
02	aramid/carbon - 100% cotton	88.20 ^a	24.84	8.06 ^a	4.85	1.38 ^{a,b}	0.18	5.00 ^a	1.94					
08	aramid/FR viscose - aramid/carbon	89.70 ^a	13.01	4.93 ^a	1.42	2.01 ^{b,c}	0.18	3.32 ^a	0.62					
04	aramid/FR viscose - 100% cotton	252.70 ^b	68.40	42.34 ^b	21.84	19.03 ^d	2.08	2.63 ^a	0.51					
01	FR cotton - 100% cotton	268.20 ^b	62.74	43.43 ^b	19.98	23.08 ^e	1.38	2.30 ^a	1.52					
05	FR cotton - FR cotton	458.40 ^c	96.07	137.50 ^c	57.74	23.47 ^e	1.68	2.07 ^a	1.09					
20% RH														
07	aramid/PBI - aramid/carbon	9.33 ^a	2.05	0.06 ^a	0.02	0.64 ^a	0.20	9.20 ^b	1.82					
03	aramid /PBI - 100% cotton	28.87 ^b	3.20	0.53 ^a	0.11	0.69 ^a	0.19	36.03 ^e	2.93					
06	aramid/carbon - aramid/carbon	20.88 ^{a,b}	5.06	0.29 ^a	0.14	0.79 ^a	0.22	6.63 ^a	1.43					
02	aramid/carbon - 100% cotton	51.95 ^c	8.38	1.69 ^a	0.60	0.87 ^a	0.31	8.91 ^b	1.65					
08	aramid/FR viscose - aramid/carbon	58.45 ^c	3.00	2.11 ^a	0.67	1.54 ^a	0.21	12.49 ^c	0.86					
04	aramid/FR viscose - 100% cotton	117.68 ^d	29.74	9.13 ^b	4.75	15.32 ^b	3.20	32.99 ^d	3.45					
01	FR cotton - 100% cotton	194.68 ^e	18.79	23.99 ^b	4.48	19.34 ^c	1.93	12.96 ^c	1.35					
05	FR cotton - FR cotton	258.20 ^f	22.45	42.19 ^b	7.16	19.96 ^c	2.78	10.24 ^{b,c}	1.76					

a,b,etc In each column, means with the same letter superscript indicate homogeneous subsets (highest and lowest means are not significantly different) when subjected to Duncan's multiple range test ($p < 0.05$)

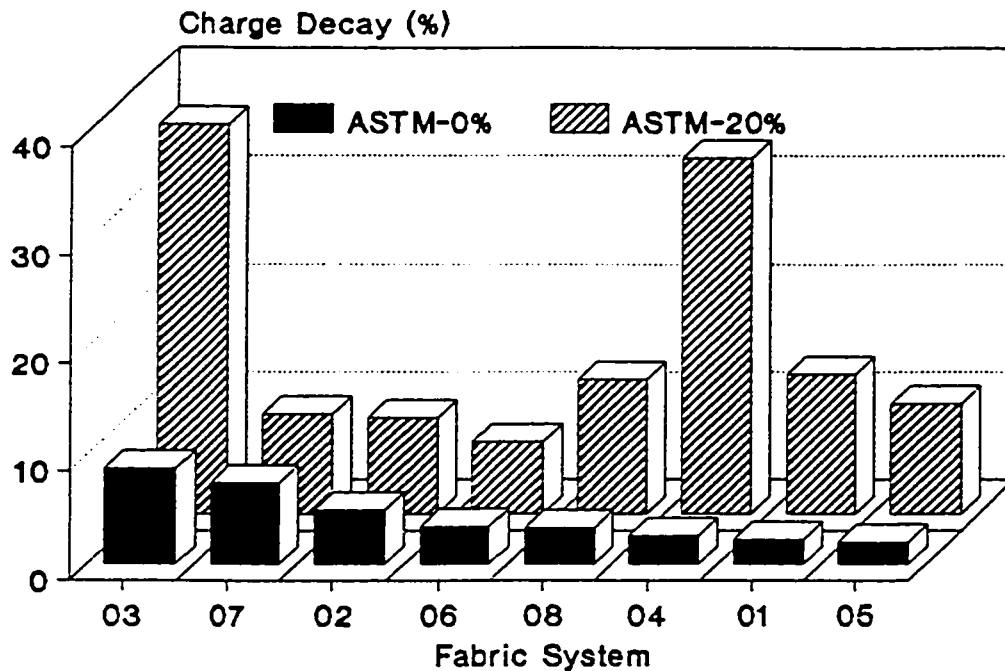


Figure 3.4. Mean charge decays at 5 seconds for proposed ASTM Method F.23.20.05

As in the case of peak discharge potentials, discharge energies at 0 and 20% RH showed similar trends in direction with very few exceptions. Larger homogeneous subsets are observed for discharge energies than for peak discharge potentials, but that could be explained by the fact that variations in both peak discharge potential and transferred charge are incorporated into energy data since energy is calculated from potential and charge.

Conclusions

The proposed ASTM method F23.20.05 was modified to measure potentials and energies from the discharge of a capacitor which has been previously charged from the tribo-electrification of a fabric system. The system was developed to provide: 1) easy evaluation by automatically recorded frictional charge (voltage) and its decay curve, as well as the discharge of a previously charged capacitor, 2) high accuracy and reproducibility, 3) adequate size of specimens, and 4) easy and quick operation.

In general, results for this method were in agreement with other studies and the theory of electrostatics. For example, results showed that anti-static fabrics generated tribo-electric discharge potentials and energies which are smaller in magnitude than non-antistatic fabrics, humidity seemed to have the greatest effect on systems with all cotton inner fabrics, and while

variation of the outer layer in a fabric system seems to have the greatest effect on the variables measured, variation of the inner layer in the system may have a lesser but significant effect, confirming what was observed in previous research (Gonzalez, 1995).

Tribo-electrification is responsible for most electrostatic nuisances and hazards in real-life situations, so it should be the preferred method of charging. In the past, some investigators have reported that tribo-charging is notoriously unreliable and considerable effort may be needed to achieve consistent charging (e.g., Chubb, 1988). The relatively low variation in potential and charge decay data yielded by this test method may be explained by the highly controlled tribo-charging process and environmental conditions maintained during the study.

References

Bailey, A. G., Smallwood, J. M., & Tomita, H. (1991). Electrical discharges from the human body. In B. C. O'Neill, Electrostatics'91 Vol. 118, (pp. 101-106). Bristol, UK: IOP Publishing Ltd.

Ballou, J. W. (1954). Static electricity in textiles. Textile Research Journal, 24(1), 146-155.

Baumgartner, G. (1987). A method to improve measurements of ESD dissipative materials. In EOS/ESD Symposium Proceedings Vol. EOS-9 (pp. 18-27). Rome, NY: The EOS/ESD Association and IIT Research Institute.

Chubb, J. N. (1988). Measurement of static charge dissipation. In J. L. Sproston (Ed.), Electrostatic Charge Migration (pp. 73-81). Bristol, UK: IOP Publishing Ltd.

Chubb, J. N., & Malinverni, P. (1993). Comparative studies on methods of charge decay measurement. Journal of Electrostatics, 30, 273-284.

Crow, R. M. (1991). Static electricity: A literature review (U) (Technical Note 91-28). Ottawa, ON: Defence Research Establishment Ottawa.

Crown, E. M., Smy, P. R., Rizvi, S. A., & Gonzalez, J. A. (1995, June 30). Ignition hazards due to electrostatic discharges from protective fabrics under dry conditions. In Final Report Presented to Alberta Occupational Health and Safety, Heritage Grant Program. Edmonton, AB: University of Alberta.

Crugnola, A. M., & Robinson, H. M. (1959). Measuring and predicting the generation of static electricity in military clothing (Textile series, Report No. 110). Natick, MA: Quartermaster Research & Engineering Command, US Army.

Gompf, R. H. (1984). Tribo-electric testing for electrostatic charges on materials at Kennedy Space Center. In EOS/ESD Symposium Proceedings Vol. EOS-6 (pp. 58-63). Rome, NY: The EOS/ESD Association and IIT Research Institute.

Gonzalez, J. A. (1995). Development of a laboratory protocol to predict the electrostatic propensity of protective clothing systems. Unpublished master's thesis. Edmonton, AB: University of Alberta.

Hidson, D. J. (1976). Electrostatic ignition energies of common fuels: A review of some relevant literature (U) (DREO Memo 18/76). Ottawa, ON: Defence Research Establishment Ottawa.

McLean, H. T. (1955). Electrostatic charges on fabrics. American Dyestuff Reporter, 44(15), 485-489.

Owens, J. E., & Klein, W. G. (1990). The hidden hazard of "static-dissipative" garments in clean rooms. In EOS/ESD Symposium Proceedings Vol. 12 (pp. 41-44). Rome, NY.

Rizvi, S. A. H., Crown, E. M., Osei-Ntiri, K., Smy, P. R., & Gonzalez, J. A. (1995). Electrostatic characteristics of thermal-protective garments at low humidity. Journal of The Textile Institute, 86(4), 549-558.

Scott, R. A. (1981). Static electricity in clothing and textiles. Thirteenth Commonwealth Defence Conference on Operational Clothing and Combat Equipment, (Malaysia). Colchester, UK: Stores and Clothing Research and Development Establishment.

Stull, J. (1994). Measuring static charge generation on PC materials. Safety & Protective Fabrics, 2 (8), 24-26.

Teixeira, N. A., & Edelstein, S. M. (1954). Resistivity: One clue to the electrostatic behavior of fabric. American Dyestuff Reporter, 43(7), 195-208.

Wilson, D. (1963). The electrical resistance of textile materials as a measure of their anti-static properties. Journal of The Textile Institute, 54, 97-105.

Wilson, N. (1983). The ignition of natural gas by spark discharges from the body. In B. C. O'Neill, Electrostatics'83 Vol. 66, (pp. 21-27). Bristol, UK: IOP Publishing Ltd.

Wilson, N. (1977/78). The risk of fire or explosion due to static charges on textile clothing. Journal of Electrostatics, 4, 67-84.

Chapter 4. Modelling of Surface Charge Dissipation on Thermal Protective Fabrics¹

Preamble

There are many difficulties inherent in measuring and interpreting resistivity of textile materials. Charge migration may vary with remaining electrical stress which is affected by geometric shapes, non-linear and non-homogeneous structures, and non-ohmic behaviour of most insulating and semi-insulating materials (Baumgartner, 1984 and 1987; Chubb, 1987 and 1988; Fowler, 1989; Taylor and Secker, 1994). This has made the direct measurement of charge decay from a material surface a much more attractive option for characterizing its dissipative properties.

This chapter describes the development of theoretical models and numerical techniques for predicting the charge dissipation of fabric systems considering decay as a function of time and time constant. Charge decay results for two-layer systems from tests following the proposed ASTM Method correlated well ($R > .90$) with the exponential model of the form $V = V_0 \exp(-t/\tau)$. Time constants for various fabrics that comprise the different fabric systems were also calculated and compared to those determined during previous small-scale experiments.

Introduction

The ease of charge migration on materials has normally been assessed by measurements of surface or volume resistivity. Such measurement is not an appropriate approach with many textile materials for the following reasons: i) conduction may vary with the remaining electrical stress in the material (i.e. the material does not obey Ohms Law); ii) the material surface is non-homogeneous (e.g., conduction is provided by localized conducting fibres); and iii) charge migration may be affected by the initial distribution of charge and by geometric effects, for example the proximity of earthed surfaces (Chubb, 1987).

A more appropriate general approach for assessing the charge migration of insulating and semi-insulating textile materials is to examine directly how quickly static charges scatter on the material surface and/or the surroundings. This involves generating (tribo-charging) or depositing some static charge on the surface (corona charging), and then measuring how quickly

¹The paper: "Gonzalez, J. A., Rizvi, S.A.H., Crown, E.M., & Smy, P.R. (1997). Mathematical modelling of electrostatic propensity of protective clothing systems. In The Proceedings of the 19th EOS/ESD Symposium 1997 (pp. 153-161), Santa Clara, CA", was based in part on this chapter.

this charge is dissipated until the surface potential or charge density falls to an acceptably low value.

There are substantial differences in the ways in which a charge is neutralized. Dissipation depends on whether charge is located on an insulated conductor or on an intrinsically insulative material. In both cases, there are even greater differences that depend on whether the neutralization is caused by charge carriers already present or if these are being created by the process itself. Furthermore, it is important to differentiate clearly between the terms "charge decay" and "electrostatic discharge" to avoid confusion. The former is used for the neutralization processes, which are not based on a change of the conductivity of the conducting medium, and the latter is reserved for processes involving breakdown and ionization.

If a charge is located on an insulator surface there is in principle no way by which the charge may ever be removed. If, however, the charged insulator is completely surrounded by a conducting fluid such as air, in contact with all points of the surface, the charge may be neutralized by oppositely charged ions being attracted to the insulator (Jonassen, 1991). The rate of charge decay seems to depend on grounding conditions, material bulk, and moisture content of both ambient air and textile surface (Onogi et al, 1996). These authors and others (Chubb, 1988; Das-Gupta, 1988; etc.) have modelled charge dissipation from single-layer materials and incorporated some of the variables mentioned above, but there has been no attempt to model decay of charge from multiple-layer non-homogeneous materials.

Modelling Charge Decay

If the rate of charge dissipation into the air is linearly proportional to the charge density on the surface (i.e. a first-order "reaction"), the static charge at t seconds after rubbing can be expressed by the following equation:

$$V = V_0 e^{-t/\tau} \quad \text{Eq. 4.1}$$

where V_0 is the charge at $t=0$ s after rubbing (peak potential), and τ is the time constant (rate of charge dissipation); the time constant for a single layer is determined by

$$\tau = (\epsilon_0 KAR) / d \quad \text{Eq. 4.2}$$

(Haase, 1977), where R is the square of the resistivity² of the fabric, K is the dielectric constant (relative permittivity $=\epsilon/\epsilon_0$), A is area of the specimen, and d is its thickness. Table 4.1 shows time constants determined for single-layer fabrics that make up the different two-layer systems,

²Surface resistivity data were used for calculations, but it seems that using volume resistivity would be more appropriate. Due to equipment limitations, only surface resistivity measurements could be obtained.

and for those systems, as well as regression coefficients (R^2) values from analyses of the fit of empirical data to the exponential model. Fabric systems have been ordered in descending order in terms of charge decay.

Table 4.1. Peak potentials, charge decays, time constants and regression coefficients (R^2) following proposed ASTM Method F23.20.05^a at 0 and 20% RH

Fabric System (Outer - Inner Layer)	Peak Potential (kV)	Charge Decay^b (%)	Time Constant (s)	R^2
0% RH				
Single-Layer Systems				
meta-aramid/PBI ^c	2.13	8.45	62.62	.8982
meta-aramid/carbon	1.28	5.47	106.00	.9014
meta-aramid/FR viscose	20.86	2.92	198.97	.9201
100% cotton	23.60	2.12	276.24	.8982
FR cotton	25.48	1.61	365.36	.8788
Two-Layer Systems				
meta-aramid/PBI - 100% cotton	2.49	8.84	55.77	.9819
meta-aramid/PBI - meta-aramid/carbon	0.83	7.23	79.16	.9109
meta-aramid/carbon - 100% cotton	1.38	5.07	120.50	.8452
meta-aramid/FR viscose - aramid/carbon	2.01	3.48	157.43	.9444
meta-aramid/carbon - aramid/carbon	1.17	3.42	170.88	.8302
meta-aramid/FR viscose - 100% cotton	19.03	2.63	190.80	.9280
FR cotton - 100% cotton	23.08	2.25	267.09	.8627
FR cotton - FR cotton	23.47	2.09	260.82	.9065
20% RH				
Single-Layer Systems				
meta-aramid/PBI	0.93	34.16	11.81	.9901
meta-aramid/FR viscose	12.14	26.09	16.44	.9989
100% cotton	16.10	9.24	52.97	.9970
FR cotton	14.18	6.74	71.53	.9992
meta-aramid/carbon	0.72	6.07	81.69	.9984
Two-Layer Systems				
meta-aramid/PBI - 100% cotton	0.69	36.03	11.57	.9884
meta-aramid/FR viscose - 100% cotton	15.32	32.99	12.45	.9991
FR cotton 100% cotton	19.96	12.96	37.68	.9916
meta-aramid/FR viscose - aramid/carbon	1.54	12.49	48.83	.9865
FR cotton - FR cotton	19.34	10.24	48.10	.9883
meta-aramid/PBI - meta-aramid/carbon	0.64	9.20	53.62	.9687
meta-aramid/carbon - 100% cotton	0.87	8.91	59.90	.9686
meta-aramid/carbon - aramid/carbon	0.79	6.63	80.42	.9588

^a Using vinyl rubbing wheel ^b Percentage of charge decay at five seconds

^c This non-commercial meta-aramid/PBI fabric has a topical anti-static treatment

It can be observed from Table 4.1 that both single- and two-layer fabric systems generally show similar trends in magnitudes of peak potential and time constant at 0% RH with a few exceptions, and opposite trend in charge decay. Therefore, it can be stated that the lower the peak potential a fabric system generates, the faster its charge decay at 0% RH. Those fabric systems with aramid/PBI and aramid/carbon fabrics, considered anti-static ones, yielded the lowest peak potentials and the fastest charge decays. But these observations differ at 20% RH.

Fabric systems show different trends in magnitude of peak potential and time constant at 20% RH, and the statement given in the previous paragraph that the lower the peak potential, the faster the charge decay is no longer valid. It can be seen from Table 4.1 that those fabric systems with cellulose-based fabrics yielded the fastest charge decays, although the lowest peak potentials were generated by those systems with fabrics considered anti-static. In both cases at 0 and 20% RH, regression coefficients (R^2) show strong fit between empirical data and the exponential model of the form $V = V_0 \exp(-t/\tau)$, confirming what other investigators have previously reported (Wilson, 1963; Jonassen, 1991; Onogi et al, 1996).

Different charge decay curves for two-layer systems were plotted using the exponential model and with values at 20% RH (Figure 4.1). The vertical axis Potential (kV) at the left side of the Figure 4.1 corresponds to the fabric systems with the word (*LEFT*) underneath, and the one at the right side corresponds to the systems with the word (*RIGHT*) underneath. It can be

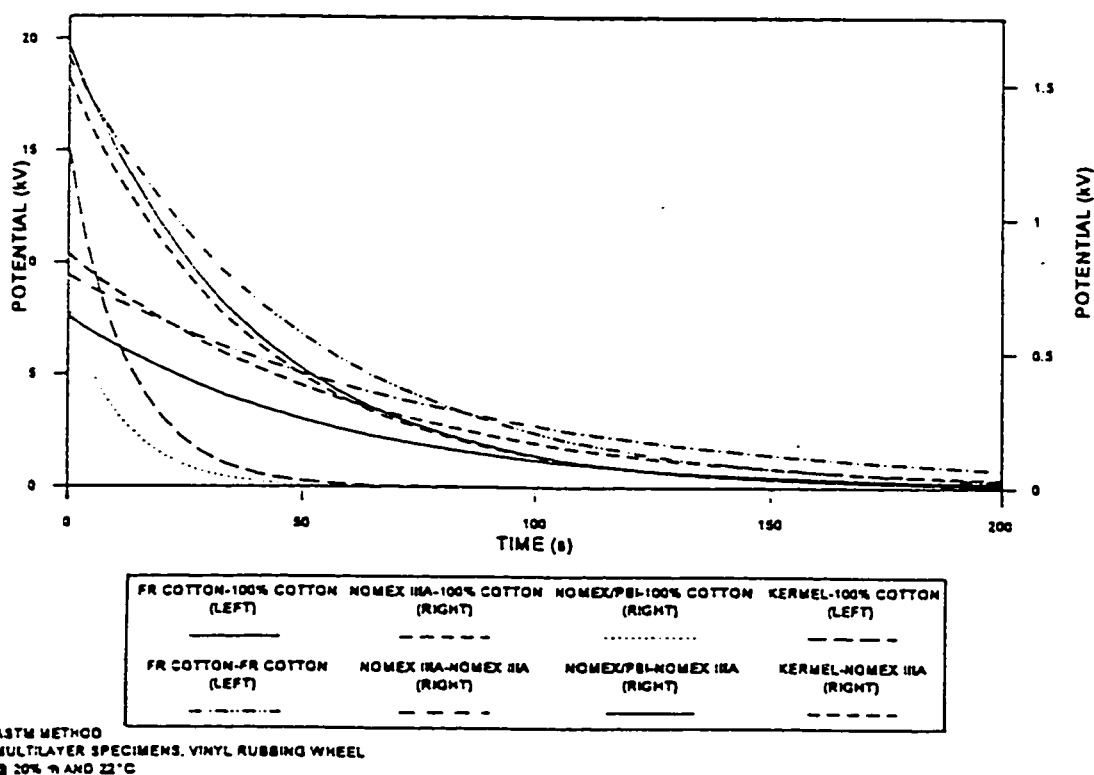


Figure 4.1. Charge decay curves for different fabric systems at 20% RH

observed that those systems with cellulose-based fabrics and/or anti-static finish decay to zero in less than 100 seconds, but the rest of the systems decays in more than 175 seconds.

Most previous research has dealt with charge decay of single layer materials, for example, a textile surface (Ramer and Richards, 1968; Taylor and Elias, 1987; Jonassen, 1991; Chubb and Malinverni, 1993; Onogi et al, 1996, Onogi, Sugiura and Matsuda, 1977). The current research focuses on two-layer systems where there is a suppression effect of the charge on the outer layer caused by an inductively charged inner layer. Thus, charge decay in two layers of fabric tested together differs from their charge decay values as single layers, and there is a corresponding change in time constant of the system (Table 4.1). In the case of testing a two-layer system following the proposed ASTM method, the variation in time constant from single to two-layer systems can be explained as follows: If τ_1 = time constant of outer layer (as single layer), and τ_2 = time constant of a two-layer system, measured from outer layer, and there is no change in fabric-system capacitance ($C = \epsilon_0 KA/d$); the change in τ is given by a change in resistivity as the fabric system becomes a two-resistor in parallel system. The total resistivity of the system would be:

$$R_T = \frac{(R_1)(R_2)}{R_1 + R_2} \quad \text{Eq. 4.3}$$

where R_1 is the resistivity of the outer layer and R_2 is the resistivity of the inner layer. Therefore, a new relationship can be established combining equations 4.2 and 4.3:

$$\text{If } \tau_1 = \frac{(\epsilon_0 KAR_1)}{d} \text{ and } \tau_2 = \frac{(\epsilon_0 KAR_T)}{d}, \text{ therefore:}$$

$$\frac{\tau_1}{R_1} = \frac{\tau_2}{R_T}$$

Eq. 4.4

Comparison Between Calculated and Observed Charge Decay Results

Equation 4.4 can be used to determine the charge decay rate of a two-layer system from single-layer testing, knowing the resistivity of both layers. The time constant τ_2 of the system, calculated using equation 4.4, can then be incorporated in equation 4.1 to determine the charge decay of a two-layer system at any specified time.

Substituting data in equations 4.2 and 4.4, time constants were calculated for single- and two-layer fabric systems. These values are compared to values determined from empirical data in Table 4.2. Time constants calculated using equation 4.2, although not identical, followed the same trend as those calculated from empirical data.

Table 4.2. Calculated time constants for various fabric systems at 0 and 20% RH ^a

Fabric System (Outer - Inner Layer)	Resistivity ^b		Calculated Time Constant (s)	
	Outer	Inner	From Eq. 4.2	From Empirical Data
0% RH				
meta-aramid/PBI - 100% cotton	2.52	21.89	56.14	55.77
meta-aramid/FR viscose-100% cotton	10.72	21.89	133.58	190.80
FR cotton - 100% cotton	15.63	21.89	213.14	267.09
FR cotton - FR cotton	15.63	15.63	182.68	260.82
20% RH				
meta-aramid/PBI - 100% cotton	0.18	1.13	10.19	11.57
meta-aramid/FR viscose-100% cotton	0.43	1.13	11.95	12.45
FR cotton - 100% cotton	1.39	1.13	32.27	37.68
FR cotton - FR cotton	1.39	1.39	35.77	48.10

^a Other fabric systems were not evaluated because aramid/carbon fabrics are not suitable for current resistivity tests

^b Surface resistivity data following AATCC Test Method for Electrical Resistivity of Fabrics (76-1989)

Discussion and Conclusions

Several mathematical equations related to charge dissipation processes have been developed. Charge decay parameters for 2-layer systems, calculated from the equations using data from single-layer measurement, fit well with empirical data from the same two-layer systems. In using data from single-layer testing, some negative effects observed during testing of charge decay, for example when charge flows only through conductive features of the specimen (Chubb, 1988), or a field suppression effect caused when non-homogeneous materials with different resistivity layers are used (Baumgartner, 1987), can be avoided and more reliable results may be achieved. With the use of the numerical technique presented here, one can reliably and accurately determine a static parameter to characterize multi-layer fabric systems.

Static charge is known to discharge between two bodies in the air by so-called electrostatic spark when the electric field between them is higher than 2.7 MV/m. However, electrons cannot be emitted from the surface to air without higher energy for the emission. In the case of testing following the proposed ASTM Method F23.20.05, electron emission from the fabric surface cannot be the cause of charge dissipation because there is no air breakdown during the event. From experimental results and theoretical considerations, it may be assumed that water molecules and ion population on the surface and in air play an important role in

neutralizing the static charge. Equations 4.2 and 4.4 take into account all these three conditions since resistivity measurements are also affected by those conditions.

The variations in trend that fabric systems show at 0 and 20% RH in Table 4.1 may be explained by the moisture content on the surface of the fabrics and in air. At 0% RH, there is no moisture in either ambient air or the textile, hence the charge may only be neutralized by oppositely charged ions in air and on the surface which are attracted to the insulator. Since a static eliminator is applied for 30 s at the beginning of the test, it may be assumed that the actual ionic population is minimal causing the dissipation process to be very slow. On the other hand, the ionic population increases around 20% RH since a small amount of moisture is found in air and a mono-layer of water molecules is developed on the textile surface (Sereda and Felman, 1964). This moisture may contribute with ions to the total ionic population already existing in air for a faster dissipation of the static charge.

Therefore, these two assumptions may explain why non-cellulose anti-static fabrics show the fastest charge decays at 0% RH as dissipation depends solely, in this case, on the anti-static mechanisms of the fabrics, but the cellulose-based fabrics rely on few oppositely charged ions available in air and on the surface to dissipate charge. At 20% RH, those systems with cellulose-based fabrics begin to absorb moisture at a higher rate than aramid fibers. This absorbed moisture increases the ionic population on the surface and may speed up the neutralization process, and therefore these systems yield faster decays than aramid-based fabrics. It seems that the topical anti-static finish on aramid/PBI increases its moisture content as well, as the system with this fabric combined with 100% cotton showed the fastest decay at 20% RH.

The equations developed here show the strong relationship between charge decay and resistivity of textile materials which has been the focus of several studies (Ramer and Richards, 1968; Jonassen, Hansson and Nielsen, 1979; Taylor and Elias, 1987). Although it is generally accepted that insulative materials such as textiles do not obey Ohms Law, it seems that the effect of multi-layer resistivity can be determined by Eq. 4.3, something that resistivity tests can not achieve.

When the time constant of the outer layer (τ_1) defined by Eq. 4.2 is substituted into equation 4.4, the time constant of the fabric system is: $\tau_T = \epsilon_0 K A R_T / d$, which is the general equation for time constant ($\tau = RC$). This means that the time constant of a fabric system is the product of the total resistance of a two-resistor in parallel system and the capacitance of the outer layer. Therefore, the influence of the inner layer, namely a suppression effect, is represented only for the change of the resistivity of the assembly.

References

- AATCC. (1989). AATCC Committee RA32. Electrical Resistivity of Fabrics (76-1989). Research Triangle Park, NC: American Association of Textile Chemists and Colourists.
- Baum, E. A., Lewis, T. J., & Toomer, R. (1977). Decay of electrical charge on polyethylene films. Journal of Physics D: Applied Physics, 10, 487-496.
- Baumgartner, G., & Havermann, R. (1984). Testing of electrostatic materials: Fed. Std. 101C. Method 4046.1. In EOS/ESD Symposium Proceedings Vol. EOS-6 (pp. 97-103). Rome, NY: The EOS/ESD Association and IIT Research Institute.
- Chubb, J. N. (1988). Measurement of static charge dissipation. In J. L. Sproston (Ed.), Electrostatic Charge Migration (pp. 73-81). Bristol, UK: IOP Publishing Ltd.
- Chubb, J. N. (1996). Corona charging of practical materials for charge decay measurements. Journal of Electrostatics, 37, 53-65.
- Chubb, J. N., & Malinverni, P. (1993). Comparative studies on methods of charge decay measurement. Journal of Electrostatics, 30, 273-284.
- Fowler, S. L. (1989). Surface resistivity and static decay do not correlate. In EOS/ESD Symposium Proceedings Vol. EOS-11 (pp. 7-11). Rome, NY: The EOS/ESD Association and IIT Research Institute.
- Haenen, H. T. M. (1975). The characteristic decay with time of surface charges on dielectrics. Journal of Electrostatics, 1, 173-185.
- Haenen, H. T. M. (1976). Experimental investigation of the relationship between generation and decay of charges on dielectrics. Journal of Electrostatics, 2, 151-173.
- Jonassen, N., Hansson, I., & Nielsen, A. R. (1979). On the correlation between decay of charge and resistance parameters of sheet materials. In B. C. O'Neill, Electrostatics'79 Vol. 48 (pp. 215-224). Bristol, UK: IOP Publishing Ltd.
- Jonassen, N. (1991). Electrostatic decay and discharge. In EOS/ESD Symposium Proceedings Vol. EOS-13 (pp. 31-37). Rome, NY: The EOS/ESD Association and IIT Research Institute.
- Löbel, W. (1987). Antistatic mechanism of internally modified synthetics and quality requirements for clothing textiles. In B. C. O'Neill, Electrostatics'87 Vol. 85 (pp. 183-186). Bristol, UK: IOP Publishing Ltd.
- Onogi, Y., Sugiura, N., & Nakaoka, Y. (1996). Dissipation of tribo-electric charge into air from textile surfaces. Textile Research Journal, 66, 337-342.
- Onogi, Y., Sugiura, N., & Matsuda, C. (1997). Temperature effect on dissipation of tribo-electric charge into air from textile surfaces. Textile Research Journal, 67, 45-49.
- Ramer, E. M., & Richards, H. R. (1968). Correlation of the electrical resistivity of fabrics with their ability to develop and to hold electrostatic charges. Textile Research Journal, 38, 28-35.

Sereda, P. J., & Feldman, R. F. (1964). Electrostatic charging on fabrics at various humidities. Journal of The Textile Institute, 55, 288-298.

Superintendent of Documents (1969). Electrostatic properties of materials. (Federal Test Method Standard 101B, Method 4046). Washington, DC: Government Printing Office.

Superintendent of Documents (1990). Determination of electrostatic decay of fabrics (Federal Test Method Standard 191A, Method 5931). Washington, DC: Government Printing Office.

Taylor, D. M., & Elias, J. (1987). A versatile charge decay meter for assessing antistatic materials. In B. C. O'Neill, Electrostatics'87 Vol. 85 (pp. 177-181). Bristol, UK: IOP Publishing Ltd.

Taylor, D. M., Owen, D. R., & Elias, J. (1987). An instrument for measuring static dissipation from materials. Journal of Electrostatics, 19, 53-64.

Wilson, D. (1963). The electrical resistance of textile materials as a measure of their anti-static properties. Journal of The Textile Institute, 54, 97-105.

Chapter 5. Modelling the Static Charge Transfer and Measurement on Thermal Protective Fabric Systems During Small-Scale Testing¹

Preamble

This chapter describes the development of different mathematical models to explain charge transfer between layers of fabric, and to calculate charge, expressed as potential difference, on a textile surface and from the discharge of a capacitor. Mathematical equations considering peak potential as a function of fabric system, humidity and temperature have been developed. Results from calculations using those equations correlated well with data from tests based on the proposed ASTM Standard Test Method for Evaluating Tribo-electric (Static) Charge Generation on Protective Clothing Materials (F23.20.05). Additional equations derived to predict peak discharge potential from a capacitor such as a clothed human body produced good agreement with data from tests following a modified ASTM Method F23.20.05.

Introduction

The charge on the surface of a material can apply a force on another charged objects in its vicinity. This ability to act at a distance is explained by introducing the concept of an electric field surrounding charged objects. Free electrons will be accelerated by the forces applied to them by the field. At high electric field strengths, these electrons will collide with and excite the electrons of the molecules in the air. As a result, the energy of the collisions can strip the electrons off the molecules causing a cascade effect that breaks down the electrical resistance of the air. The result is a spark (ESD) or a series of sparks.

At the most basic level, contact or frictional charging is a simple phenomenon. When two different but electrically neutral materials come into contact, charges must transfer from one surface to the other in order to bring the contacting materials into thermodynamic equilibrium. If the surfaces are separated sufficiently quickly and the two materials remain isolated from earth they will retain these excess charges. Several studies have been carried out to know more about the nature of this phenomenon and to develop models for explaining it.

Hersh and Montgomery (1956) found that the direction of charge transfer was determined by the relative position of the Fermi levels in two contacting materials, and that the Fermi level depended not only on chemical composition, but also on temperature and on the

¹The paper: "Gonzalez, J. A., Rizvi, S A H., Crown, E. M., & Smy, P. R. (1997). Mathematical modeling of electrostatic propensity of protective clothing systems. In The Proceedings of the 19th EOS/ESD Symposium 1997 (pp. 153-161), Santa Clara, CA", was mainly based on this chapter.

detailed molecular structure. They stated that Fermi energy for an insulator is about half the sum of the ionization energy² and the electron affinity³ in the case of long chain molecules. Chowdry and Westgate (1974) found that the charge transferred in a metal-insulator contact was dependent on the work function difference between the metal and the insulator. This indicates that electron transfer is the mechanism responsible for the charging.

Shinohara, Yamamoto, Anzai and Endo (1976) reported that the magnitude and sign of electrostatic charges of polymers were determined by internal conditions such as the chemical structure, orientation, crystallinity, surface state of materials, and impurities, as well as by external conditions such as the atmosphere, and the method of electrification. They found that the maximum charge changes from positive to negative as the substituents of the polymer chain change from electron-releasing to electron-attracting. The charging sign changes as the nature of polar group changes.

Lowell (1976) found that the charge transferred by a single non-sliding contact to a metal was independent of the metal work function. If, however, the contact was repeated many times, or if sliding occurs, then the charge depended on the metal work function. Also, he reported that the observed charge increase was associated with the mechanical deformation of the polymer which occurs during contact with the hard metals. The charge in the polymer would increase towards the equilibrium value during the short intervals of deformation-induced conductivity. If the duration of the deformation was not sufficient to allow equilibrium to be reached in a single contact, the charge would increase as a result of subsequent contacts. The charge was eventually saturated at the value given by the condition for thermodynamic equilibrium; this saturation charge depended on the metal Fermi level, although not linearly. Furthermore, Ohara (1979) observed that the basic process of contact or frictional electrification was the process in which segments of polymer molecules, brought to the surfaces by thermal motion, approach or mutually contact causing charge transfer between both surfaces. Peaks of charge were observed in the temperature and friction speed-dependence of frictional electrification, as friction speed determines the number of close contacts and separations between molecules on the two surfaces in a unit time.

Taylor and Secker (1994) stated that charge transfer from metals to insulators could be explained in terms of electron transfer from a solid of low work function to one of higher work function. They also stated that the contacts between one insulator and another may readily be described by electron transfer in much the same way as metal-insulator contacts. They reported

²Ionization energy is defined as the amount of energy required to remove the electron from an atom or ion.

³Electron affinity of a semiconductor is defined as the energy difference between the bottom of the conduction band and the vacuum level (Taylor and Secker, 1994, p. 88).

evidence for the existence of polymer work function (equilibrium Fermi energy), also presented by Davies (1970) and by Gallo and Lama (1976).

Textile materials which make up clothing are good insulators when they are dry and can build up large charges. They eventually discharge to a lower potential as described in the previous chapter. But charged clothing can induce a charge on the body. As someone slides across a car seat to get out of a car, a charge is built up on the clothing which then induces a charge on the body (Rizvi et al, 1995). When the person touches the car metallic door, the electric field near the finger tips exceeds the breakdown value and electrons flow as a spark to or from the car frame to neutralize the induced charge on the body (Wilson, 1979).

These events tend not to occur at high humidities because textile materials absorb moisture from the atmosphere and become good conductors of electricity. Thus, when areas of two fabrics rub together, the areas of separated charge are in electrical contact and electrons flow to neutralize static charges.

Most previous research has dealt with the generation of charge and/or the subsequent discharge from a surface or a person, but no relevant literature was found regarding transfer of charge between layers. The developed mathematical models reported here are aimed at explaining how charge is transferred from an outer layer to an inner layer, and how to determine the amount of either surface charge expressed as potential difference (proposed ASTM Method F23.20.05), or discharge potential from a capacitor (modified ASTM Method).

Modelling Electrostatic Propensity

In the development of the mathematical models for two-layer fabric systems, peak potentials are considered a function of fabric system, humidity, and temperature, according to the following general form:

$$V = f(V_S, V_H, V_T)$$

Where:

V = predicted peak potential for a two-layer system,

V_S = fabric system effect on peak potential,

V_H = humidity effect on peak potential, and

V_T = temperature effect on peak potential

Equations have been derived from this general form to determine both peak potential from a textile surface and peak discharge potential from a capacitor, and were tested using empirical data.

System Component: Mathematical Model for a Two-Layer System Following ASTM Draft Method No. F23.20.05

The electrostatic process inherent to this method comprises three different phases: i) tribo-electrification of the outer-layer fabric by rubbing wheel, ii) induced charging by contact of inner-layer fabric by outer layer, and iii) measurement of discharge potential from the surface of the fabric.

During the second phase, the charging of the inner layer begins at the same time as the tribo-electrification of the outer layer. In Figure 5.1a, both the rubbing wheel and fabric system are at $DV = 0$ after a de-ionization process. Then, in Figure 5.1b the rubbing wheel rubs the outer fabric, where most of the energy, converted from friction work done at the interface, dissipates as heat and only a very small amount is converted into electrical energy (Harper, 1967). In Figure 5.1c, both the rubbing wheel and the fabric system become charged with equal but opposite charge. Since during the event there is no separation at the interface but rubbing occurs between two layers of fabric, their electrification is rather complicated.

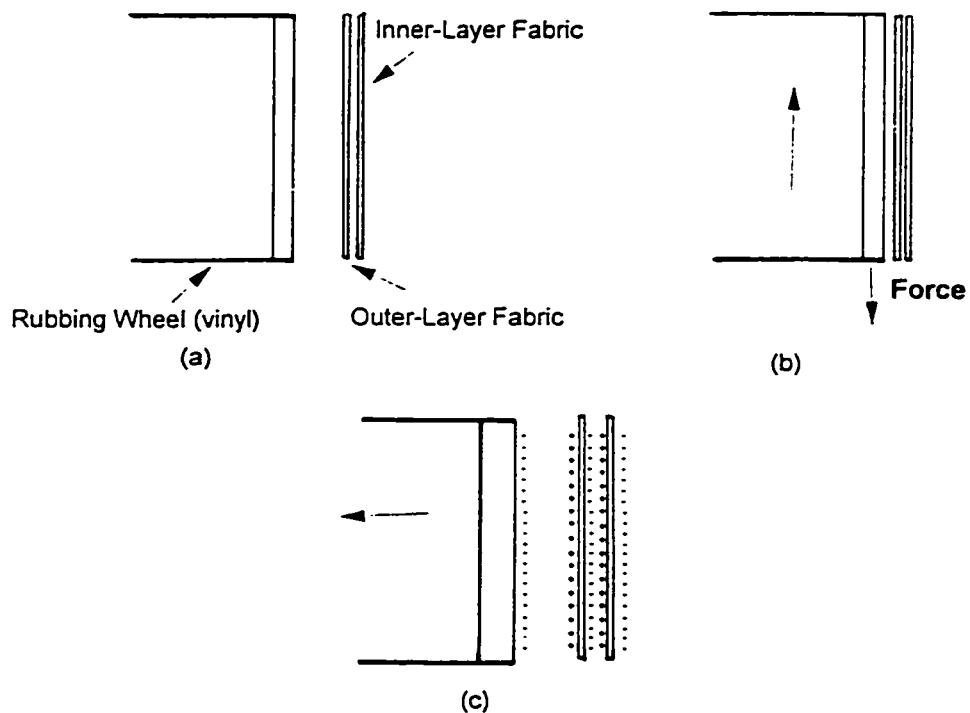


Figure 5.1. (a) Before rubbing process. (b) Tribo-electrification stage. (c) After rubbing

The system component of the peak potential equation for modelling the process following the proposed ASTM Method is based on measurement of charge on a textile surface and implies insulator-insulator contact only. Potential difference of a uniformly charged insulator (Figure 5.2) may be determined as follows:

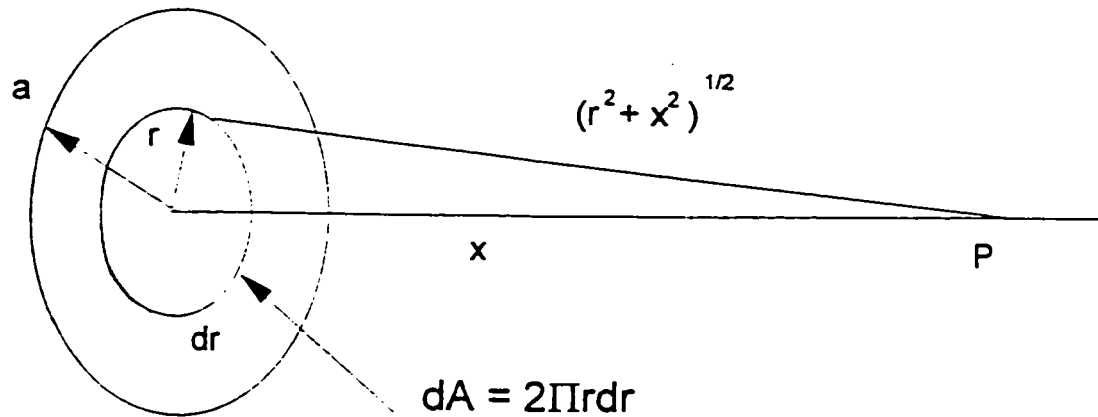


Figure 5.2. Measuring charge from a uniformly charged insulator

The measurement of the electrical potential is along the axis of a uniformly charged disk of radius a and charge density σ . The potential dV at some point P due to the charge element dq is given by:

$$dV = k \frac{dq}{r} \quad \text{Eq. 5.1}$$

Then, the disk is divided into a series of charged rings with a radius r and width dr , as indicated in Figure 5.2. The area of the ring is

$$dA = 2\pi r dr$$

and the charge on the ring is $dq = \sigma dA = \sigma 2\pi r dr$. Hence, the potential at the point P due to this ring is derived from Eq. 5.1

$$dV = \frac{k\sigma 2\pi r dr}{\sqrt{r^2 + x^2}} \quad \text{Eq. 5.2}$$

To find the total potential at P , all rings making up the disk are added up, i.e. integrating dV from $r = 0$ to $r = a$.

$$V = \pi k \sigma \int_0^a \frac{2r dr}{\sqrt{r^2 + x^2}} = \pi k \sigma \int_0^a (r^2 + x^2)^{-1/2} 2r dr$$

The solution for this integral is

$$V = 2\pi k\sigma(\sqrt{a^2 + x^2} - x) \quad \text{Eq. 5.3}$$

But $k = (4\pi\epsilon_0)^{-1}$. Then, the equation 5.3 becomes:

$$V = \frac{\sigma}{2\epsilon_0}(\sqrt{a^2 + x^2} - x) \quad \text{Eq. 5.4}$$

Equation 5.4 calculates the total potential on the surface of the outer layer. For the transfer of charge from the outer layer to the inner layer, three assumptions must be taken into account: i) there is a full contact between layers, ii) there is a change in the medium through which charge will be transferred from outer to inner layer, and iii) the distance x becomes t , the thickness of the inner fabric. Therefore, the equation 5.4 becomes:

$$V_1 = \frac{\sigma_1}{2\epsilon}(\sqrt{a^2 + t^2} - t)$$

Where: ϵ is the permittivity, σ_1 is the surface charge density, and t the thickness of the inner layer. But $\epsilon = K\epsilon_0$, then:

$$V_1 = \frac{\sigma_1}{2K\epsilon_0}(\sqrt{a^2 + t^2} - t) \quad \text{Eq. 5.5}$$

Equation 5.5 calculates the charge on the inner layer induced by the charged outer layer. This induced charge on the inner layer will cause a suppression effect on the initial charge generated by tribo-electrification on the outer layer and calculated by equation 5.4. The final potential on the outer layer will be:

$$V_p = \frac{\sigma_2}{2\epsilon_0}(\sqrt{a^2 + x^2} - x) \quad \text{Eq. 5.6}$$

Where: σ_2 is the surface charge density on the outer layer. But $\sigma_2 = CV_1/A$; then, equation 5.6 becomes:

$$V_p = \frac{CV_1}{2\epsilon_0 A}(\sqrt{a^2 + x^2} - x) \quad \text{Eq. 5.7}$$

Combining equations 5.5. and 5.7, the peak potential from the outer layer of the fabric system can be calculated:

$$V_p = \frac{C\sigma_1}{4KA\epsilon_0^2}(\sqrt{a^2 + t^2} - t)(\sqrt{a^2 + x^2} - x) \quad \text{Eq. 5.8}$$

But $\sigma_1 = CV/A$; then, equation 5.8 becomes:

$$V_p = \frac{C^2 V}{4KA^2 \epsilon_o^2} (\sqrt{a^2 + t^2} - t) (\sqrt{a^2 + x^2} - x) \quad \text{Eq. 5.9}$$

Where:

V_p = peak potential of a two layer system

C = total capacitance of the system

V = potential difference between rubbing wheel and outer layer

K = dielectric constant of inner fabric

A = rubbing area of specimen

ϵ_o = permittivity of free space

a = specimen radius

t = inner-layer fabric thickness

x = gap between outer-layer fabric and measuring probe

Equation 5.9 means that the peak potential for a two-layered system is directly proportional to the peak potential of the outer-layer fabric and inversely proportional to the dielectric constant of the inner-layer fabric. Therefore, knowing the total capacitance of the measuring system, the peak potential of the outer layer, the dielectric constant of the inner-layer fabric, and the thickness of the inner fabric, it is possible to predict the peak potential from a two-layered fabric system following the proposed ASTM Method, Draft No. F23.20.05.

Substituting the following data in equation 5.9, peak potentials were calculated for eight two-layer systems. These calculated values are compared to observed values from previous testing in Table 5.1. Calculated results for two fabric systems, aramid/carbon - aramid/carbon and aramid/FR viscose - aramid/carbon, did not correlate well with observed values as most of the systems did.

$$C = 9 \times 10^{-12} \text{ F}$$

$$x = 5.08 \times 10^{-2} \text{ m}^*$$

$$A = 1.27 \times 10^{-2} \text{ m}^2$$

$$a = 6.35 \times 10^{-2} \text{ m}$$

$$t = 1 \times 10^{-3} \text{ m}$$

$$K = 2.5 \text{ (FR cotton)}, 3.2 \text{ (100\% cotton)**}, 6.0 \text{ (aramid/carbon)}$$

Note: the values of K were obtained at 0% RH

* As per manufacturer's specification (2 in = 5 cm)

** Value for 100% cotton taken from Morton and Hearle, 1975.

Table 5.1. Results of calculations using theoretical model of the system component following proposed ASTM Method, F23.20.05 at 0% RH

Fabric System (Outer - Inner)	Observed Peak Potential (kV) Outer Layer	Peak Potential (kV) Two-Layer	
		Calculated	Observed
aramid/PBI - aramid/carbon	2.13	0.64	0.83
aramid/carbon - aramid/carbon	1.28	0.38	1.17
aramid/carbon - 100% cotton	1.28	1.22	1.38
aramid/FR viscose - aramid/carbon	20.86	6.27	2.01
aramid/PBI - 100% cotton	2.13	2.03	2.49
aramid/FR viscose - 100% cotton	20.86	19.92	19.03
FR cotton - 100% cotton	25.48	24.33	23.08
FR cotton - FR cotton	25.48	24.29	23.47

System Component: Mathematical Model for a Two-Layer System Following a Modified ASTM Method

In this case, the transfer of charge is between an insulator and a conductor. The charge generation on the side of the outer layer facing the rubbing wheel and the transfer of charge from the outer layer to the inner layer remain the same, as in previous section. The charge on the side of the inner layer touching the conducting plate can be expressed as follow:

$$V_2 = \frac{\sigma_1}{2K\epsilon_0} (\sqrt{a^2 + t^2} - t) \quad \text{Eq. 5.10}$$

But $\sigma_1 = (C_1 V_1)/A$. Then:

$$V_2 = \frac{C_1 V_1}{2AK\epsilon_0} (\sqrt{a^2 + t^2} - t) \quad \text{Eq. 5.11}$$

The change in the order of potential observed in the modified ASTM Method -from kilovolts to volts- is caused by the change in capacitance of the system (C in Figure 5.3). Therefore, the potential in the capacitor V_p can be expressed as: $V_p = Q_2 / C_2$. But $Q_2 = C_1 V_2$. Therefore:

$$V_p = \frac{C_1 V_2}{C_2} \quad \text{Eq. 5.12}$$

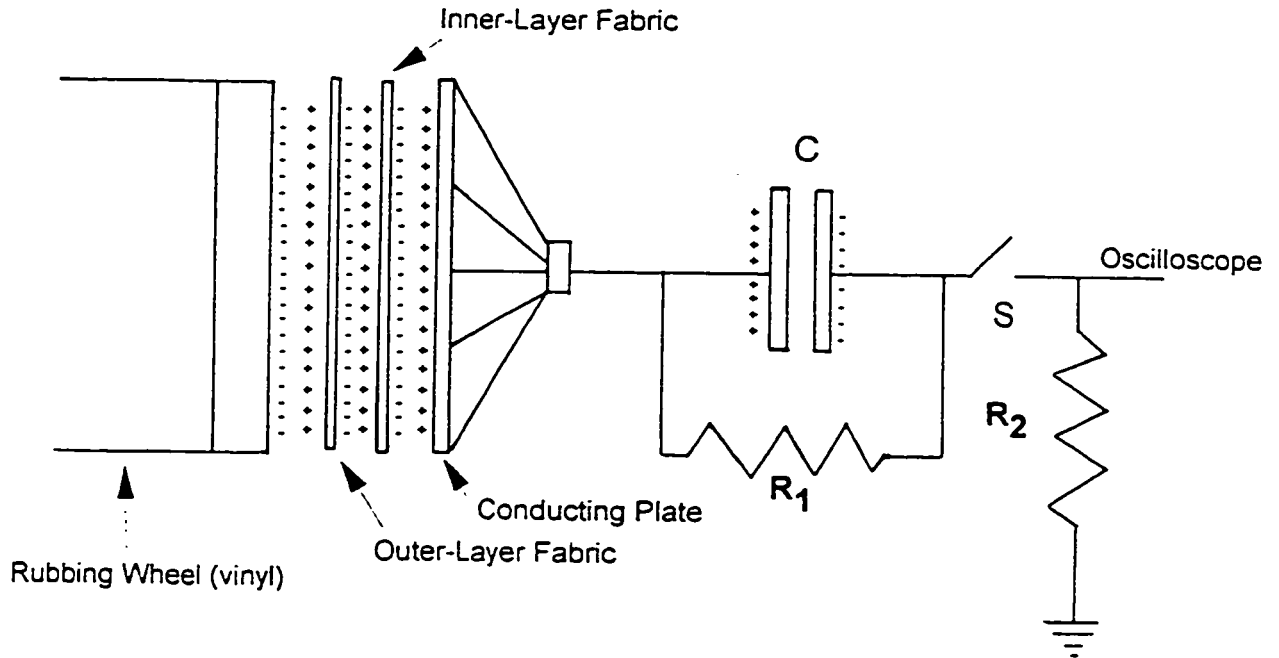


Figure 5.3. Diagram of modified ASTM Method

Combining equations 5.11 and 5.12:

$$V_p = \frac{C_1^2 V_1}{2AK\epsilon_0 C_2} (\sqrt{a^2 + t^2} - t) \quad \text{Eq. 5.13}$$

Equation 5.13 calculates the peak potential at the point of discharge s measured through R_2 (Figure 5.3), where:

V_p = peak potential from capacitor

C_1 = capacitance of proposed ASTM system

V_1 = potential at outer layer

A = surface area of specimen

K = dielectric constant of inner specimen

C_2 = capacitor in RC unit

a = specimen's radius

t = inner layer thickness

Substituting the following data in equation 5.13, peak discharge potentials from a capacitor were calculated for eight two-layer systems. These calculated values are compared to observed values from previous testing in Table 5.2:

$$C_1 = 5 \times 10^{-12} \text{ F}$$

$$C_2 = 220 \times 10^{-12} \text{ F}$$

$$A = 1.27 \times 10^{-2} \text{ m}^2$$

$$a = 6.35 \times 10^{-2} \text{ m}$$

$$t = 1 \times 10^{-3} \text{ m}$$

$$K = 2.5 \text{ for FR cotton}$$

$$K = 3.2 \text{ for 100\% cotton}$$

$$K = 6.0 \text{ for aramid/carbon}$$

Note: the values of K were obtained at 0% RH

As only V_1 changes through different fabric systems with 100% non-FR cotton inner layer, equation 5.13 becomes:

$$V_P = (9.8686 \times 10^{-3}) V_1$$

Table 5.2. Results of calculations using theoretical model of the system component following a modified ASTM Method at 0% RH

Fabric System (Outer - Inner)	Observed Peak Potential (kV) Outer Layer	Peak Potential (V) Two-Layer	
		Calculated	Observed
aramid/PBI - 100% cotton	2.13	20.0	67.4
aramid/PBI - aramid/carbon	2.13	6.6	71.7
aramid/carbon - 100% cotton	1.28	12.6	88.2
aramid/carbon - aramid/carbon	1.28	4.0	88.8
aramid/FR viscose - aramid/carbon	20.86	64.8	89.7
aramid/FR viscose - 100% cotton	20.86	205.9	262.7
FR cotton - 100% cotton	25.48	251.5	268.4
FR cotton - FR cotton	25.48	251.1	458.4

The fabric systems with anti-static fabrics, aramid/carbon and aramid/PBI, had calculated peak potentials that did not correlate well with observed values, even though they were in the same order of magnitude. Those fabric systems with cellulose-based fabrics as an outer layer correlate well to some extent with observed peak potentials.

Humidity Component

From early investigations to date, it has been established that one of the most important factors in determining electrostatic characteristics of textile materials is their moisture content (Hearle, 1953; Sereda and Feldman, 1964; Kolyer and Rushworth, 1990; Onogi et al, 1996 and 1997). Different electrostatic characteristics have been evaluated at different relative humidities, and in all cases it was found that electrostatic charges on textiles decreased exponentially as their moisture content increased, and these changes were related to the moisture regain of the fibres.

Hearle (1953) defined several empirical equations relating the electrical resistance of a fibre and its moisture content. He tested more than 30 different fibres at various humidities and found that all the samples showed sigmoidal relations between log resistance ($\log R_s$) and log moisture content ($\log M$) over a wide range. At low moisture contents, the resistance could be expressed by the relation:

$$\log R_s = -n^1 M + \log K^1 \quad \text{or} \quad R_s = K^1 e^{(-n^1 \ln 10)M}$$

where n^1 and K are empirical constants. Over a range of about 30 to 90 % RH, Hearle found that all the hygroscopic fibres except nylon could be represented by relations of the type

$$\log R_s = -n \log M + \log K \quad \text{or} \quad R_s M^n = K$$

given a linear relation with a reasonable approximation.

Sereda and Feldman (1964) tested electrostatic charging on four different fabrics at relative humidities ranging from 0 to 65%. They found that electrostatic charges seem to reach maximum values at a relative humidity corresponding to that of a mono-molecular layer of water existing on the surface of the material. They stated that the absorbed water on the surface contributed to a higher static potential either by contributing hydrogen ions to a metal or by allowing a more effective transfer of electrons from the metal. As there was no full contact between the specimen surface and the metal, the absorbed water might have acted as a medium for distributing the electrons on the insulating surface. They also added that because of the dipole nature of the water, it may modify the character of the surface in a way to make available more sites for the trapping of electrons. This effect of water interaction might explain the observed decrease in charge generated at conditions of humidity below the level when a mono-molecular layer of water is present on the textile surface.

Koyler and Rushworth (1990) tested surface resistivity on 12 antistatic materials at different humidities and temperatures. They found that surface resistivity was mainly affected by two factors: the moisture content of the specimens, which is controlled by the ambient relative humidity, and by the ambient temperature. Surface resistivity decreased exponentially as the moisture content and temperature increased, but showed a sigmoidal relationship at very low moisture levels, as Hearle (1953) had previously reported.

Onogi et al (1996; 1997) have investigated the different mechanisms utilized by textile fibres to dissipate static charge. They found that charges on the surface not only dissipate by electric conduction into the earth but also by penetrating into the material bulk and by scattering into the air. Charges can dissipate to some degree into the air by accompanying the vaporization of water molecules. They stated that the amount of free water, above the critical water content of a textile fibre, plays a very important role in atmospheric dissipation of tribo-electric charges.

In the current experiments, electrostatic charges, expressed as potential difference, decrease exponentially as the relative humidity increases. But this charge decrease varies for different fibres tested as their moisture regain differs, which is in agreement with what other researchers have found. The empirical data from tests following the proposed and modified ASTM Methods were found to fit ($R^2 > .80$) the exponential model well.

At low relative humidities (i.e. up to 30%) the decrease in peak potential following either proposed or modified ASTM methods can be expressed by the relation:

$$V = V_0 e^{bH} \quad \text{Eq. 5.14}$$

where V is the potential at RH %, V_0 is the potential at the lowest humidity conditions (e.g., 0% RH and 0°C), b is a humidity constant and H is the relative humidity (%). Values for b and regression coefficient R^2 obtained from non-linear regression analyses following the exponential model, are given in Tables 5.3 and 5.4 for proposed and modified ASTM methods, respectively.

Peak potential data from some fabric systems for both proposed and modified ASTM methods yielded $R^2 < .7$. Aramid/FR viscose and FR cotton were among the fabrics with low regression coefficients, but more than 65% of the systems showed coefficients above .75.

Table 5.3. Values of constant "b" and R² for proposed ASTM Method between 0 & 30% RH

Fabric System	Humidity Constant "b"	R ²
Single-Layer:		
100% non-FR cotton	-0.02066	.9998
FR cotton	-0.02867	.9965
aramid/carbon	-0.00237	.9350
aramid/PBI	-0.00297	.9993
aramid/FR viscose	-0.06555	.6705
Two-Layer:		
FR cotton - 100% cotton	-0.04165	.7810
aramid/carbon - 100% cotton	-0.04719	.8533
aramid/PBI - 100% cotton	-0.08992	.9522
aramid/FR viscose - 100% cotton	-0.12929	.6282
FR cotton - FR cotton	-0.03661	.7295
aramid/carbon - aramid/carbon	-0.03227	.8916
aramid/PBI - aramid/carbon	-0.02321	.8872
aramid/FR viscose - aramid/carbon	-0.05611	.7969

Table 5.4. Values of constant "b" and R² for modified ASTM Method between 0 & 30% RH

Fabric System	Humidity Constant "b"	R ²
Single-Layer:		
100% non-FR cotton	-0.06363	.9569
FR cotton	-0.04661	.8369
aramid/carbon	-0.05343	.6052
aramid/PBI	-0.06260	.6783
aramid/FR viscose	-0.08422	.8447
Two-Layer:		
FR cotton - 100% cotton	-0.05995	.6008
aramid/carbon - 100% cotton	-0.11519	.7096
aramid/PBI - 100% cotton	-0.05679	.9684
aramid/FR viscose - 100% cotton	-0.14683	.7347
FR cotton - FR cotton	-0.07555	.8961
aramid/carbon - aramid/carbon	-0.07126	.9998
aramid/PBI - aramid/carbon	-0.03163	.9999
aramid/FR viscose - aramid/carbon	-0.09961	.7011

Temperature Component

A review of the literature on the electrostatic properties of textile materials shows that the information about the effect of temperature is limited, with only scattered, outdated results under various conditions and materials being available. In a study of electrical conduction in nylon as a function of draw ratio and temperature Sharman, Hersh and Montgomery (1953) found that the conductivities decreased as the temperature decreased from 45 to 15 °C at constant regain, but at none of the temperatures and regains studied could the temperature dependence be accounted for as a simple rate process. They also found that a non-linear relationship might be established between log conductivity and log moisture regain over small ranges of regain, but the deviation from linearity was greatest at low temperatures. They determined that curves of log conductivity against the reciprocal of temperature were approximately parallel at different regains. Furthermore, Hearle (1954) found that a decrease in temperature, increasing the restraints on the dipoles, causes a decrease in permittivity in solid materials.

Hearle's research (1953) on the electrical resistance of textile materials found that the resistance of fibres decreases as the temperature increases, a rise of 10 °C causes a decrease in the order of five times. He established the following empirical equations:

$$-\frac{d(\log R)}{dT} = a - bM - cT$$

where T is temperature (°C), M is moisture content, and a , b , and c are empirical constants for a given material. On integration, this becomes:

$$\log R = (\log R)_{T, M=0} - (a - bM)T + \frac{c}{2}T^2$$

Clark and Preston (1955) found that Hearle's equations fit the results for viscose rayon at 24.5% regain down to -60 °C, with an increase in log Rs as the temperature decreases according to a nearly linear relation. They also found that these results were similar to Hearle's observations (1953) at higher temperatures.

Koyler and Rushworth (1990) determined in their study of anti-static materials that resistance decreased exponentially with temperature at constant relative humidity. At high relative humidity, the temperature effect becomes small or nil as materials moved from the

semi-conductive toward the conductive state. Thus, they recommended to give both temperature and relative humidity when reporting surface resistivity data.

Onogi et al (1997), in a study of the tribo-electric charge dissipation from textile surfaces, concluded that the rate constant of charge dissipation into the air depends not only on the amount of free water in the textile material, but also on the vapour pressure of water (absolute humidity). It is well known that the vapour pressure of water strongly depends on the ambient temperature.

In this study, it has been determined that peak potential from a textile surface exponentially decreases as the temperature increases at constant relative humidity, confirming the previous research. At constant relative humidity levels, the decrease in peak potential due to temperature change can be expressed by the relation:

$$V = V_0 e^{cT} \quad \text{Eq. 5.15}$$

where V is the potential at T °C, V_0 is potential at the lowest humidity conditions (e.g., 0% RH and 0 °C), c is a temperature constant, and T is the temperature (°C). Values for constant c and regression coefficient R^2 , which were obtained from non-linear regression analyses following the exponential model, are given in Table 5.5 for proposed ASTM Method. Due to restriction in available space inside the cold room where the experiment at low temperature was carried out, there was no testing following the modified ASTM Method.

Table 5.5. Values of temperature constant "c" for proposed ASTM Method at 0% RH

Fabric System	Temperature Constant "c"	R ²
Single-Layer:		
100% non-FR cotton	-0.00509	.9992
FR cotton	-0.00726	.6070
aramid/carbon	-0.01584	.9728
aramid/PBI	-0.00098	.7740
aramid/FR viscose	-0.00542	.8969
Two-Layer:		
FR cotton - 100% cotton	-0.01742	.7281
aramid/carbon - 100% cotton	-0.02663	.6020
aramid/PBI - 100% cotton	-0.00719	.8340
aramid/FR viscose - 100% cotton	-0.00470	.9860
FR cotton - FR cotton	-0.01132	.7281
aramid/carbon - aramid/carbon	-0.05281	.6394
aramid/PBI - aramid/carbon	-0.04267	.9530
aramid/FR viscose - aramid/carbon	-0.04532	.5493

In general, correlations were good as 9 out of 13 fabric systems showed $R^2 > .7$, although some regression coefficients were lower than .7 in a few cases.

Combined Effect of Humidity and Temperature on Peak Potential

Several researchers have reported that the effect of either humidity or temperature on peak potential cannot be evaluated unless both variables are taken into account together (Hearle, 1954; Koyler and Rushworth, 1990; Onogi et al, 1997; etc.). The following equation has been developed including both variable effects, and making humidity dependant on temperature:

$$V_p = V_o \exp[b \exp(cT)]H \quad \text{Eq. 5.16}$$

where: V_p = peak potential, V_o = peak potential at maximum conditions, b = humidity constant, c = temperature constant, T = temperature in °C, and H = relative humidity in %.

Values for b and c are shown from Table 5.3 to Table 5.5. Equation 5.16 was tested using commercial software, the student edition of MATLAB version 4. Comparison between calculated and observed results at selected testing conditions are shown in Table 5.6. Appendices 7a to 7e show 3-D plots showing humidity and temperature effect on peak potentials for different single-layer fabrics.

Table 5.6. Comparison between calculated and observed results following proposed ASTM Method F23.20.05 at 22 °C

Fabric System	Calculated			Observed ^a		
	0%	20%	30%	0%	20%	30%
Single-Layer:						
100% non-FR cotton	25.31	16.32	12.95	23.70	16.10	13.00
FR cotton	24.97	13.18	9.42	25.41	14.18	11.16
aramid/carbon	0.74	0.70	0.67	0.75	0.72	0.55
aramid/PBI	1.72	0.97	0.71	1.77	0.99	1.25
aramid/FR viscose	14.81	3.65	1.74	14.99	12.14	1.76

^a Absolute values

Only one fabric system in one condition (aramid/FR viscose at 20% RH) showed low correlation between calculated and observed peak potentials. The rest of the systems and conditions correlated well.

Complete Mathematical Model

To develop a full mathematical model for predicting the peak potential of two layer systems from data of single layer testing following either the proposed or modified ASTM methods, the three components, system, humidity and temperature, are then combined together.

For proposed ASTM Method:

$$V_p = \left[\frac{C^2 V}{4KA^2 \epsilon_o^2} (\sqrt{a^2 + t^2} - t) (\sqrt{a^2 + x^2} - x) \right] \left[\exp(b \exp(cT)H) \right] \quad \text{Eq. 5.17}$$

For modified ASTM Method:

$$V_p = \left[\frac{C_1^2 V_1}{2AK\epsilon_o C_2} (\sqrt{a^2 + t^2} - t) \right] \left[\exp(b \exp(cT)H) \right] \quad \text{Eq. 5.18}$$

Table 5.7 shows comparisons between calculated results using equation 5.17, and observed results obtained following the proposed ASTM Method at both 20 and 30% RH. It is important to note that results are shown as absolute values because the developed equations can not determine the polarity of potential. There were some discrepancies between calculated and observed peak potentials at both 20 and 30% RH. Aramid/FR viscose - 100% cotton fabric system showed the greatest discrepancy at both humidities, as it was observed during the development of the different components of the model. Aramid/carbon and aramid/PBI fabric systems showed also some discrepancies at 30% RH.

Discussion and Conclusions

Theoretical models have been developed to predict peak potential of two-layer systems from single-layer data following either proposed or modified ASTM Methods at any relative humidity and temperature. It has been demonstrated that peak potentials calculated using

Table 5.7. Results of calculations using theoretical model of the system component following proposed ASTM Method, F23.20.05 at 20 and 30% RH and 22 °C

Fabric System (Outer - Inner)	Observed Peak Potential (kV)	Peak Potential (kV) Two-Layer	
	Outer Layer @ 0% RH	Calculated	Observed ^a
20% RH			
aramid/PBI - aramid/carbon	2.13	0.35	0.64
aramid/carbon - aramid/carbon	1.28	0.36	0.79
aramid/carbon - 100% cotton	1.28	1.14	0.87
aramid/PBI - 100% cotton	2.13	1.11	0.69
aramid/FR viscose - aramid/carbon	20.86	1.43	1.54
aramid/FR viscose - 100% cotton	20.86	4.54	15.32
FR cotton - 100% cotton	25.48	12.42	19.96
FR cotton - FR cotton	25.48	12.40	19.34
30% RH			
aramid/FR viscose - aramid/carbon	20.86	0.68	0.16
aramid/FR viscose - 100% cotton	20.86	2.17	0.27
aramid/carbon - 100% cotton	1.28	1.10	0.32
aramid/carbon - aramid/carbon	1.28	0.34	0.42
aramid/PBI - 100% cotton	2.13	0.82	1.17
aramid/PBI - aramid/carbon	2.13	0.26	1.40
FR cotton - 100% cotton	25.48	8.87	5.94
FR cotton - FR cotton	25.48	8.86	7.23

^a Absolute values

equation 5.17 fit well, in most cases, with empirical data from two-layer systems following the proposed ASTM method.

Equations 5.14 and 5.15 suggest that the peak potential of a two-layer system is directly proportional to the peak potential of the outer fabric measured as single layer and indirectly proportional to the dielectric constant of the inner fabric. The latter means that there will be more transfer of charge from the outer layer to the inner layer (i.e. suppression effect on the outer layer caused by the inner layer), as the dielectric constant of inner layer increases. This has been confirmed by empirical testing where an inner layer of fabric with conductive fibres like aramid/carbon causes a greater decrease in peak potential of the outer layer in two-layer systems than cellulose based fabrics at low humidities. The exponential decrease in potential due to humidity and temperature effects confirms several research works carried out for the last 40 years. Also, it confirms that humidity has a greater effect than temperature on electrostatic characteristics of textile materials.

The lack of correlation in some of the cases reported may have been caused by any of the following reasons: i) lack of intimate contact between either the vinyl rubbing wheel and the outer layer or the inner and outer layers during test, ii) topical finish on the surface of some fabrics which might have been removed by rubbing as the same specimens were used for testing through the investigation, iii) no intimate blend in case of fabrics with multi-fiber content that could expose uneven blend at the interface, iv) scaffolding effect that tends to place one of the component fibers in a blend on top of the yarn surface, and v) some wear due to abrasion which may have caused small variations at microscopic level on the surface of the fabric. One, or a combination of any of these reasons may account for some of the discrepancies between calculated and observed peak potentials.

For example, fabric systems of aramid/FR viscose - 100% cotton which had the greatest discrepancy may have been affected by lack of intimate contact, blend characteristics, and/or by the scaffolding effect. The lack of contact at the interface could have been caused by actual repellence between layers due to the polarity of each fabric according to the triboelectric series developed during the research (Appendix 8). Poor fiber blending and/or scaffolding effect would tend to present different fibers at the interface causing variation on charge generated; systems with aramid/FR viscose revealed the highest variability. If FR viscose fibers are exposed to the abrasion work of the rubbing wheel, either fibers or FR finish may be lost causing variation.

In the case of aramid/PBI fabric, it was determined that it has a topical anti-static finish. Changes on the surface due to loss of the finish by abrasion may account for the variation shown at both 20 and 30% RH (Table 5.7).

References

ASTM. (1994). ASTM Committee F-23 on Protective Clothing. Standard Test Method for Evaluating Triboelectric (Static) Charge Generation on Protective Clothing Materials (ASTM F23.20.05). Philadelphia, PA: American Society for Testing and Materials.

Chowdry, A., & Westgate, C. R. (1974). Comments on "Contact charging of polymers" [Letter to The Editor]. Journal of Physics D: Applied Physics, 7, L149-L151.

Clark, J. F., & Preston, J. M. (1955). Electrical resistance of viscose rayon at low temperatures. Textile Research Journal, 25, 797-798.

Davies, D. (1970). Charge generation on solids. Advances in Static Electrification, 1, 10-21.

Gallo, C. F., & Lama, W. L. (1976). Classical electrostatic description of the work function and ionization energy of insulators. IEEE Transactions on Industry Applications, IA-12(1), 7-11.

Harper, W. (1967). Contact and frictional electrification. London, UK: Oxford University Press.

Hearle, J. W. S. (1953). The electrical resistance of textile materials: Parts I to IV. Journal of The Textile Institute, 44, 117-198.

Hersh, S. P., & Montgomery, D. J. (1956). Static electrification of filaments. Theoretical Aspects. Textile Research Journal, 26, 903-913.

Koyler, J. M., & Rushworth, R. (1990). Humidity and temperature effects on surface resistivity. Evaluation Engineering, 29(10), 106-110.

Lowell, J. (1976). The electrification of polymers by metals. Journal of Physics D: Applied Physics, 9, 1571-1585.

Morton, W. E., & Hearle, J. W. S. (1975). Physical Properties of Textile Fibres. London, UK: The Textile Institute & William Heinemann Ltd.

Ohara, K. (1979). Contribution of molecular motion of polymers to frictional electrification. In J. Powell, Electrostatics'79 Vol. 48 (pp. 257-264). Bristol, UK: IOP Publishing Ltd.

Onogi, Y., Sugiura, N., & Nakaoka, Y. (1996). Dissipation of triboelectric charge into air from textile surfaces. Textile Research Journal, 66, 337-342.

Onogi, Y., Sugiura, N., & Matsuda, C. (1997). Temperature effect on dissipation of triboelectric charge into air from textile surfaces. Textile Research Journal, 67, 45-49.

Rizvi, S. A. H., Crown, E. M., Osei-Ntiri, K., Smy, P. R., & Gonzalez, J. A. (1995). Electrostatic characteristics of thermal-protective garments at low humidity. Journal of The Textile Institute, 86, 549-558.

Scott, R. A. (1981). Static electricity in clothing and textiles. Thirteenth Commonwealth Defence Conference on Operational Clothing and Combat Equipment (Malaysia). Colchester, UK: Stores and Clothing Research and Development Establishment.

Sereda, P. J., & Feldman, R. F. (1964). Electrostatic charging on fabrics at various humidities. Journal of The Textile Institute, 55, 288-298.

Sharman, E. P., Hersh, S. P., & Montgomery, D. J. (1953). The effect of draw ratio and temperature on electrical conduction in nylon filaments. Textile Research Journal, 23, 793-798.

Shinohara, I., Yamamoto, F., Anzai, H., & Endo, S. (1976). Chemical structure and electrostatic properties of polymers. Journal of Electrostatics, 2, 99-110.

Taylor, D. M., & Secker, P. E. (1994). Industrial Electrostatics: Fundamentals and Measurements. Somerset, England: Research Studies Press Ltd.

Wilson, N. (1979). The nature and incendiary behaviour of spark discharges from the body. In B. C. O'Neill, Electrostatics'79 Vol. 48 (pp. 73-83). Bristol, UK: IOP Publishing Ltd.

Chapter 6. Development of Mathematical Models to Predict the Static Propensity of Thermal Protective Clothing Systems¹

Preamble

This chapter describes empirical and theoretical models to assess electrostatic propensity of clothing systems. Experimental data were used for obtaining empirical models to determine the best relationship between data from small-scale testing and human-body experiments. These empirical models form the basis for a theoretical model developed during this investigation.

A proposed ASTM method and a simple modification were evaluated and compared in order to select the method(s) that could best assess the electrostatic propensity of protective garment systems worn by workers in hazardous environments under dry conditions. Experiments were conducted at both 0% and 20% relative humidity (RH) and room temperature. Several one- and two-layer fabric systems were tested, including combinations of aramid/PBI, aramid/carbon, aramid/FR viscose, non-FR cotton and FR cotton.

Using the linear model of the form $Y = a + mX$, data from both tests were regressed with peak potentials obtained during human-body experiments. At 0% RH, regression coefficients (R^2) were .85 and .92 for peak potentials from fabric surface (proposed ASTM F23.20.05) and from a capacitor (modified ASTM), respectively. At 20% RH, regression coefficients were .86 and .94 for peak potentials from proposed ASTM and modified ASTM, respectively.

Based on these empirical models, the theoretical model was then analyzed, where the most influencing variables on charge generation were incorporated as constant m . Constants were determined for use in the equation to predict human-body potentials from either proposed or modified ASTM data.

Introduction

The charged human body is a primary cause of ESD (Greason, 1992). The charging process for the human body involves both tribo-electrification and induction processes. Typical charge densities due to contact electrification are in the range of 10 nC/cm², and in a surface of

¹The papers: "Gonzalez, J.A., Rizvi, S.A., Crown, E.M., & Smy, P.R. (1997). A modified version of proposed ASTM F23.20.05: Correlation with human body experiments on static propensity. In J. O. Stull & A. D. Schwoppe, Performance of Protective Clothing Vol. 6, ASTM STP 1273 (pp. 47-61). Philadelphia, PA: American Society for Testing and Materials", and "Gonzalez, J.A., Rizvi, S.A., Crown, E.M., and Smy, P.R. (1997). A laboratory protocol to assess the electrostatic propensity of protective clothing systems. Unpublished manuscript.", were based in part on this chapter.

100 cm², like shoe soles, the calculated charge will be 1 μC . Since the human body can be modelled as a neutral conductor, insulated from ground by footwear worn, the charge trapped on the footwear causes a polarization of charge on the human body. A charge equal and opposite in polarity to the footwear's charge moves to the feet, leaving a charge equal in magnitude and polarity to the trapped charge distributed over the human body. If the person now makes contact with a grounded conducting object, a charge will flow to balance the polarized charge.

In cold regions like Alberta, the absolute humidity level declines extremely with very cold temperatures, so the electrostatic hazard can be more significant than in warmer regions. People who work outdoors in extremely cold conditions may be required to wear thermal protective clothing when working in hazardous circumstances. Rizvi et al (1995) showed that clothing made of thermal protective fabrics such as aramid or flame retardant cotton may generate enough energy to ignite a fuel vapour-air mixture. Cellulose-based fibres are often mistakenly considered less prone to static electricity than thermally stable synthetic fibres such as aramid. This belief is based on the high moisture regain of those cellulose-based fibres at higher relative humidity, and on the mid-position of cotton in the tribo-electric series². For example, at 50% RH, the cotton products have somewhat lower values than aramid fibres, but at 20% RH, aramid fabrics have a slightly lower apparent surface resistivity than regular cotton or FR cotton fabrics. The decrease of resistivity with an increase in humidity is greater for cotton than for fabrics made of most synthetic fibres (Hearle, 1953).

Key considerations in the analysis of a process to determine the degree of hazard associated with human static discharges are the mechanisms by which the electrostatic energy is generated, stored, and discharged. The amount of static generation depends not only on the atmospheric conditions but also on the substance being rubbed against, the degree of rubbing, the charge generation characteristics of the clothing and footwear of the person involved (Hersh and Montgomery, 1955; Ramer and Richards, 1968; Wilson, 1977/78). Energy storage is dependent on the capacitance of the body while the energy discharge is controlled largely by the body resistance and the configuration of the discharge point (Berkey, Pratt and Williams, 1988).

Values for body parameters are widely reported in numerous references, and there is some agreement among data acquired using a considerable range of techniques (Cleves and Sumner, 1962; Tucker, 1968; Wilson, 1977/78 and 1979; Sullivan and Underwood, 1985, Sperber and Blink, 1987; Rizvi et al, 1995). Among these were the direct use of commercial capacitance bridges and various systems for determining body resistance and capacitance from recorded discharges from subjects charged to controlled initial voltages. Capacitance data are

²A tribo-electric series ranks different materials according to charge polarity generated when materials, in pairs, are rubbed against each other and separated (frictional separation).

reported for subjects of different physical characteristics and for clothing combinations. Fisher (1989) summarized body capacitance and resistance data from several sources. He reported that body capacitance over 400 pF cannot be expected, with mean values of 164 and 290 pF for standing and sitting conditions, respectively. He also noted that body resistance apparently exhibits a much broader range of values, as it is dependent on skin moisture, the particular portion of the body involved in the discharge path, and the contact area and degree of pressure applied in touching a metal object.

Wilson and Cavanaugh (1972) documented the results of charge generation after testing various types of footwear and clothing. They measured voltages and charge generated on a person, as well as body capacitance. More work was done developing specifications for identification of safe fabrics used in flammable environments (Wilson, 1977/78 and 1979). Body resistance and voltage data at different relative humidity levels were reported, and ignition testing was conducted with coal gas and natural gas. Wilson concluded that the stored energy on a body must be 60 to 100 times the minimum ignition energy (MIE) to have an ignition due to human ESD, that the static propensity of an unknown material should be determined empirically, and that less than 10% of the charge energy lost by the body is released in the spark gap.

Movilliat and Monomakoff (1977) carried out an extensive comparison between capacitive sparks and those generated by humans. They concluded that for discharge between non-pointed electrodes, the spark energy from a human discharge is of the same order of magnitude as the energy of a capacitor discharge when both capacitances are the same. They also stated that for all practical purposes, the capacitance of the body will not fall below 90 pF.

In modelling the electrostatic propensity of a human body, several studies have been carried out mainly aimed for the electronic industry. The Electrical Overstress (EOS) / Electrostatic Discharge (ESD) Association Standard for ESD Sensitivity Testing: Human-body Model (HBM) - Component Level (EOS/ESD-S5.1-1993) establishes the test procedure for evaluating the ESD sensitivity of components to a defined HBM. The purpose of this standard is to ensure reliable test data from tester to tester, regardless of the component type being tested, so that accurate comparisons can be made for component level ESD sensitivity to a defined HBM.

Establishment of correlation between human-body model and ESD testers is a recurring problem. Different studies have been done with the purpose of establishing calibration procedures in ESD testers to improve that correlation. Consiglio and Morgan (1988) developed a calibration procedure which significantly improved the correlation between HBM and ESD simulators. They found that charging voltage, effective charging capacitance, and open circuit voltage were meaningful DC parameters to control the energy in and out of the HBM circuit. Also, measurements of effective charging capacitance across a range of charging voltages was

necessary. Current waveform rise-time and peak current appeared to be the most important waveform parameters to control, with discharge time of less importance.

Sperber and Blink (1987) developed a human model appropriate for ESD testing of the automotive electrical system. They measured and determined body capacitance and resistance, as well as body voltages and energies for two conditions, inside and outside a vehicle. They found that two models are required to explain the ESD phenomenon in a vehicle: one, when the occupant is inside the car, and a second, when the person gets off the vehicle, reaches back and discharges, because the values for capacitance, voltage and energy varied in each condition.

A simulator to replicate severe human body ESD events was developed at the Electromagnetic Testing Division at Sandia National Laboratories, USA (Barnum, 1991). The device is configured as a coaxial transmission line, which allows control of parasitic inductance and capacitance to achieve a desired waveform, and operates reliably at voltages up to 35 kV. It is reported that measurements using the simulator are very reliable and there is good correlation between those measurements and severe human body discharges. It was concluded that in ESD testing it is important to obtain high fidelity sub-nanosecond data which is inherent in ESD events, and that careful selection and calibration of instrumentation is required for accurate measurements.

Greason (1995) investigated different configurations involving a clothed human body with multiple charged sources and an electronic system, when a person approaches a work station and assumes a seated position in a chair. He determined that if a finite amount of charge is assumed for the footwear and clothing worn by a worker, a body potential will result which is a function of the amount of charge and the capacitance coefficient³ of the systems, as well as the present environment and the previous history of human body grounding. He concluded that the nature of the coupling factors⁴ in effect at the initial grounding of the human body determines the amount of charge transferred to the body.

Part of the present research was planned to improve the correlation between small-scale tests and real-life static discharges by developing a laboratory protocol that can accurately and reliably assess the electrostatic propensity of protective clothing systems that workers wear in hazardous environments under cold and dry conditions. Also, a theoretical model was developed to explain a defined correlation between small-scale and human-body data.

³Self-capacitance coefficient of the form C_{ii} is defined as the charge on body i when the potential of body i is raised to a potential of 1 V with all other conductors in the systems are grounded.

⁴A coupling factor k_1 describes the degree to which electric flux associated with the charge on a body B terminates on a body A . If all electric flux from Body B terminates on body A , $k_1 = 1$; if all flux from body B terminates on other bodies excluding body A , $k_1 = 0$. Then, k_1 is defined by $c_{12} = -k_1 c_{22}$, where c_{12} and c_{22} are mutual capacitance coefficients.

Method in Empirical Modelling

This research was conducted under low humidity conditions at room temperature on two-layer specimens of thermal protective fabrics. The independent variables were test method, relative humidity and fabric system. In the proposed ASTM Method F23.20.05 (proposed ASTM) the dependent variables were peak potential [kV] and percentage of charge decay at 5 s. In the modified ASTM Method F23.20.05 (modified ASTM) the measured variable was peak discharge potential [V]. Fabric characteristics, and detailed description of proposed and modified ASTM Methods are given in Chapter 3 of the present dissertation.

Data Analyses

Using commercially available, SPSS version 6.1 software, the following statistical analyses were performed, with the level of significance for testing hypotheses set at $p < .05$.

- 1) Pearson's correlation coefficient to test the null hypothesis of no significant correlation between small-scale test results and data from human-body experiments (Rizvi et al, 1995; Rizvi, Crown, Gonzalez and Smy, in press).
- 2) Multiple linear regression to build a testing model to predict the electrostatic propensity of protective clothing.

Results and Discussion in Empirical Modelling

To test the null hypothesis that there was no significant correlation between small-scale data and those from the human-body experiments, Pearson's correlation analysis was performed between both peak potentials and charge decay from small-scale tests and human-body discharge potentials. All correlations but one were significant at both 0 and 20% RH; therefore this null hypothesis was rejected (Table 6.1)

TABLE 6.1--Correlations* (R) between human-body discharge potentials and energies, and both peak potentials, and charge decays.

Parameter	0% RH		20% RH	
	HBE-Pot ^a	HBE-Ene ^b	HBE-Pot ^a	HBE-Ene ^b
ASTM-Pot	.921*	.890*	.929*	.920*
ASTM-Dec	.527*	.326	.580*	.414
Mod. ASTM-Pot	.960*	.930*	.969*	.940*

* $p < 0.01$

^a Human-body experiment peak potential

^b Human-body experiment discharge energy

Small-scale results are more highly correlated with human-body discharge potential than with human-body discharge energy. Both types of peak potentials have higher correlations than does charge decay with human-body discharge potentials. At both 0% and 20% RH, the highest correlations were, in order, those between modified ASTM potential and human-body potential, modified ASTM potential and human-body energy, proposed ASTM potential and human-body potential.

Various empirical models, built with the help of multiple linear regressions (Table 6.2), suggested appropriate test protocols. The highest regression coefficient (R^2) was obtained when all parameters were regressed with human-body data, where R^2 at 0 and 20% RH were .93 and .94, respectively. At 0% RH, in terms of single parameters, modified ASTM potential, proposed ASTM potential, and proposed ASTM charge decay had regression coefficients of .92, .85, and .28, respectively; and at 20%, R^2 were .94, .86, and .34, respectively.

According to preliminary plotting of data, a linear relationship exists between small-scale and human-body potentials (Figure 6.1). Different plots were obtained to confirm the assumption of linear relationship: standardized residuals vs. standardized predicted values, histogram of standardized residuals, normal probability (P-P plot), and actual vs. predicted values. The combination of all three parameters (Regression No. 1 in Table 6.2) was selected and named Test Battery 1.

Table 6.2. Correlation coefficients (R) and regression coefficients (R^2) among small-scale parameters and human-body data at 0 and 20% RH.

Regression No.	Parameter	0% RH		20% RH	
		R	R^2	R	R^2
1	MOD. ASTM - potential	.96	.93	.97	.94
	PROP. ASTM - potential				
	PROP. ASTM - charge decay				
2	MOD. ASTM - potential	.96	.92	.97	.94
3	PROP. ASTM - potential	.94	.89	.93	.86
	PROP. ASTM - charge decay				
4	PROP. ASTM - potential	.92	.85	.93	.86
5	PROP. ASTM - charge decay	.53	.28	.58	.34

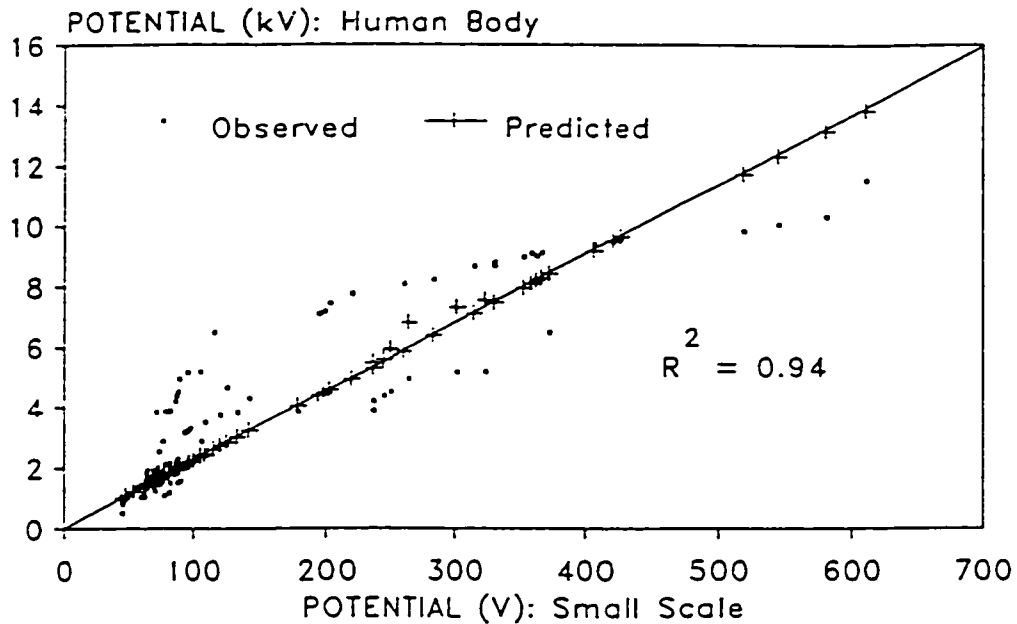


Figure 6.1. Linear relationship between Test Battery 1 and human-body data at 20% RH

Theoretical Modelling

As was previously shown (Figure 1.2), the modelling process can be divided into three steps: 1) modelling charge decay, 2) modelling the electrostatic potential from either a textile surface (proposed ASTM method) or a capacitive system (modified ASTM method), and 3) modelling the relationship between small-scale and human-body data, or prediction of electrostatic propensity of clothing systems.

The first two steps are reported in Chapters 4 and 5. Here, an equation is being reported which can predict human-body discharge potentials from small-scale peak potentials using linear model $Y = a + mX$, where $a = 0$. It was previously found that small-scale and human-body potentials fit the linear model well, and those methods using a capacitive discharge system (e.g., modified ASTM method) yielded the highest regression coefficients ($R^2 > .9$).

The new equation relates the differences among different variables involved in a human-body/ESD event (Rizvi et al, 1995; Rizvi et al, in press)⁵ and those in the test methods utilized, expressed as a ratio. Therefore, constant m can be calculated using the following equation:

$$m = \left(\frac{C_a}{C_b} \right) \left(\frac{F_{sa}}{F_{sb}} \right) \left(\frac{v_a}{v_b} \right) \left(\frac{A_b}{A_a} \right) \quad \text{Eq. 6.1}$$

⁵ See Appendices 2a and 2b for detailed information about the methods followed during human-body experiments.

Where:

C_a = human-body capacitance

C_b = small-scale capacitance

F_{sa} = human-body frictional force

F_{sb} = small-scale rubbing force

v_a = human-body sliding speed

v_b = small-scale rubbing speed

A_a = human-body area of contact

A_b = small-scale area of contact

Calculations using the new equation were carried out using values for the variables defined above (Table 6.3). Two different approaches were followed: i) taking into account the total frictional force exerted by a person when sliding off a car seat, and the total area of contact between the person and the car seat, and ii) including only the frictional force exerted by the person's back and the area of the person's back. Results from data at 0% RH following the second option were in agreement with empirically determined constant m ; but at 20% RH, results from data following the first option were in agreement with constant m (Table 6.4).

Table 6.3. Values of variables for small-scale and human-body experiments

Method	Capacitance [pF]	Force [N]	Speed [m/s]	Area [m ²]
0% RH				
Human-body Experiment ^a	198.75	340.40	0.1333	0.2774
Human-body Experiment ^b	198.75	116.58	0.1333	0.1535
Modified ASTM method	1.31	6.06	1.3333	0.0127
Proposed ASTM method	0.0711	6.06	1.3333	0.0127
20% RH				
Human-body Experiment ^a	184.34	265.70	0.1333	0.2774
Human-body Experiment ^b	184.34	90.99	0.1333	0.1535
Modified ASTM method	1.27	4.73	1.3333	0.0127
Proposed ASTM method	0.1431	4.73	1.3333	0.0127

^a Taking into account the total friction force and area of contact

^b Including only friction force and contact area from person's back

Table 6.4. Results from calculations of constant "m"

Human-body/Small-scale Experiments	Calculated Constant m		Empirical Constant "m"
	Option 1	Option 2	
0% RH			
HBE-Modified ASTM	38.99	24.13	22.81
HBE-Proposed ASTM	718.48	444.66	362.70
20% RH			
HBE-Modified ASTM	37.30	23.08	39.70
HBE-Proposed ASTM	331.10	204.92	423.20

Option 1: Taking into account the total friction force and area of contact

Option 2: Including only friction force and contact area from person's back

To predict human-body potentials from small-scale data, equations 5.17 and 5.18 can be combined with equation 6.1. The new equations will incorporate the different effects of clothing systems and environmental conditions with other variables involved in the relationship between small scale and human body.

For the proposed ASTM method:

$$V_{HB} = \left[\left(\frac{C_a}{C_b} \right) \left(\frac{F_{sa}}{F_{sb}} \right) \left(\frac{v_a}{v_b} \right) \left(\frac{A_b}{A_a} \right) \right] \left[\frac{C_2 V}{4KA^2 \epsilon_o^2} (\sqrt{a^2 + t^2} - t) (\sqrt{a + x} - x) \right] [\exp(b \exp(cT)H)]$$

Eq. 6.2

For the modified ASTM method:

$$V_{HB} = \left[\left(\frac{C_a}{C_b} \right) \left(\frac{F_{sa}}{F_{sb}} \right) \left(\frac{v_a}{v_b} \right) \left(\frac{A_b}{A_a} \right) \right] \left[\frac{C_1^2 V_1}{4KA \epsilon_o C_2} (\sqrt{a^2 + t^2} - t) \right] [\exp(b \exp(cT)H)]$$

Eq. 6.3

The hazard involved with the electrostatic propensity of human-body discharge potentials may be assessed by combining either equations 6.2 or 6.3 with the equation used to determine the electrostatic energy stored in a charged capacitor:

$$U_{HB} = \frac{1}{2} C V_{HB}$$

Eq. 6.4

where C is the human-body capacitance which has been evaluated between 150 and 300 pF by different researchers. Then, the calculated energy can be compared to minimum ignition energies for different flammable gases, vapours, dust, etc. to determine safety levels in wearing specific clothing systems.

Discussion and Conclusions

Peak potentials and charge decays from a textile surface and peak discharge potentials from a capacitor were measured for two-layer specimens. The general pattern of data given by these methods was predictable on the basis of other studies and the theory of static electricity. However, the magnitude of electrostatic discharges for each fabric system and the relationships among the two methods and the human-body experiment were unknown. Rizvi et al (1995 and in press) determined that measuring peak discharge potentials and total discharge energies from a clothed human body was a reliable method to assess the electrostatic hazard of a person involved in different physical activities.

According to correlation and linear regression analyses, it is possible to establish a small-scale laboratory protocol to predict accurately and reliably, from data on two-layer fabric systems, the electrostatic propensity of garment systems made from those fabrics and worn by workers in hazardous environments. As an individual test method, the modified ASTM Method showed the best relationship compared to the human-body data with coefficients of determination of .92 and .94 at 0 and 20% RH, respectively. These high values mean that more than 92% of the human-body discharge potentials can be predicted by the results from this test. Also, peak potential measured following the proposed ASTM method correlates reasonably well with human-body data and is perhaps the more generic parameter.

Theoretical equations based on the linear model and with the incorporation of different variables involved in both human-body and small-scale ESD events confirm what has been previously reported: firstly, the combined effect of clothing system, humidity and temperature, and secondly, the proportionality of those variables from both small-scale and human-body levels given in equation 6.1 and showed in Table 6.4. The influence of such factors as contact pressure, contact area, capacitance of the system, and rubbing speed on the magnitude of charge generation was previously studied by other researchers (Hersh and Montgomery, 1955; Ramer and Richards, 1968; Wilson, 1977/78). Results from calculations using those equations suggest that the electrostatic propensity of clothing systems, expressed in terms of human-body discharge potentials, can be predicted using either equations 6.2 and 6.3.

The discrepancies in constant m between empirical and calculated values using options 1 and 2 at 0 and 20% RH observed in Table 6.4 may be explained by potential inaccuracy in the

calculated friction force existing between the subject and the back of the car seat, as three subjects with different physical build were involved during human-body experiments. Different characteristics of subjects are reported in Appendix 2a, Table 2. Also, the vinyl material used in small-scale testing was slightly different from the one which was the car seat cover.

Furthermore, in using equation 6.4 to determine the total discharge energy, one can assess the hazard involved in an ESD event in real-life conditions. Discharge energy is an important parameter to determine criteria for both incendive and non-incendive sparks due to electrostatic discharges (Owens, 1984; Glor, 1988; Rizvi, Smy, Crown, and Osei-Ntiri, 1991). This criterion could be implemented as a standard, based on MIE for different gas mixtures predicting safe wearing of protective clothing under hazardous environments.

References

Barnum, J. R. (1991). Sandia's severe human body electrostatic discharge tester (SSET). In EOS/ESD Symposium Proceedings Vol. EOS-13 (pp. 29-33). Rome, NY: The EOS/ESD Association and IIT Research Institute.

Berkey, B. D., Pratt, T. H., & Williams, G. M. (1988). Review of literature related to human spark scenarios. Plant/Operations Progress, 7(1), 32-36.

Cleves, A. C., & Sumner, J. F. (1962). The measurement of Human Capacitance and resistance in relation to electrostatic hazards with primary explosives (Report No. 18/R/62). Aldermaston, England: Atomic Weapons Research Establishment.

Consiglio, R. J., & Morgan, I. H. (1988). A method of calibration for human body model ESD testers to establish correlatable results. In EOS/ESD Symposium Proceedings Vol. EOS-10 (pp. 155-161). Rome, NY: The EOS/ESD Association and IIT Research Institute.

Fisher, R. J. (1989). A severe human ESD model for safety and high reliability system qualification testing. In EOS/ESD Symposium Proceedings Vol. EOS-11 (pp. 55-58). Rome, NY: The EOS/ESD Association and IIT Research Institute.

Glor, M. (1988). Electrostatic Hazards in Powder Handling. Letchworth, England: Research Studies Press.

Greason, W. D. (1992). Electrostatic discharge: A charge driven phenomenon. Journal of Electrostatics, 28, 199-218.

Greason, W. D. (1995). Quasi-static analysis of electrostatic discharge (ESD) and the human body using a capacitance model. Journal of Electrostatics, 35, 349-371.

Hearle, J. W. S. (1953). The electrical resistance of textile materials: Parts I to IV. Journal of The Textile Institute, 44, 117-198.

Hersh, S. P., & Montgomery, D. J. (1955). Static electricity of filaments. Experimental techniques and results. Textile Research Journal, 25, 279-295.

Movilliat, P., & Monomakhoff, H. (1977). Ignition of gas mixtures by discharge of a person with static electricity. In Proceedings of International Conference on Safety in Mines (pp. 230-242). Varna, Bulgaria.

Owens, J. E. (1984). Hazards of personnel electrification: Nomex vs. NoMoStat. Wilmington, DE: E. I. DuPont de Nemours & Co.

Ramer, E. M., & Richards, H. R. (1968). Correlation of the electrical resistivities of fabrics with their ability to develop and to hold electrostatic charges. Textile Research Journal, 38, 28-35.

Rizvi, S. A. H., Crown, E. M., Gonzalez, J. A., & Smy, P. R. (in press). Electrostatic characteristics of thermal-protective garment systems at various low humidities. Journal of The Textile Institute.

Rizvi, S. A. H., Crown, E. M., Osei-Ntiri, K., Smy, P. R., & Gonzalez, J. A. (1995). Electrostatic characteristics of thermal-protective garments at low humidity. Journal of The Textile Institute, 86, 549-558.

Rizvi, S. A. H., Smy, P. R., Crown, E. M., & Osei-Ntiri, K. (1991). Characterization of incendive and non-incendive spark discharges from surfaces of charged fabrics in an open hazardous environment. In M. W. King, International Conference on Fibre & Textile Science - 1991. Ottawa, ON. (pp. 187-190). London, UK: The Institute of Textile Science, The Fiber Society, The Textile Institute.

Sperber, W., & Blink, R. P. (1987). Characterization of electrostatic discharge generated by an occupant of an automobile. IEEE International Symposium on EMC, 360-363.

Sullivan, S. S., & Underwood, D. D. (1985). The automobile environment: Its effects on the human body ESD model. In EOS/ESD Symposium Proceedings Vol. EOS-7 (pp. 103-106). Rome, NY: The EOS/ESD Association and IIT Research Institute.

Tucker, T. J. (1968). Spark initiation requirements of a secondary explosive. Annals of the New York Academy of Sciences, 152, 643-653.

Wilson, L. G., & Cavanaugh, P. (1972). Electrostatic hazards due to clothing (Report No. 665). Ottawa, ON: Defence Research Establishment Ottawa.

Wilson, N. (1979). The nature and incendiary behaviour of spark discharges from the body. In B. C. O'Neill, Electrostatics'79 Vol. 48. Oxford (pp. 73-83). Bristol, UK: IOP Publishing Ltd.

Wilson, N. (1977/78). The risk of fire or explosion due to static charges on textile clothing. Journal of Electrostatics, 4, 67-84.

Chapter 7. Summary, Conclusions, Implications and Recommendations

In this chapter, the purpose, objectives, method, and findings of the overall study are summarized. Conclusions are then stated followed by implications and recommendations for industry and for further research.

Summary

The purpose of this research was to develop theoretical models and numerical techniques for explaining and predicting the static phenomenon during small-scale testing of two-layer fabric systems, and for assessing the electrostatic propensity of thermal protective clothing systems. The investigation addressed the following problems:

- 1.- How and why the charge dissipation process is affected by tribo-electrification, and does it vary from single- to multiple-layer fabric systems? Specifically, which elements or variables are involved and affect charge decay, and how can charge dissipation modelling help in decreasing the static hazard?
- 2.- What is the process of charge transfer between layers of fabrics during a small-scale test? What are the determinants of peak potential from either a surface or a capacitor? Can mathematical models discriminate measurements following different test methods?
- 3.- How can the relationship between human-body model and a small-scale tester be improved? Can a mathematical model be developed to predict the static behaviour of clothing systems from small-scale test data?
- 4.- Is there any small-scale test protocol which can reliably and accurately measure electrostatic characteristics of textile systems?, and can measurements taken by the method be meaningful for prediction of static hazard from a clothed person?

A human ecological perspective was introduced to the modelling process, so all interactions between a clothed person and each of the surrounding environments could be evaluated individually, as well as their interactions regarding the static hazard. Based on previous studies, the following assumptions were made:

- 1.- There is a combined effect of ambient temperature and moisture content of both the fibre and environment on static propensity of textile materials.
- 2.- Potentials from a textile surface and from a capacitor, generated as a result of tribo-electrification, differ in mechanisms of charge transfer and subsequent discharge.
- 3.- Potentials from either the textile surface or the capacitor are better predictors of electrostatic behaviour of clothing systems than is charge decay.

4.- An accurate and reliable prediction of static propensity is possible only if all the elements involved in an ESD event are taken into account in the model or models.

The study consisted of four parts. In the first part, mathematical models, based on theoretical knowledge, were developed to describe the electrostatic phenomenon, and theoretical models and numerical techniques were developed to predict the electrostatic propensity of thermal protective clothing systems. Then, the electrical and physical characteristics of thermal protective fabrics, used in the models, were measured, and tribo-electric charges and their subsequent dissipation or discharge were studied under different environmental conditions and on single- and two-layer specimens. The accuracy and reliability of results obtained from calculations using the mathematical models were then verified with the observed data. Finally, theoretical human-body models were also determined based on empirical data from small-scale tests and human-body experiments obtained in previous research (Crown, Smy, Rizvi and Gonzalez, 1995).

A modification to the draft ASTM Test Method for Evaluating Triboelectric (Static) Charge Generation on Protective Clothing Materials (F23.20.05) procedure is reported. The modification was developed to measure peak potentials and energies from a capacitor, as well as peak potentials and decay rates from the surfaces charged by tribo-electrification. The test system simulates a clothed human body rubbing an insulated surface and touching a grounded object, generating a spark of several thousand volts. Results from tests following both the proposed ASTM method and its modification were found reliable and accurate.

Mathematical models for charge decay of surface charges on thermal protective fabric surfaces are also reported. These models are used to determine the effect of surface characteristics on the static propensity of fabric systems, for example: time constant, capacitance of fabric surface, and other parameters of interest. Charge decay models could help to understand more fully the static phenomenon of surface charges generated by tribo-electrification, and why and how the charge decay of those charges differ from other types of surface electrification, induction-conduction and corona charging, as well as the suppression effect of multiple layers on charge dissipation.

Theoretical models to explain charge transfer between layers of fabric, measurement of charge from a textile surface, and electrostatic discharge from a capacitor, and the corresponding effects of humidity and temperature on potential and charge decay of fabric systems were developed and reported. With the use of these mathematical models, it is possible to explain the process involved in the charge generation, its transfer through fabric layers, and its consequent dissipation and/or discharge. Also, it is possible to explain how and why relevant independent variables mentioned above affect the static phenomenon.

Empirical models were the basis for theoretical equations and numerical techniques to assess the electrostatic propensity of thermal protective clothing systems in real-life conditions since small-scale and human-body data fit the linear model well. Therefore, the theoretical model was based on this model where different variables, for example, sliding speed, friction force, capacitance, etc., were incorporated. Different equations were determined for correlating data from either proposed or modified ASTM methods with human-body data.

Limitations

Before drawing conclusions from this study, the following limitations should be considered:

- 1.- Charge decay models can not be used for calculations of time constant for fabric systems with one or both layers containing conductive fibres. Fabrics with conductive fibres are not suitable for testing surface resistivity following known textile test method, (e.g. AATCC 76-1989), because their surface resistivity cannot be measured. A small charge applied between electrodes, in current standard test methods, flows through those conductive fibres, and the actual resistance measured in this case is the impedance of the equipment (Baumgartner, 1987).
- 2.- Use of the mathematical models developed here for calculating peak potentials from either a textile surface or a capacitor is limited to low relative humidity levels up to 30%. Beyond this level, new humidity constants for different fabrics should be determined. The limitation in use of the mathematical model for calculating peak potentials of two-layer systems is due to the change in the rate of moisture absorption of a fibre as the relative humidity increases, and its corresponding effect on the static propensity (Sereda and Feldman, 1964; Morton and Hearle, 1975). This change in absorption rate causes a change in humidity and temperature constants, b and c in equations 5.11 and 5.12, respectively. Constants b and c were determined for relative humidity ranging between 0 and 30%. The reported effect was mainly observed for those cellulose-based fabrics tested during the investigation.

Conclusions

The use of a human ecological framework provided a holistic and interdisciplinary approach to the study of the electrostatic phenomenon on textile materials and human beings, where the main effects of each variable involved and the interactions of those variables could be evaluated and incorporated into the developed equations. Incorporation of a human ecological

framework into textile science recognizes the dynamic, interdependent human-environmental relationships, the multi-disciplinary nature of the study of clothing and textiles, the integration of generalist and specialist knowledge, and the mission directed towards global well-being. Therefore, a human ecological perspective can promote broad-based, long term solutions to problems of everyday life as they relate to one of the most intrinsic of human environments, textiles and clothing.

An early objective of the researcher was to determine appropriate test method(s) to measure accurately and reliably electrostatic characteristics of textile materials (Gonzalez, 1995; Gonzalez et al, 1997). The draft ASTM method F23.20.05 was modified to measure potentials and energies from the discharge of a capacitor which has been previously charged from the tribo-electrification of a fabric system. The system was developed to provide: i) easy evaluation by automatically recorded frictional charge (voltage) and its decay curve, as well as the discharge of a previously charged capacitor, ii) high accuracy and reproducibility, iii) adequate size of specimens, and iv) easy and quick operation.

The objectives established at the beginning of this research to answer the research questions were achieved as it is explained in detail in the section which follows.

Objective 1

"To develop mathematical equations based on known theory to explain electrostatic phenomena in real-life conditions, and models to establish relationships between small-scale and human-body data." This objective was achieved as equations 4.4 for charge decay, and 5.17 and 5.18 for peak potential which incorporated the system, humidity and temperature components were developed for small-scale level; peak potentials of two-layer systems can be calculated by using results derived from single-layer tests. Equations 6.2 and 6.3 were developed to predict human-body peak discharge potentials from small-scale data calculated using equations 5.17 and 5.18, respectively.

The effect of multi-layer resistivity, which prevents resistivity tests from giving accurate measurements, can be calculated by considering a two-layer system as a two-resistor-in-parallel system (Eq. 4.3). According to the developed equations in Chapter 4, 4.2 and 4.4, the time constant of a two-layer fabric system is $\tau = R_p C$. This means that the time constant of a fabric system is the product of the total resistance of the parallel systems and the capacitance of the outer layer. Therefore, the influence of the inner layer-namely suppression effect-on the outer-layer charge decay is represented by the change in resistivity of the assembly.

Equations 5.6 and 5.10 suggest that the peak potential of a two-layer system is directly proportional to the peak potential of the outer fabric measured as single layer and indirectly proportional to the dielectric constant of the inner fabric. The effect of the inner-layer dielectric

constant is translated in more transfer of charge from the outer layer to the inner layer (i.e. suppression effect caused by the inner layer onto the outer layer) as the dielectric constant increases (Morton and Hearle, 1975). This has been confirmed by empirical testing where an inner layer of fabric with conductive fibres like aramid/carbon causes a greater decrease in peak potential of the outer layer in two-layer systems than cellulose based fabrics at low humidities. The exponential decrease in static potential due to humidity and temperature confirms several research works carried out for the last 40 years. Also, the combination of the humidity and temperature components in the complete theoretical model confirms that humidity has a greater effect than temperature on electrostatic characteristics of textile materials (Hearle, 1953).

Objective 2

"To measure some physical characteristics of the fabrics used during the investigation, and use these parameters in testing the models: a) dielectric constants ($K = \epsilon/\epsilon_0$) of fabrics at 0% RH; b) friction constants between two textile surfaces at different relative humidity levels and temperatures; and c) surface resistivity of fabrics at different relative humidity levels." Results of the measurement of these physical characteristics were used to test the different mathematical models. Dielectric constants were used in testing equations 5.17 and 5.18 (pp. 60 and 63) and shown in Appendix 3; friction constants were used in determining frictional forces included in equation 6.1 (Appendix 4); surface resistivity values for the different fabrics, shown in Appendix 5, were used in calculating time constants in testing equation 4.2.

Objective 3

"To measure peak potential of static discharges from fabric systems and capacitor at different relative humidity levels and temperatures." Appendix 6 shows the results obtained in measuring peak potentials from fabric surfaces and capacitor following the draft ASTM Method F23.20.05 and the modified ASTM Method, respectively. These peak potentials were measured for single- and two-layer test specimens at 0, 20 and 30% RH and room temperature. Also, peak potentials were measured following the draft ASTM Method at 4° and 30° C and 0% RH. No measurements following the modified ASTM Method were obtained due to limitations of space inside the cold room used for testing a low temperature.

Objective 4

"To measure charge decay time for the surface charge on fabric systems at different relative humidity levels and temperatures." The results of this objective are shown in Appendix 6. Values of percentages of the decayed charge at five seconds were recorded for single- and two-layer test specimens at 0, 20, and 30% RH and 4°, 22°, and 30° C.

Objective 5

"To determine mathematical relationships between peak potentials and charge decay and relative humidity, temperature, or fabric system; including interaction effects." Mathematical relationships were established between peak potentials and relative humidity, temperature, and fabric system. It was found that peak potential decreases as the relative humidity and temperature increase according to the exponential model of the general form $V = V_o \exp(ax)$, where a is a practical constant and x is the independent variable which could be either relative humidity (H) or temperature (T) as shown in equations 5.14 and 5.15. Values for the humidity (b) and temperature (c) constants are shown in Tables 5.3, 5.4 and 5.5. The mathematical relationship between peak potential and fabric system was established with equations 5.9 and 5.13 for surface potential and capacitive potential, respectively.

Objective 6

"To verify the developed theoretical mathematical models with observed data." The different mathematical models developed during this research were successfully tested as the calculated results were compared to observed values during small-scale testing; these comparisons are shown in Tables 4.2, 5.1, 5.2, 5.6, and 5.7.

Charge decay parameters for a two-layer system calculated from single-layer measurement using the equations fit well with empirical data from testing two-layer systems. In using data from single-layer testing, some negative effects observed during testing of charge decay, for example when charge flows only through conductive features of the specimen (Chubb, 1988), or a field suppression effect caused when non-homogeneous materials with different resistivity layers are used (Baumgartner, 1987), can be avoided and more reliable results may be achieved. The developed equations show the strong relationship between charge decay and resistivity of textile materials which has been the focus of several studies (Ramer and Richards, 1968; Jonassen, Hansson and Nielsen, 1979; Taylor and Elias, 1987).

In the case of peak potentials from either textile surface or capacitor calculated using the models, comparison between those calculations and observed data showed good agreement in most cases. In either case, following the proposed or the modified ASTM methods, the equations show how the inner layer affects the value of the peak potential as more conductive fabrics (i.e. higher dielectric constant) allow more charge to be transferred from the outer layer to inner layer and cause a suppression effect. They also show how the capacitance of the measuring system may change the final output of the static event. Despite the limitation stated previously regarding appropriate relative humidity range, the use of the models could be

extended to higher relative humidity levels with the determination of new humidity and temperature constants.

Objective 7

"To establish numerical techniques for the prediction of the static propensity of protective clothing systems by using: a) observed data from small-scale and human-body testing and, b) calculated data from mathematical equations developed in Objective 1." These two sub-objectives were achieved in Chapter 6. Empirical modelling was used to establish a numerical technique to predict the static propensity of thermal protective clothing systems. According to correlation and linear regression analyses, it was possible to establish a small-scale laboratory protocol to predict, from data on two-layer fabric systems, the electrostatic propensity of garment systems worn by workers in hazardous environments. A linear relationship of the general form $Y = a + mX$ was found between small-scale and human-body data. Based on this linear relationship and using equations developed for small-scale level, numerical techniques were determined for predicting body peak discharge potentials from small-scale peak potentials derived from single-layer tests. Theoretical equations based on the linear model and with the incorporation of variables involved in both human-body and small-scale ESD events-for example, friction force, sliding or rubbing speed, capacitance, etc.-were developed.

Incorporation of those variables into the model, as well as the system, humidity and temperature components, integrates and confirms to a great extent what was reported previously by other researchers regarding major determinants of sparking potential (Hersh and Montgomery, 1955; Wilson, 1987; Berkey et al, 1988). Furthermore, it is proposed that the hazard involved with the electrostatic propensity of human-body discharge potentials may be assessed by combining either equations 6.2 or 6.3 with the equation used to determine the electrostatic energy stored in a charged capacitor.

General Conclusions

One of the achievements of this research was to develop mathematical models which can determine electrostatic characteristics-namely peak potential and charge decay-of two-layer fabric systems by using data derived from single-layer tests. This can facilitate the determination of electrostatic propensity of fabric systems as less work will be required in testing only the outer layer of the systems as single layer, and combine these results with previously obtained data of dielectric constant, surface resistivity, and friction constant for the inner-layer fabrics.

Different mathematical equations were developed to explain the electrostatic phenomenon at small-scale level during test following the draft ASTM Method and its modification. Surface charge decay and peak potential from either a textile surface or a charged

capacitor can be evaluated by analyzing the different factors incorporated into the developed equations. Such analyses of the effect of dielectric and friction constants, humidity and temperature on those parameters can help to modify polymer and/or fabric structures to decrease the electrostatic propensity of textile materials and reduce the hazard involved with static discharges.

Modelling the relationship between small-scale and human-body data shows a simple linear relationship where human-body potentials can be calculated from small-scale data theoretically or empirically obtained, with incorporation as a constant of those variables acting during both human-body and small-scale static events. Their incorporation allows one to predict potentials under different conditions of a person's weight and height, surface electrification, and environment.

Tribo-electrification is responsible for most electrostatic nuisances and hazards in real-life situations, so it should be the preferred method of charging. In the past, some investigators, (e.g., Chubb, 1988), have reported that tribo-charging is notoriously unreliable and considerable effort may be needed to achieve consistent charging. The relatively low variation yielded here by results on potentials and charge decay may be explained by the high control of both the tribo-charging process of the equipment and experimental conditions maintained during the study.

Most of the variation observed in some of the comparisons shown in this dissertation could be explained by the fact that the same test specimens were used throughout the study. Changes on the surface structure of these fabric specimens due to the abrasive action of the frictional charging during tests may account for differences in calculated and observed values. Variation may also be explained by the loss of some topical finishes that some of the test fabrics had due to abrasion during tribo-charging.

Implications and Recommendations

Implications and Recommendations for Industry

It has been demonstrated that both peak potential and charge decay parameters calculated from the equations using data from single-layer measurements fit well with empirical data from the two-layer systems of the same fabrics. Use of the models, therefore, will allow one to determine in advance how fabrics will behave when used together with other fabrics in a clothing system. Such predictions will be useful for manufacturers in designing two-layer garments, and for users in combining garments of different fabrics into clothing systems.

The use of single-layer measurements with the equations will allow the evaluation of two-layer systems, something which is not possible in some tests like surface resistivity and charge decay because the charge applied or generated on the textile surface of the system tends to flow

through the more conductive layer of the system. Also, with the use of only single-layer measurements, quicker and more cost effective testing can be carried out for laboratories evaluating static propensity of textile systems because there is no need to evaluate each possible combination of fabrics.

The prediction of human-body potentials at low humidities makes it possible to know in advance the static hazard that a clothed person may have working in a hazardous environment. This static hazard can be determined by the calculation of the total discharge energies from those predicted potentials using equation 6.4. These calculated energies can then be compared to the MIE of different flammable gases, vapours, dust, etc. to determine safety levels of wearing clothing systems under specific environments.

Implications and Recommendations for Further Research

The following are suggestions for further work in this field:

- 1.- Further analysis of the meaning of the models of the electrostatic phenomenon, and its implications for the static propensity of textile materials, i.e. how those parameters found to play important roles in an ESD event can be varied or eliminated so the static hazard may be reduced.
- 2.- Some means to measure surface resistivity from fabrics containing conductive fibers should be developed.
- 3.- Further research is required to determine new humidity and temperature constants for relative humidity above 30% and temperatures below zero degree Celsius. Also, more work is recommended to incorporate into the models the change in absorption rate, as well as the effect of mono-molecular layer of water. The convenience of use of absolute temperatures (K) should be also considered.
- 4.- Further study on static electrification is needed to predict the polarity of the charge and its incorporation into the developed models.
- 5.- More research is required to improve the accuracy of human-body models at different relative humidity levels.
- 6.- More work is needed to determine if the models used for predicting body potentials are valid for other typical physical human activities.
- 7.- Further work should be pursued to develop a safety code for wearing protective clothing in flammable and explosive environments. This code could be based on MIE for different gases, mixtures, dust, etc.

References

Baumgartner, G. (1987). A method to improve measurements of ESD dissipative materials. In EOS/ESD Symposium Proceedings Vol. EOS-9 (pp. 18-27). Rome, NY: The EOS/ESD Association and IIT Research Institute.

Berkey, B. D., Pratt, T. H., & Williams, G. M. (1988). Review of literature related to human spark scenarios. Plant/Operations Progress, 7(1), 32-36.

Chubb, J. N. (1988). Measurement of static charge dissipation. In J. L. Sproston (Ed.), Electrostatic Charge Migration (pp. 73-81). Bristol, UK: IOP Publishing Ltd.

Crown, E. M., Smy, P. R., Rizvi, S. A., & Gonzalez, J. A. (1995, June 30). Ignition hazards due to electrostatic discharges from protective fabrics under dry conditions. In Final Report Presented to Alberta Occupational Health and Safety, Heritage Grant Program. Edmonton, AB: University of Alberta.

Gonzalez, J. A. (1995). Development of a laboratory protocol to predict the electrostatic propensity of clothing systems. Unpublished master's thesis, University of Alberta, Edmonton, AB.

Hearle, J. W. S. (1953). The electrical resistance of textile materials: Parts I to IV. Journal of The Textile Institute, 44, 117-198.

Jonassen, N., Hansson, I., & Nielsen, A. R. (1979). On the correlation between decay of charge and resistance parameters of sheet materials. In B. C. O'Neill, Electrostatics'79 Vol. 48. Oxford. (pp. 215-224). Bristol, UK: IOP Publishing Ltd.

Morton, W. E., & Hearle, J. W. S. (1975). Electrical resistance. In W. E. Morton, & J. W. S. Hearle, Physical Properties of Textile Fibres (2nd ed.) (pp. 502-528). London: William Heinemann Ltd and The Textile Institute.

Ramer, E. M., & Richards, H. R. (1968). Correlation of the electrical resistivities of fabrics with their ability to develop and to hold electrostatic charges. Textile Research Journal, 38, 28-35.

Sereda, P. J., & Feldman, R. F. (1964). Electrostatic charging on fabrics at various humidities. Journal of The Textile Institute, 55, 288-298.

Taylor, D. M., & Elias, J. (1987). A versatile charge decay meter for assessing antistatic materials. In B. C. O'Neill, Electrostatics'87 Vol. 85. Oxford (pp. 177-181). Bristol, UK: IOP Publishing Ltd.

Wilson, N. (1987). Effects of static electricity on clothing and furnishing. Textiles, 16(1), 18-23.

APPENDICES

Appendix 1. Some Characteristics of Textile Fibers which Make up the Fabric Systems

100% Non-FR Cotton

Cotton fibers are made up of natural cellulose. Two anhydroglucose units combine first to form cellobiose units which then combine to form cellulose. About 70 - 75% of the cotton fiber is crystalline, and 30 - 25% is amorphous. At 65% relative humidity and 21 °C, its moisture regain¹ is 8.5%.

FR Cotton

FR cotton was FR finished with the Proban chemical² and chemically polymerized with ammonia gas. FR cotton fiber has a moisture regain³ of 7 - 8% at 21° C and 65% relative humidity

Aramid/Carbon Sheath Core

Aramid/carbon sheath core (Nomex IIIA ®) fiber is made of 98% aramid fiber and 2% sheath core fiber. Aramid is a "manufactured fiber in which the fiber-forming substance is any long-chain synthetic polyamide in which at least 85% of the amide (CONH) linkages are attached directly to two aromatic rings (TFPIA⁴).” The aramid component of the used fiber is made of 93% of meta-aramid fiber (Nomex ®) and 5% of para-aramid fiber (Kevlar ®). The sheath core fiber is made of 96% of nylon 6,6 fiber (sheath) and 4% core which is made of 70% polyethylene fiber and 30% carbon fiber. The moisture regain³ of aramid fibers is 4 - 5% at 21° C and 65% relative humidity.

Aramid/PBI (Polybenzimidazole)

Aramid/PBI fibers are a blend of 60% aramid and 40% PBI which is a "manufactured fiber in which the fiber-forming substance is a long-chain aromatic polymer having recurring imidazole groups as an integral part of the polymer chain (TFPIA³).” Aramid/PBI fiber has a moisture regain³ of 7 - 8% at 21° C and 65% relative humidity.

Aramid/FR Viscose

Aramid/FR viscose fibers are made of 50% Kermel ® fiber and 50% FR viscose fiber. Kermel ® is a polyamide-imide fiber (aramid) made from trimellitic anhydride chloride and either a diamine or a diisocyanate. FR viscose is a cellulose-based man-made fiber in which substituents have replaced not more than 15% of the hydrogens of the hydroxyl groups, and has a fire retardant finish of a halogenated alkyl phosphate type. The moisture regain³ of this blend is 7.5% at 21° C and 65% relative humidity.

¹ Hatch, K. (1993). Cotton fibers. In Textile Science (p.166). Minneapolis/St Paul, MN: West Publishing Co.

² (CH₂OH)₄P⁺X⁻, tetrakis(hydroxymethyl)-phosphonium (THP) salt, where X=Cl,OH,(1/2)(SO₄)²⁻ as a condensate with urea

³ Moisture regain was determined following ASTM 2654 Standard Test Methods for Moisture in Textiles

⁴ The Textile Fiber Products Identification Act (USA)

Appendix 2a.**ELECTROSTATIC CHARACTERISTICS OF THERMAL PROTECTIVE GARMENTS AT LOW HUMIDITY**

A revised version of this paper has been published as:

Reference: Rizvi, S. A. H., Crown, E. M., Osei-Ntiri, K., P. R. Smy, & Gonzalez, J. A. (1995). Electrostatic characteristics of thermal protective garments at low humidity. Journal of The Textile Institute, 86, 549-558.

ABSTRACT:

The electrostatic discharge between a clothed human body and ground has been investigated under conditions of low atmospheric humidities. Measurements were carried out for two experimental configurations which arose from electrostatic charge build up from two different types of human activity. Discharge current wave forms and other discharge parameters were monitored for each clothing system and a correlation between the discharge energy and each fabric system was established. Maximum discharge energies up to 15 mJ and peak potentials up to 13 kV were observed.

Introduction

Electrostatic charges which develop on fabrics can produce many undesirable effects. Some fibers have high resistivity at moderate humidities, and so the fabrics retain any generated charge for some time because of the low electrical leakage. Often, these charges are harmless, causing only "cling" between adjacent layers of fabrics; in other situations [1] they produce sparks which can be dangerous in flammable environments such as those encountered in the petrochemical and gas industries.

At present, there is no accepted policy regarding electrostatic charges on clothing nor are there any generally accepted standards in the gas and petrochemical industries. In Alberta, as in most jurisdictions clothing policy and standards are essentially left to the discretion of each individual firm. A variety of anti-static techniques are now being used in the hazardous workplace. These range from temporary organic additives to the use of permanent conductive fibers in the fabrics. Fabrics of particular interest here are the fabrics used in flame retardant thermal protective clothing specifically intended for use in hazardous situations.

Most of the research reported to date on clothing hazards of this kind has been conducted at normal values of room temperature and significant levels of humidities (e.g. about 20%) [2-4] and no thorough investigation has been carried out into the static propensity of the thermal protective fabrics now available in the market. In Canada and in some other parts of the world many industrial workers are required to carry out their duties in very cold and therefore very dry atmospheres. In this paper, we report on a study of the accumulation and subsequent discharge of the electrostatic charge from a human body wearing thermal protective garments at low humidities. Because charges generated on the outer layers of garments can be induced onto the body which in turn can generate a spark on contact with an earthed or large

conductor, other parameters such as the potential (developed on a human subject due to some activity), charge and energy in a spark have also been determined. In most of the work reported so far [2,5], the emphasis was only on the outermost garment but here the effect of variations of the inner layers has also been investigated.

The purpose of the study was to determine the characteristics of discharges from different thermal protective garment systems and to determine the resulting electrostatics hazard in flammable environments under cold dry conditions. The research hypothesis was that the electrostatic propensity of the protective garment systems would differ.

Methods

When considering garment systems (i.e. layers of clothing) on the human body, the situation becomes more complex than when one is merely testing single layers of fabric. This is especially so if some of the layers are blends of different fibers. Because of their relative places on the tribo-electric series, charges generated on such fabrics through the contact layers within the system may tend to cancel each other out. It is therefore more likely that significant charges will be generated and retained on the garment system or the body when it is in contact with some other external material (for example, in rubbing against a car seat when getting out of a car) or through the removal of one part of the system (i.e. the outer layer). For this reasons, two different experiments were performed, one involving frictional rubbing and the other, removal of the outermost garment.

Materials:

In this study different thermal protective garment systems were used. Combinations of 100% Aramid, Aramid/carbon, Aramid/stainless steel and FR cotton were used as the outer garments (parka or coverall) and 100% Aramid, Aramid/carbon, 100% cotton and FR cotton were used as shirt. While 100% cotton under garments (vest, underwear, socks) were used. In experiment one, coveralls were

worn over shirts and pants while in experiment two insulated parkas were worn over and then removed from shirts and pants (Table 1). There were total of 15 different garment combinations for three subjects for the first experiment. As the pattern in both experiments was expected to be somewhat similar, only 8 different garment combinations for two subjects were investigated in the second experiment. The garments for each experiment were all purchased from the same source and were of the same design and color. All subjects wore identical insulating rubber-soled (2 cm thick) shoes during the experiment.

Procedure:

All experiments were conducted in a room sized, zero humidity chamber, at room temperature. The relative humidity in the chamber was carefully controlled and monitored. It could be varied from normal levels down to close to 0%, while the temperature remained at 22°C. Standard procedures were followed for the conditioning of the garment systems in both experiments. First all the garments were washed following CGSB method and then conditioned by hanging them in the environmental chamber, keeping them separated to allow free circulation of air, for at least 24 hours prior to conducting the experiment. All garment systems were tested on three different subjects having significantly different physical characteristics of height and weight. Each experiment was replicated for each subject at least ten times.

The independent variables in both experiments were the garment systems and the human subjects. The dependent variables included discharge potential, total charge transferred and discharge energy. The two experiments involved two different types of physical activity. The first experiment consisted of the frictional charging of a human subject wearing a specified garment system and sliding across a vinyl covered bench car seat. The car seat was permanently stationed in the environmental chamber. The sideways force and the normal reaction exerted during the sliding process were carefully monitored.

The second experiment measured the charge accumulated on a human subject when carrying out simple movements such as walking for a fixed number of steps at a predetermined speed and then removing an outer garment such as a parka. In both experiments the quantity of charge and the discharge energy were measured as the human body (a conductor) touched a grounded object at the end of each test

Measurement of Dependent Variables

Discharge potential was measured across a grounding resistor. The "ground", used to measure the parameters of the discharge, was a pointed conical steel electrode of 1 mm end diameter which was in turn grounded through a 100 kilo-ohm resistor. The subject touched the grounded electrode with an index finger immediately after performing one of the two sets of physical activities. The discharge potential was recorded across the grounding resistor by using a Tektronix model 2430A digital oscilloscope with a 1000x {P-6015} Tektronix probe (impedance 100M Ω). Little charge was lost during the interval between body charging and discharge as was verified by the charge decay curves described elsewhere [6]. The digitized information so obtained was used to provide a hard copy of the discharge voltage wave form from which the transferred charge, discharge energy, peak current, current duration and other parameters of interest were calculated.

The total charge flow (transferred), Q , was calculated by the time integral of the discharge potential, V , divided by the grounding resistance:

$$Q = \int i \, dt = (1/R) \int V \, dt \quad (1)$$

The total energy was determined via equation.(1) by calculating the product of the total charge and the potential:

$$E = (1/2) QV \quad (2)$$

The measurements can be considered as being done in two parts; Experiment 1 and Experiment 2. All three parameters, discharge potential, charge transferred, and

discharge energy were measured as a function of time.

Statistical Analysis:

A statistical analysis of all experimental data was carried out using commercially available software, SPSS vers. 6.0. One of the available statistical analysis tools -ANOVA (analysis of variance) both one way and multivariate were used to analyze the various clothing configurations.

An ANOVA test was performed on each set of data for all the garment combinations. A hypothesis was formulated that there were no significant differences among the means of the discharge potentials and energies for the garment combinations with the same outer garment. So, a null hypothesis was postulated that the mean of all the discharge potentials for the four main garment groups were same.

Results:

Experiment 1:

ANOVA analysis by using SPSS software resulted in the rejection of the null hypothesis at the 0.05 significance level for both the discharge potentials and energies. Thus the ANOVA test confirmed that all the four garment groups are distinct. Statistical tests were repeated for each of the three subjects separately with very similar results.

When the results from different subjects were compared, it was found that the results for each subject were statistically different at the 0.05 significance level. It was found that the discharge potential and energy could vary by up to 50% from one subject to another under similar conditions.

Two way analysis confirmed that there was a significant difference between the (garment) systems, as well as between the subjects. Moreover, there was a significant interaction between the systems and the subjects. The same trend was observed for both the measured discharge potentials and the energies.

It was found that the peak discharge potentials and consequently the discharge

energies varied with the different garment combinations and subject. Because safety studies, of necessity, focus on the "worst case" scenario, the maximum, as well as mean discharge potentials and energies for all three subjects together are shown in Figures 1 and 2. The same trend was observed for each individual with very few exceptions. For all three subjects the highest (both mean and maximum) discharge potentials were observed with garment system 8. The lowest discharge potentials were observed for garment systems 11 for the subjects "K" and "J". But, for the subject "R" the lowest mean potential was observed for the garment system 7. However, a statistical analysis confirmed that there was no significant difference at 95% confidence level between garment systems 11 and 7.

Among the subjects, subject "R" had the lowest potential with a mean of only 5.22 kV for all the fifteen garment systems, followed by the subject "K", with an average of 5.82 kV. The highest mean value was observed for subject "J" with an average potential of 6.4 kV. Therefore, it is evident that discharge potential could vary up to 20% from one subject to another.

The difference in the results from one subject to another can be attributed to either statistical variation or to the physical characteristics of the individuals. Some correlation was found between the physical characteristics of a subject, as shown in Table 2, and the charging process, the higher the weight to height ratio of an individual subject, the more likely the subject will be charged to a higher discharge potential.

Although significant differences in the results were observed for different subjects wearing the same garment systems it was found that the largest variation in potential as well as in the energy arose from the use of different garment systems.

The discharge parameters in Figures. 1 & 2 are plotted in increasing order of magnitude. It was found (Figure 3) that the inner garments like pants do not significantly affect the discharge parameters. Therefore, the different garment systems are grouped, according to the material in the coverall (outer layer) based on the results

shown in Figure 4. It was confirmed by the SPSS analysis using Duncan's Multiple Range Tests for both the discharge potentials and energies. Because within each group (the homogeneous subsets) highest and lowest means were not significantly different.

In general all the garment combinations could be grouped according to their outer garments except garment systems 9 and 15. This discrepancy could be explained if friction between similar surfaces results in higher potentials while friction between static outer layer and anti-static inner layer produces less energy. Within each of the Aramid and FR cotton groups, it was found that the systems with shirts and coveralls of the same material (garments systems 9 and 8) produced the highest discharge potentials in their respective groups. So, the garment system 9 with similar fabrics (100% Aramid) yielded a significantly higher discharge potential/energy than all the garment combinations in the respective group. On the other hand, garment system 15 should have produced higher potential/energy but the systems with the inherently anti-static fibers (Aramid/carbon) as the inner layer produced less discharge potential/energy.

The lowest and the highest mean discharge potentials of 1.71 kV and 12.60 kV were observed for the garments systems 11 and 8, respectively. Thus, a garment combination with FR-cotton could result in seven times higher discharge potentials than a garment combination with anti-static Aramid/carbon fibers in the outer layer. Consequently, the spark energy could vary by a factor of up to 10X depending on which combination of garments was used posing a significant increase in the risk involved.

The characteristics of each group of garment systems can be studied by comparing the average discharge potentials for the various groups. The Aramid/carbon group had the lowest average discharge potential value of 3.11 kV among all the four groups. Next was the Aramid/s.steel group with an average of 4.78 kV. Aramid and FR cotton groups had further higher average discharge potential values of 6.64 and

7.33 kV, respectively. The increase in the average discharge potential from Aramid/carbon to Aramid/s.steel was more than 50%, and from Aramid/s.steel to Aramid was almost 40%, whereas the increase from Aramid to FR cotton was just over 10%.

Besides the average values of the discharge parameters it is also important to know the variations in the results within each group of garment systems. It was found that the Aramid/carbon group had the lowest standard deviation of 0.91 kV compared with 1.05 kV for Aramid/s.steel. Aramid and FR cotton had even higher standard deviations of 1.66 kV and 1.79 kV, respectively.

Another parameter of interest was the absolute value of the electrostatic energy stored on the human body. The average as well as the maximum discharge energies for all the three subjects for different garment systems are shown in Figure 2. The values are presented in increasing order of magnitude.

It was found that under conditions of near zero humidity, typical of the situation experienced on an extremely cold day, sliding off a car seat may charge a person wearing protective garments up to a potential of 13 kV and so produce a maximum discharge energy of 15 mJ in a body discharge. FR cotton as interior as well as exterior layer (garment system 8) produces the highest discharge energy (average energy of 6.8 mJ and maximum energy of 14.9 mJ) followed by 100% Aramid (garment system 9) as the inner and outer fabric (average energy of 5.9 mJ and maximum energy of 11.2 mJ). On the other hand, the garment system 11 with Aramid/carbon as the outer layer and Aramid as the inner layer yielded the least with an average energy of 0.7 mJ and a maximum energy of 1.4 mJ only. . As shown in Figure 2, both mean and maximum energies vary by almost an order of magnitude among the various garment systems. It was also found that the maximum values could be twice as large as the average values.

Experiment 2

A statistical analysis of experimental data was also carried out for experiment 2. A one way ANOVA test of both potentials and energies confirmed that all the three garment groups were distinct. These statistical tests were repeated for the two subjects with very similar results.

The two way ANOVA analysis confirmed that there was a significant difference between the garment systems, as well as between the subjects. It was found to be same as in experiment 1 for both potentials and energies. The 2-way analysis showed some interaction between the garment systems and the subjects.

Eight different garment systems (Table 1) were selected for the experiment. Both the mean and maximum discharge potentials and energies for two subjects are shown in Figs. 5 & 6. In experiment 2, Aramid/carbon (garment system 203) yielded the lowest (average potential of 1.4 kV and maximum potential of 2.3 kV) and the Aramid (garment system 204) produced the highest values (average potential of 1.4 kV and maximum potential of 2.3 kV). While FR cotton produced the intermediate values.

The systems (203) with the anti static fibers (Aramid/carbon) in the parka layer produced the lowest energies (average energy of 0.2 mJ and maximum energy of 0.6 mJ). The garment system (204) which produced the highest energies (average energy of 3.2 mJ and maximum energy of 5.8 mJ) had no anti-static fibers in the system and included parkas and shirts made of 100% Aramid and 100% cotton, respectively.

Comparison of the results for each experiment gives some insight into the discharge process. When charge is produced by separation of layers it is expected that layers of different materials will produce more charge than with layers of the same material, which is just the opposite scenario observed in experiment 1. The garment

system 207 (garment system 8 in experiment 1) with FR cotton no longer produced the highest energy or the highest potential as was the case in experiment 1. But the garment system 203 (garment system 11 in experiment 1) with Aramid/carbon produced the lowest energy/potential as was the case in experiment 1. This could be easily explained on the basis of the difference in charging mechanism, frictional against separation of layers.

Contrary to the results of experiment 1, a remarkable difference in the results is that the absolute values for the potentials were found to be almost half (57%) and the energy values were found to be almost one third (35%) of those in experiment 1. Consequently, in experiment 2, the corresponding variations in the potential and energy values were almost one quarter (72%) and one half (48%) than observed in experiment 1 which in turn significantly lower than reported elsewhere [3].

Some similarities were found between the two experiments. The behavior of all the 8 garment systems in experiment 2 could be grouped statistically on the basis of their outer layers as in experiment 1. The lowest discharge potential/energy was observed for the garment systems with anti-static fibers in the outer layer and the highest discharge potential/energy was observed for the garment systems with non anti-static fibers (outer layer).

Ignition Threshold

The minimum ignition energy to ignite methane and air in a closed chamber by a spark between a finger and an earthed electrode was first evaluated as 18.6 mJ [2], then 5.9 mJ [7], 1.1 mJ [8], and was as low as 0.5 mJ [5]. The experiments were performed under different conditions i.e. different gas mixtures. electrode sizes and body capacitances. At present the most commonly used value is about 1 mJ.

The experimental results show that a subject wearing an Aramid with anti-static fibers generates the lowest discharge energy. In experiment 1, the average

discharge energy for all the three subjects for the garment system 11 as shown in Figure 2 is less than 0.68 mJ which is below the minimum threshold [8] for the ignition of methane and air in a closed chamber. However, the maximum discharge energy observed (15 mJ), Figure 2, for all the three subjects exceeds this minimum threshold by a very substantial factor. In experiment 2 (Figure 4), however the average and the maximum discharge energies produced by the garment systems (garment system 201, 202, and 203) with Aramid/carbon in the outer layer were found to be less than the ignition threshold of 1.1 mJ.

Body Resistance and Capacitance:

To understand the variation in the results from one subject to another, some parameters representative of the physical characteristics of the subjects were determined (Table 2). Estimates of these parameters can be made from the discharge wave form characteristics. The body capacitance (C) can be estimated from the charge transferred in a discharge, while the equivalent series resistance (R) can be determined from the wave form decay. It was found that the subject K had the highest average body capacitance of about 230 pF followed by subjects R and J with 195 pF and 190 pF, respectively.

The subjects K, J, and R had an average body resistance of 69, 56, and 55 kilo-ohms, respectively. No correlation was found between the electrostatic discharge energy and the body capacitance. However, the average potential of each of the 15 garment combinations in experiment 1, shown in Table 2, could be correlated to some extent with the weight to height ratio.

Conclusion:

In dry conditions frictional activity such as sliding off a car seat can result in a discharge energy of up to 15 mJ and could charge a person wearing protective

garments up to 13 kV. Separation rather than rubbing of the garments decreased the energies by almost one third.

Although the nature of the inner garments does affect the discharge, it was found that the outer layer was the most significant (Fig. 4). All 15 garment systems can be classified into four distinct groups formed on the basis of the outer garments. At low relative humidities, Aramid/carbon group yielded the lowest potential/energy in both experiments with the least variation. The highest potential/energy was observed for the FR cotton and Aramid groups as the outer garments in experiments 1 and 2, respectively. In most of the cases, FR cotton garments were found to perform no better than systems containing 100% Aramid.

Garment systems with anti-static fibers (Aramid/carbon and Aramid/s.steel) are found to be the safest garment combinations in low humidity environments but they may still develop sufficient charge due to frictional work to ignite flammable gases. Among the anti-static garment systems Aramid/carbon was found to be better than Aramid/s.steel, producing much less discharge energy for all the subjects.

Unlike previously reported results [3] of charge variation of three orders of magnitude for different subjects, we found a variation of less than 50%- perhaps due to the highly controlled conditions of the experiment.

References:

- [1] Rizvi, S.A.H. and Smy, P.R. (1992), "Characteristics of incendive and non-incendive spark discharges from the surface of a charged insulator", *Journal of Electrostatics*, 27, 267-282.
- [2] Wilson, N. (1977). "The risk of fire or explosion due to static charges on textile clothing". *Journal of Electrostatics*, 4, 67-84.
- [3] Veghte, J.H. and Millard, W.W. (1963). "Accumulation of static electricity on arctic clothing", (Technical Documentary Report AAL-TOR-63-12), Alaska: Arctic Aeromedical Laboratory.
- [4] Phillips, D.E. (1982). "Testing for electrostatic generation and dissipation", Maryland: Defense Technical Information Centre (DTIC), inclosure 2, p. 1.
- [5] Crugnola, A.M. and Robinson, H.M. (1959). "Measuring and predicting the generation of static electricity in military clothing", (Report No. 110). Massachusetts: Quartermaster Research and Engineering Centre, p.9 and p.56.
- [6] Bailey, A.G., Smallwood, J.M. and Tomiat, H. (1991). "Electrical discharges from the human body", *Institute of Physics Conference Series*, No. 118, p. 102.
- [7] Movillat, P. and Monomakhoff, H. (1977), "Ignition of gas mixtures by discharge of a person charged with static electricity", Paper C3, presented at the International Conference of Safety in Mines Research, Varna, Bulgaria, p. 230-242, Oct. 1977.
- [8] Tolson, P. (1980). "The stored energy needed to ignite methane by discharges from a charged person". *Journal of Electrostatics*, 8, p.293.

LIST OF TABLES AND FIGURES

- Table 1. Garment systems for experiments 1 and 2.
- Table 2. Comparison of weight/height ratio, body capacitance and RC among three subjects.
- Figure 1. Mean and maximum body discharge potentials for experiment 1 and for three subjects.
- Figure 2. Mean and maximum body discharge energies for experiment 1 and for three subjects.
- Figure 3. Boxplot of energy by coverall by pants.
- Figure 4. Boxplot of energy by coverall by shirt.
- Figure 5. Mean and maximum body discharge potentials for experiment 2 and for two subjects.
- Figure 6. Mean and maximum body discharge energies for experiment 2 and for two subjects.

Table 1.

SYSTEM	COVERALL	SHIRT	PANTS
1	100% Aramid	100% cotton	100% cotton
2	Aramid/s.steel	100% cotton	100% cotton
3	Aramid/carbon	100% cotton	100% cotton
4	FR cotton	100% cotton	100% cotton
5	100% Aramid	FR cotton	FR cotton
6	Aramid/s.steel	FR cotton	FR cotton
7	Aramid/carbon	FR cotton	FR cotton
8	FR cotton	FR cotton	FR cotton
9	100% Aramid	100% Aramid	FR cotton
10	Aramid/s.steel	100% Aramid	FR cotton
11	Aramid/carbon	100% Aramid	FR cotton
12	FR cotton	100% Aramid	FR cotton
13	100% Aramid	Aramid/carbon	100% cotton
14	Aramid/carbon	Aramid/carbon	100% cotton
15	FR cotton	Aramid/carbon	100% cotton
SYSTEM	PARKA	SHIRT	PANTS
201	Aramid/carbon	100% cotton	100% cotton
202	Aramid/carbon	FR cotton	FR cotton
203	Aramid/carbon	100% aramid	FR cotton
204	100% aramid	100% cotton	100% cotton
205	100% aramid	FR cotton	FR cotton
206	100% aramid	Aramid/carbon	100% cotton
207	FR cotton	FR cotton	FR cotton
208	FR cotton	Aramid/carbon	100% cotton

Table 2.

	J	K	R
WEIGHT (kg)	77.00	84.00	68.00
HEIGHT (m)	1.63	1.78	1.68
RATIO WEIGHT/HEIGHT	47.24	47.19	40.48
MEAN POTENTIAL (kV)	6.10	5.71	4.87
MEAN ENERGY (mJ)	4.15	4.21	2.68
BODY CAPACITANCE (pF)	188.74	230.39	194.74
RC (μ s)	10.58	15.99	10.65

Figure 1.

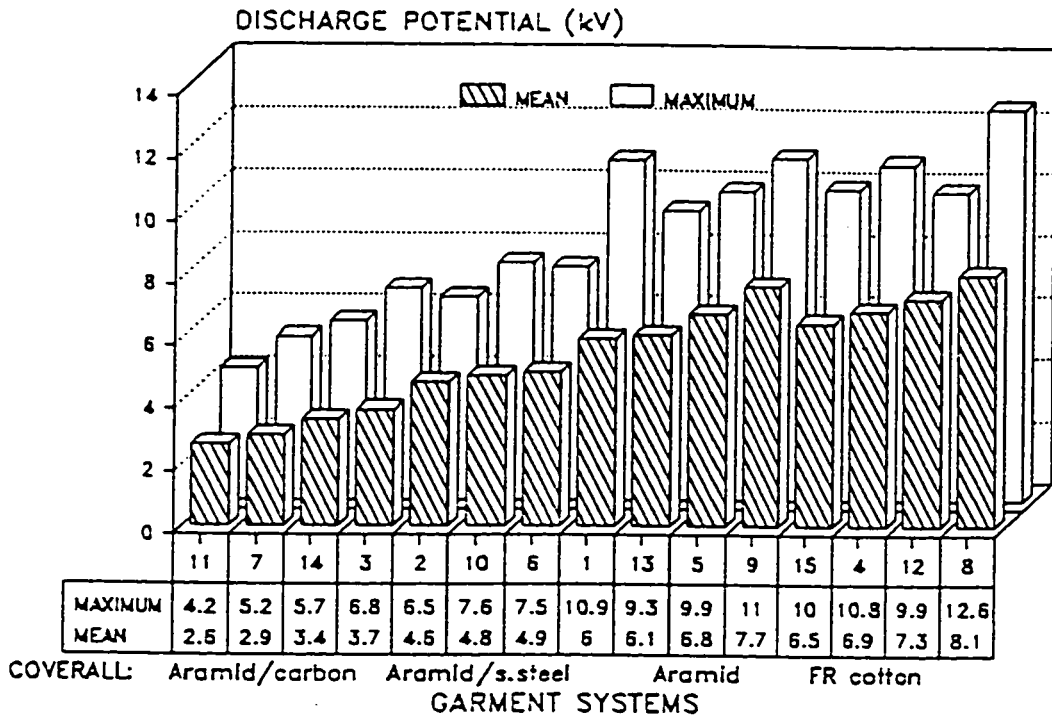


Figure 2.

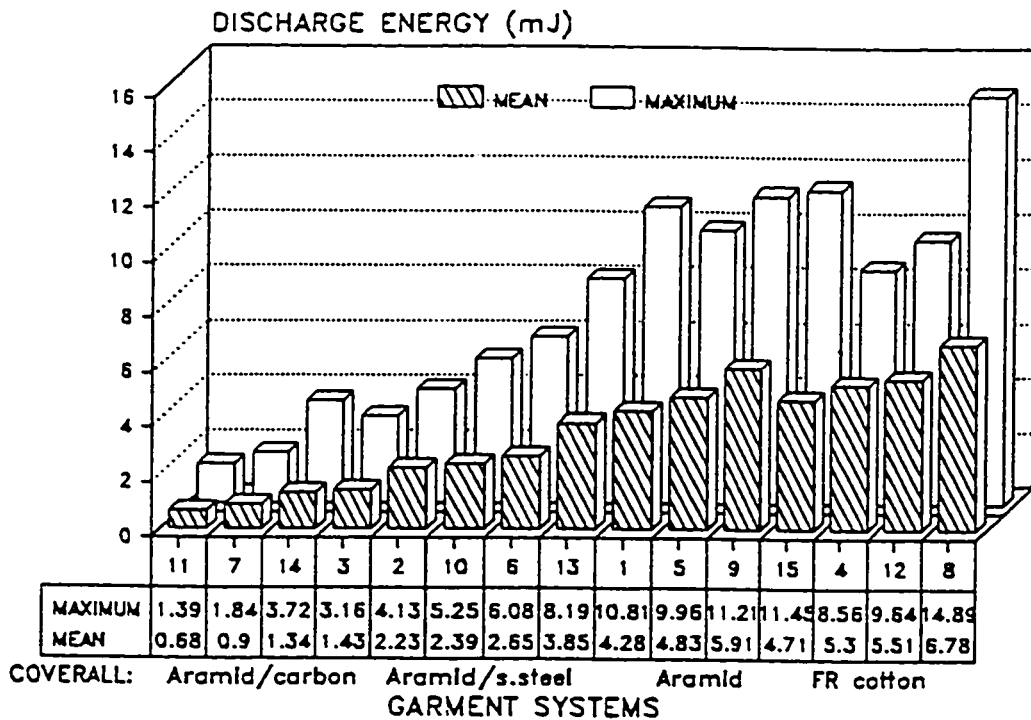


Figure 3.

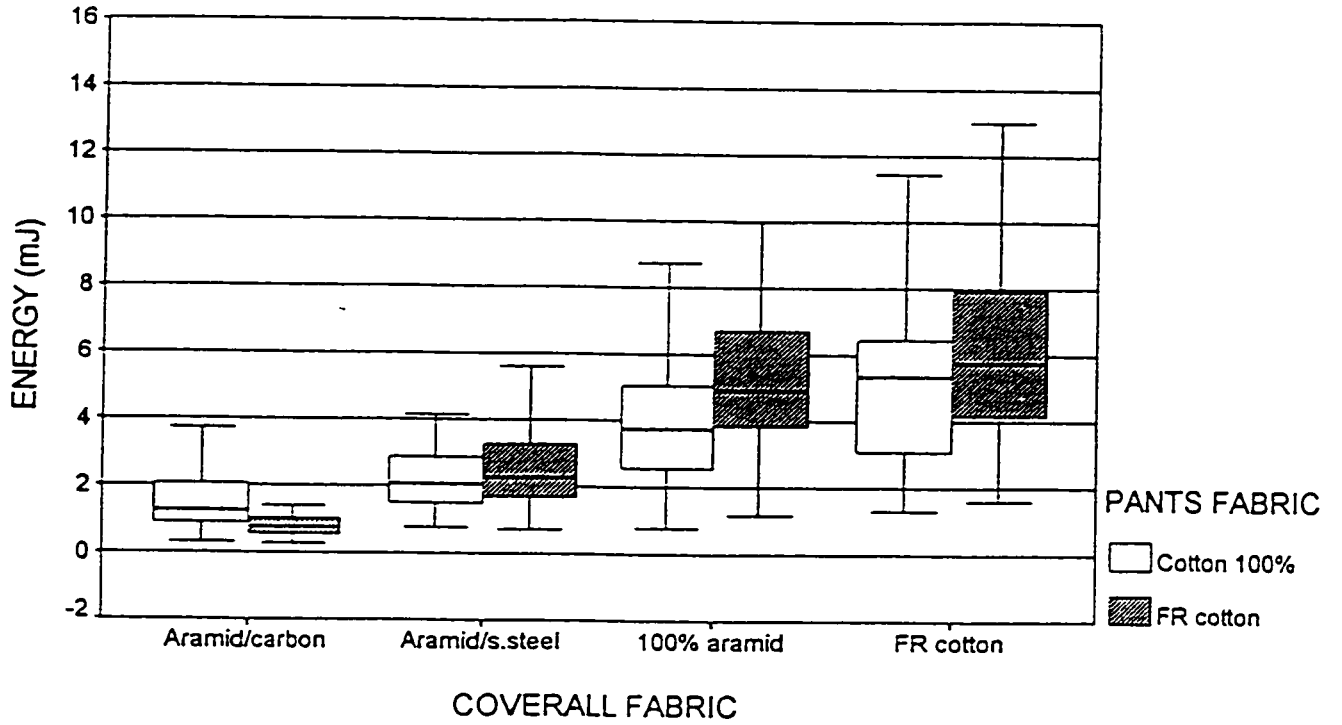


Figure 4.

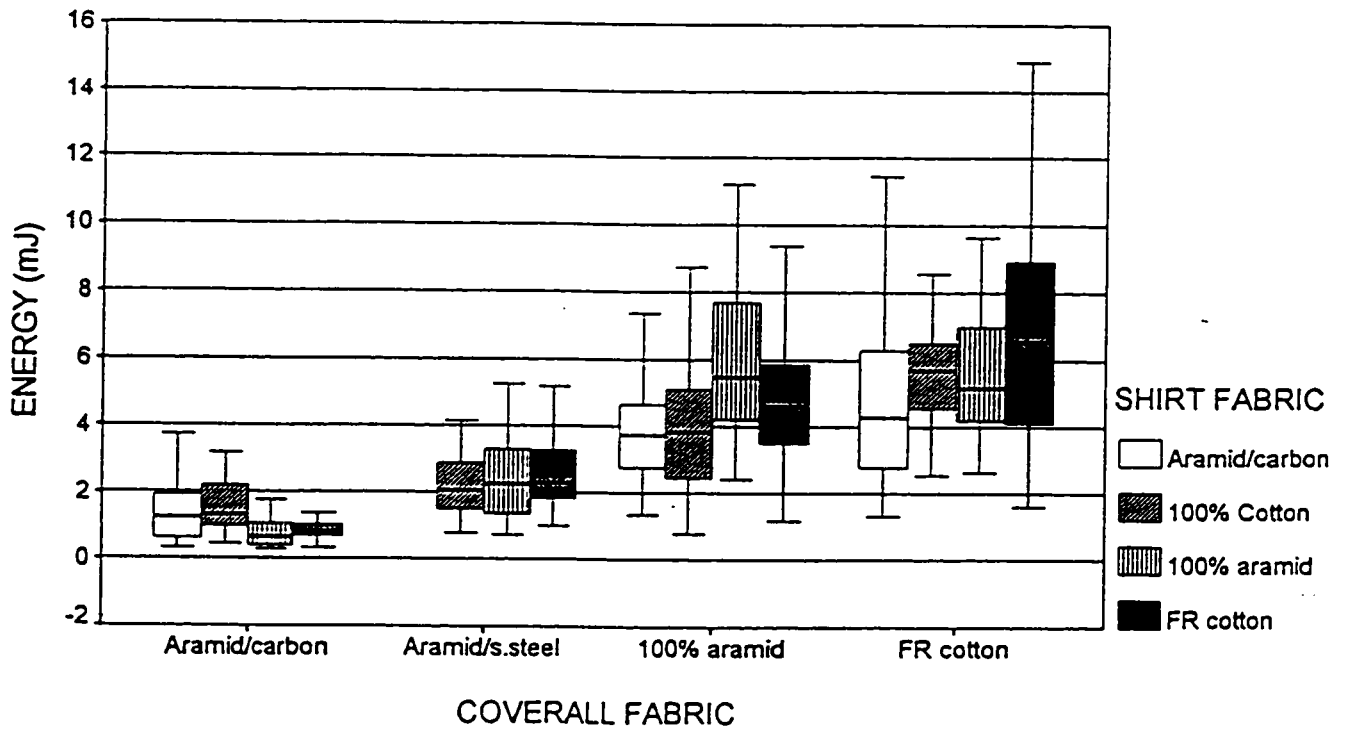


Figure 5.

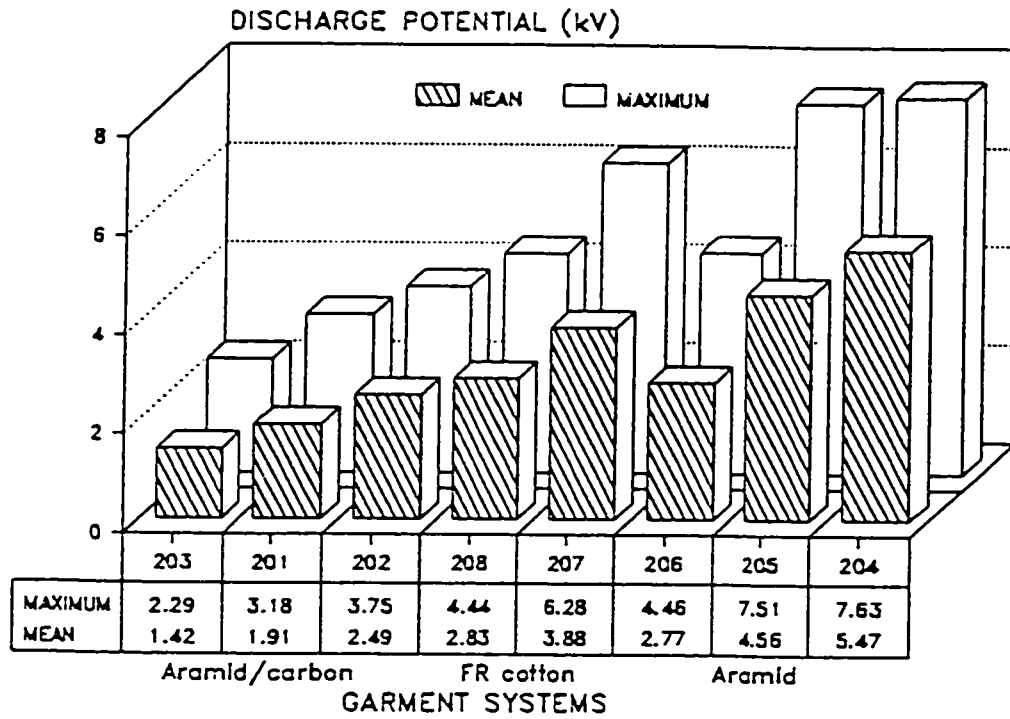
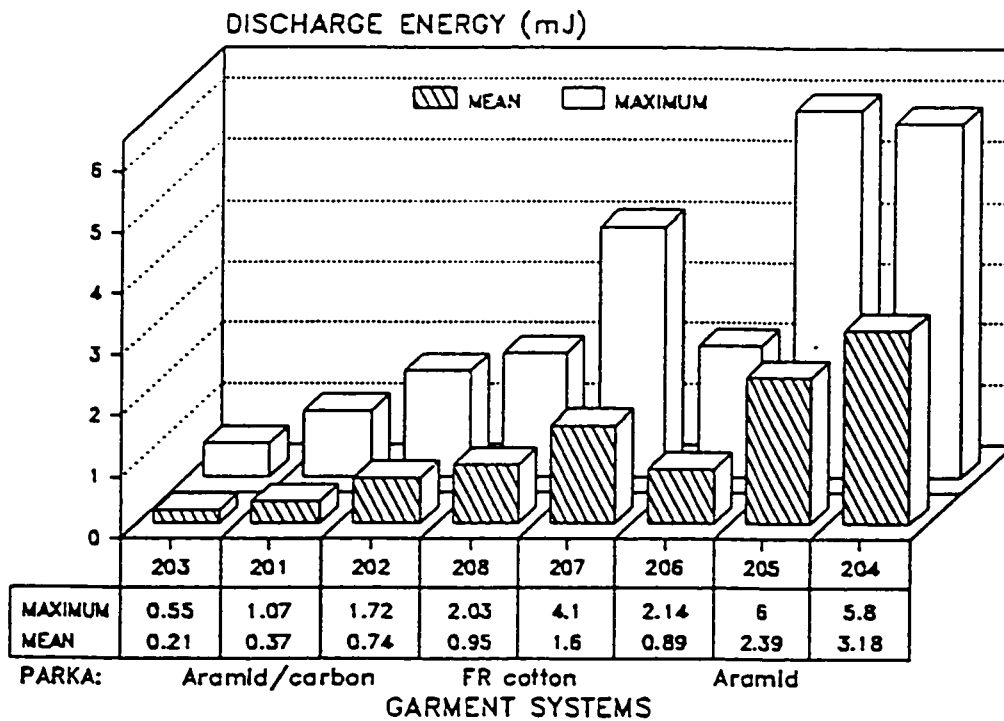


Figure 6.



Appendix 2b.**ELECTROSTATIC CHARACTERISTICS OF THERMAL PROTECTIVE GARMENTS AT VARIOUS LOW HUMIDITIES**

A revised version of this paper has been accepted for publication as:

Reference: Rizvi, S. A. H., Crown, E. M., Gonzalez, J. A., & P. R. Smy (in press).
Electrostatic characteristics of thermal protective garments at various low humidities.
Journal of The Textile Institute, (Accepted for publication).

ABSTRACT:

Electrostatic discharges to a grounded object from a human body wearing various combinations of protective garments at low humidity were investigated. Two experiments comprising different human activities were performed at 0%, 10% and 20% relative humidity and room temperature. Discharge parameters such as potential, charge and energy were determined. Differences among garment systems and the effect of humidity on such differences were determined.

1. INTRODUCTION

Electrostatic discharges from a clothed human body are of prime concern for many industries and become significant at low humidity. One important factor in determining the electrostatic propensity of a fabric is its moisture content. The moisture content, normally in equilibrium with the surrounding atmosphere, varies with the fibre, and for most fibres depends on temperature and humidity. The surface conductivity of a fabric, and hence the dissipation of electrostatic charges from a garment's surface, normally decrease as the moisture content decreases. Thus, low moisture environments such as those typically found in Canadian winter pose potential hazards. It is therefore important to gain insight into the generation and dissipation of electrostatic charges for a range of thermal-protective clothing systems comprising different combinations of garments, at low humidities common in some parts of the world.

In a previous investigation [1] discharge parameters were determined after conditioning garments at 0% humidity. In this paper the previous work is extended by including garments conditioned in ambient relative humidities of 10% and 20% and by including additional garment systems. The purpose of this research was to study the characteristics of discharges from humans wearing different thermal-protective clothing systems, and to determine the resulting electrostatic hazards in flammable environments under different humidity conditions. Although such hazards have been studied for traditional non-protective garments, in most of the work reported so far [2-4], emphasis was on relative humidities of 20% or greater.

This paper is concerned primarily with the effect of low humidities on the

generation and dissipation of electrostatic charges from a human subject wearing thermal-protective clothing and involved in a normal physical activity. Because charges generated on the outer layers of garments can be induced on the body which in turn can generate a spark on contact with an earthed or large conductor, some typical parameters such as potential, charge and energy in a discharge were investigated, providing a comparison of spark hazards while wearing different thermal-protective garments under dry conditions. It was hypothesized that the static propensity of the garment systems would differ and that the differences among systems would be affected by humidity.

2. METHODS

As in the previous work [1], two different experiments were performed. The independent variables in both experiments were garment system, relative humidity, and subject. The first experiment, performed on two subjects at 0%, 10% and 20% r.h. consisted of the frictional charging of the subject wearing a specified garment system and sliding across a vinyl-covered bench truck seat. The second experiment comprised the removal of the outermost garment in a system and was performed on two subjects at 0% and 20% r.h.

2.1 Materials

For this study thermal-protective garment systems comprising

combinations of outer and inner garments of FR-cotton, aramid /carbon, aramid¹/PBI, aramid¹/FR viscose, and non-FR cotton, were used. In experiment one, coveralls were worn over shirts and pants, while in experiment two insulated parkas were worn over, and then removed from, coveralls. Garments were all purchased from the same source and were of the same design and color. Both subjects wore identical insulating rubber-soled (2 cm thick) shoes during the experiment. Identical 100% cotton undergarments (vest, undershorts) and socks were also worn.

2.2 Procedure

A detailed description of the procedures, including conditioning of the garment systems, performance of the physical activities, and measurement of the dependent variables, is found in the earlier report [1]. As described there, total charge flow (transferred), Q , was calculated by integrating the discharge potential, V , wave form and dividing this by the grounding resistance. Total energy, E , was then determined as follows:

$$E=(1/2)QV.$$

2.3 Statistical Analysis

All experimental data were analyzed using SPSS version 6.0. For each experiment, multi-variate analysis of variance was used to determine differences among garment systems, relative humidities, and subjects, as well as

interactions among the three independent variables. One-way analysis of variance and Duncan's multiple range tests [5] were used to determine which garment systems differed significantly from each other. Significance levels were set at $p < 0.05$.

3. RESULTS

3.1 Experiment 1

Three-way analysis of variance found significant main effects of garment system, relative humidity and subject on both body discharge potential and discharge energy; thus, the null hypothesis of no differences was rejected for both parameters. Three-way and two-way interaction effects were also significant, except that for discharge potential there was no significant two-way interaction between subject and relative humidity. These results indicate that although significant, the differences in these discharge parameters among garment systems are affected by relative humidity and by subject. The analyses which follow, however, use the data for both subjects together, because with very few exceptions, the same trends were observed for each subject.

3.1.1 Peak Discharge Potential

Discharge potentials for each garment system at different relative humidities are shown in Figure 1. As in previous work [1], results of the one-

way ANOVA and Duncan's multiple range test for body discharge potential (Table I) indicate that the garment systems can be grouped according to the fabric comprising the outer (coverall) layer; they have been grouped accordingly in Table I and Figure 1. The highest discharge potentials were observed for the systems with FR cotton coveralls followed by those with aramid/FR viscose coveralls and then aramid/carbon. Aramid/PBI coveralls produced the lowest discharge potentials among all the garment combinations, although at 20% r.h. the difference between aramid/PBI and aramid/carbon coveralls was not significant. The highest mean discharge potential (for systems with FR cotton coveralls) was almost an order or magnitude greater than the lowest potential (aramid/PBI coveralls) at each humidity level.

Garment systems with 100% untreated cotton inner garments tended to generate lower potentials than those with either aramid/carbon or FR cotton inner garments, but the differences between untreated cotton and aramid/carbon inner garments are not generally significant.

Among the three relative humidity levels, the lowest potentials were observed at 20% and 10% r.h., with overall means of only 3.11 kV and 3.20 kV for the 8 garment systems. The highest mean value (3.84 kV) was observed at 0% r.h. An analysis of data for each garment system will give further insight.

Garment systems with FR cotton coveralls (16 & 17) were least affected by the humidity; mean discharge potentials increased by only 13% as the

relative humidity was decreased from 20% to 0. Approximately 24% and 36% increases in potentials were observed for systems with aramid/PBI coveralls (20 & 21) and aramid/FR viscose coveralls (22 & 23), respectively. The greatest effect of humidity was observed in the case of aramid/carbon coveralls (18 & 19); when these were combined with an aramid/carbon inner layer the mean potential almost tripled with change in humidity from 20% to 0.

In addition to mean values, maximum discharge potentials are of interest because they represent worse case scenarios. Maximum potentials are from 15% to 110% higher than their corresponding mean values at 0% r.h. and from 40% to 125% higher at 20 % r.h.

3.1.2 Body Discharge Energy

Maximum body discharge energies for each garment system and relative humidity are plotted in Figure 2. One-way analysis of variance and Duncan's multiple range test results for body discharge energy are given in Table I. Again, garment systems can be grouped according to the outer layer. Highest discharge energies were observed for systems with FR cotton coveralls followed by aramid/FR viscose coveralls. Systems with aramid/PBI and aramid/carbon coveralls produced the lowest discharge energies among all the garment combinations.

Thus, results indicate that a subject sliding off a car seat may produce a discharge energy as high as 13.1 mJ at 0% r.h. Maximum discharge energy

was not affected much by change in humidity. However, the mean discharge energy for all systems was found to increase almost 50% from 4.35 mJ at 20% r.h. to 6.59 mJ at 0% r.h.

3.2 Experiment 2

Three-way ANOVA found significant main effects of garment system, relative humidity and subject on both body discharge potential and discharge energy in Experiment 2. The null hypothesis was therefore rejected for both parameters. All interaction effects were significant except there was no significant three-way interaction for the discharge potential data. In other words, while there are significant differences in both parameters among garment systems, such differences are affected by humidity and to some extent by subject. For the analyses which follow, however, data for both subjects are treated together.

3.2.1 Peak Discharge Potential

One-way ANOVA and Duncan's multiple range test results for body discharge potential are given in Table II. Mean discharge potentials at 0% r.h. are approximately two to nine times greater than those at 20% r.h. Garment systems can be grouped by the outer layer (parka) as in Table II and Figure 3. Significantly higher discharge potentials were observed for systems with the FR cotton parka at both 0% and 20 % r.h.

While there is no significant effect of the inner garment in systems with the aramid/carbon parkas, systems with the FR cotton parkas differ significantly depending on the coverall layer. In this case, systems in which the two layers are more similar generate lower potentials than those where the two layers are made from quite different fibres.

3.2.2 Body Discharge Energy

One-way ANOVA and Duncan's multiple range test for body discharge energy are given in Table II. Garment systems can be grouped according to the parka layer (Table II and Figure 4). Significantly higher discharge energies generally were observed for systems with the FR cotton parka at both 0% r.h. and 20 % r.h. As for potentials, there were significant differences among systems with different coveralls for the FR-cotton parka group, but not for the systems with the aramid/carbon parkas. Such differences were greater at 20% r.h. than they were at 0% r.h.

Energies measured at 0% r.h. are approximately four to 50 times greater than those measured at 20% r.h. Generally, differences between 0% and 20% r.h. were somewhat greater for systems with aramid/carbon parkas than for those with FR-cotton parkas.

4. CONCLUSIONS

This research has confirmed and extended conclusions reached in our

earlier work [1]. As in the previous study, content of the outer layer of clothing systems had a greater effect on potentials and energies than did the inner layer for both experiments. The inner layer was more likely to have an effect when charges were generated simply by separation (experiment 2) than when friction through rubbing against another material was involved (experiment 1), but discharge potentials and energies were also lower in the former case. These results held for each humidity level studied. Overall, however, energies were much higher (up to 15 times) at 0% r.h. than at 20% r.h.

Systems with outer garments of anti-static materials (inherent or topical) generated lower potentials and energies than did those without. For experiment 1 at all three humidity levels, however, even the anti-static systems produced maximum discharge energies greater than the minimum ignition energy of 0.5 mJ cited [6] for methane and air. In addition, the affect on mean potentials and energies of reducing humidity from 20% to 0% r.h. was greatest for systems with aramid/carbon outer garments.

Thus, our previous conclusions [1] have been supported for a greater variety of protective clothing systems and at low humidities ranging from 0% to 20% r.h.

REFERENCES

- [1] S.A.H. Rizvi, E.M. Crown, K. Osei-Ntiri, P.R. Smy, and J.A. Gonzalez. *J. Text. Inst.*, 1995, 86, 549-558.
- [2] D.E. Phillips. 'Testing for Electrostatic Generation and Dissipation', Test Activity Report No. APG-MT-5566, Defense Logistics Agency. Defense Technical Information Center (DTIC), Alexandria, VA, USA, April, 1982.
- [3] J.H. Veghte and W.W. Millard. 'Accumulation of Static Electricity on Arctic Clothing' (Technical Documentary AAL-TDR-63-12) Arctic Aeromedical Laboratory, Aerospace Medical Division, Air Force Systems Command, Fort Wainwright, Alaska, USA, May, 1963.
- [4] N. Wilson. *J. Electrostat.* 1977/78, 4, 67-84.
- [5] R.E. Walpole and R.H. Myers. 'Probability and Statistics for Engineers and Scientists', MacMillan, New York, NY, USA, ISBN 0-02-424210-1, 4th edition, 1989, p. 486.
- [6] A.M. Crugnola and H.M. Robinson. 'Measuring and Predicting the Generation of Static Electricity in Military Clothing' (Report No. 110), Quartermaster Research and Engineering Command, US Army, Natick, MA, USA, September, 1959.

Table I
Analysis of Variance: Body Discharge Potentials and Energies at 0, 10 and 20% r.h., Experiment 1.

Code	Garment System (Outer - Inner Layers)	Mean Potential (kV)			Mean Energy (mJ)		
		0% rh	10% rh	20% rh	0% rh	10% rh	20% rh
20	aramid/PBI ¹ - 100% cotton	0.83 ^a	0.67 ^a	0.79 ^a	0.09 ^a	0.06 ^a	0.07 ^a
21	aramid/PBI ¹ - aramid/carbon	1.18 ^{a,b}	0.67 ^a	0.83 ^a	0.16 ^a	0.05 ^a	0.07 ^a
18	aramid/carbon - 100% cotton	1.63 ^{b,c}	1.36 ^b	1.12 ^a	0.34 ^a	0.19 ^a	0.24 ^a
19	aramid/carbon - aramid/carbon	2.32 ^c	1.40 ^b	0.87 ^a	0.55 ^{a,b}	0.20 ^a	0.12 ^a
22	aramid/FR-viscose - 100% cotton	3.81 ^d	3.46 ^c	2.66 ^b	1.38 ^b	1.19 ^b	0.78 ^b
23	aramid/FR-viscose - aramid/carbon	3.45 ^d	3.80 ^c	2.69 ^b	1.14 ^b	1.53 ^b	0.77 ^b
16	FR-cotton - 100% cotton	6.93 ^e	6.64 ^d	6.42 ^c	4.42 ^c	4.12 ^c	4.19 ^c
17	FR-cotton - FR-cotton	8.13 ^f	6.48 ^d	6.86 ^d	6.59 ^d	4.03 ^c	4.35 ^d

¹ This fabric has a topical anti-static treatment

^{a,b,etc.} In each column, means with the same letter indicate homogeneous subsets (highest and lowest means are not significantly different) when subjected to Duncan's multiple range test ($p < 0.05$)

Table II
Analysis of Variance: Body Discharge Potentials and Energies at 0 and 20% r.h., Experiment 2.

Code	Garment System (Outer - Inner Layers)	Mean Potential (kV)		Mean Energy (mJ)	
		0% rh	20% rh	0% rh	20% rh
211	aramid/carbon - aramid/PBI ¹	0.43 ^a	0.08 ^a	0.03 ^a	0.00 ^{a,2}
210	aramid/carbon - aramid/FR-viscose	0.39 ^a	0.14 ^a	0.03 ^a	0.00 ^{a,2}
212	aramid/carbon - aramid/carbon	0.42 ^a	0.15 ^a	0.03 ^a	0.00 ^{a,2}
209	aramid/carbon - FR-cotton	0.62 ^a	0.18 ^a	0.05 ^a	0.01 ^a
213	FR-cotton - FR-cotton	3.60 ^b	0.43 ^b	1.28 ^b	0.02 ^a
214	FR-cotton - aramid/FR-viscose	4.41 ^c	1.85 ^c	2.07 ^c	0.34 ^b
215	FR-cotton - aramid/PBI ¹	4.49 ^d	2.31 ^d	2.19 ^c	0.54 ^c
216	FR-cotton - aramid/carbon	5.51 ^e	3.01 ^e	3.36 ^d	0.88 ^d

¹ This fabric has a topical anti-static treatment
² < 0.01 mJ

^{a,b,etc.} In each column, means with the same letter indicate homogeneous subsets (highest and lowest means are not significantly different) when subjected to Duncan's multiple range test ($p < 0.05$)

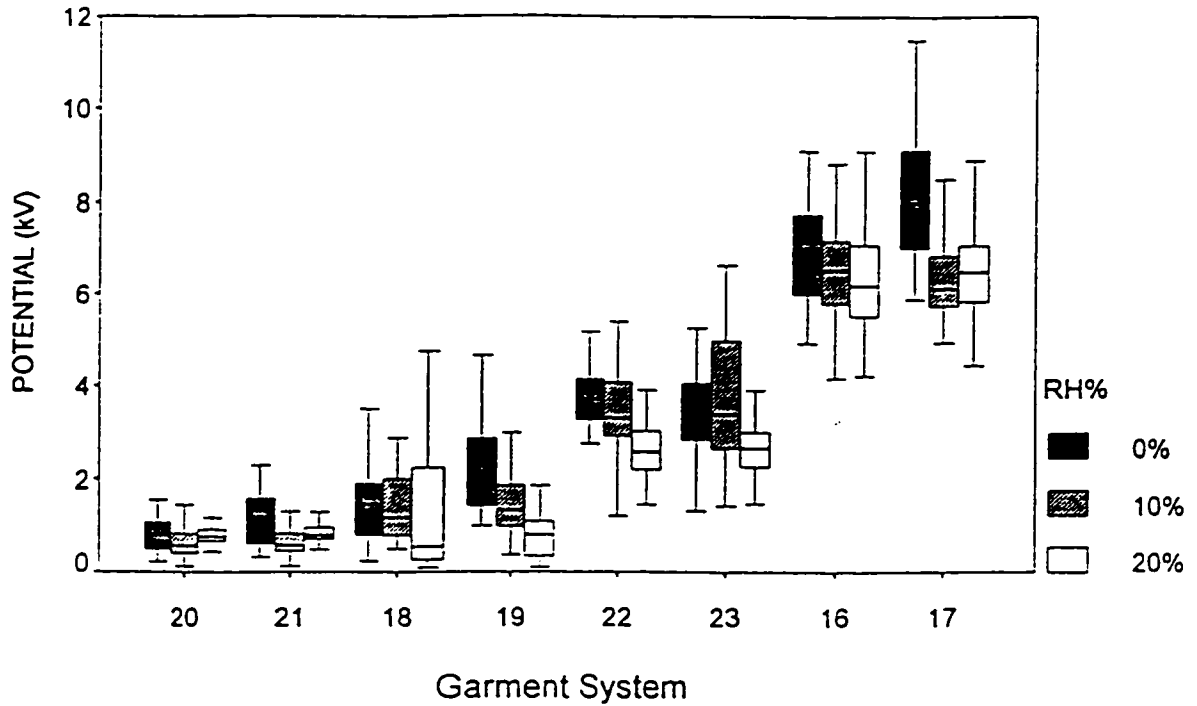


Fig. 1 Discharge potentials showing minimum and maximum values, and interquartile ranges at different relative humidity levels: experiment 1

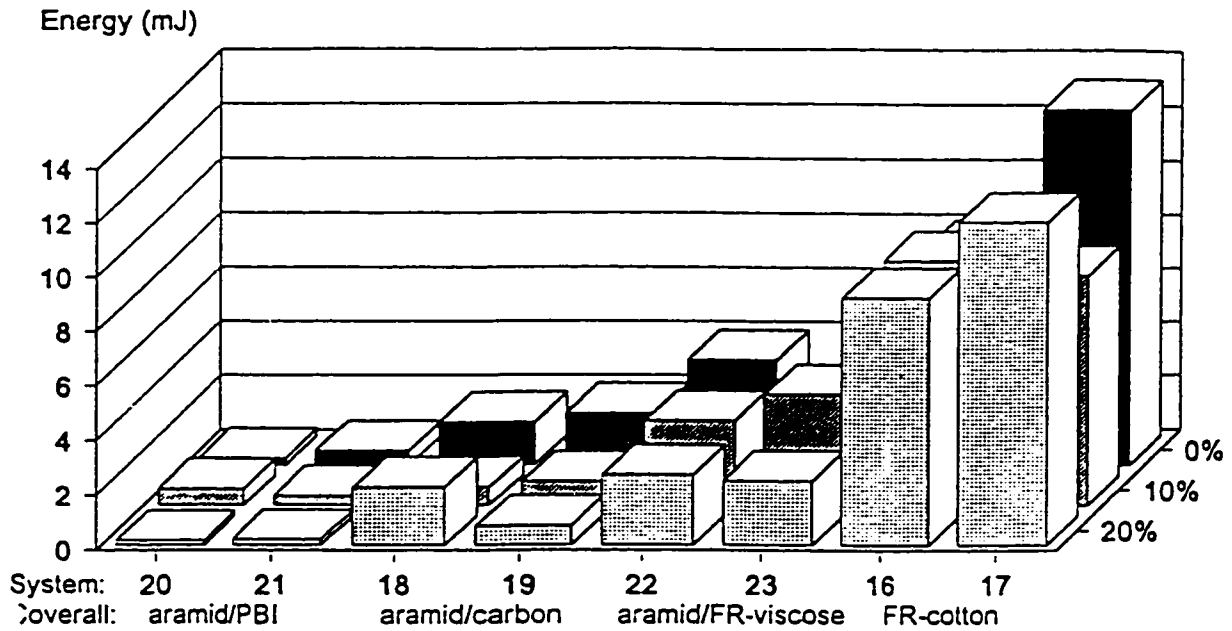


Fig. 2 Maximum body-discharge energies at different relative humidity levels: experiment 1

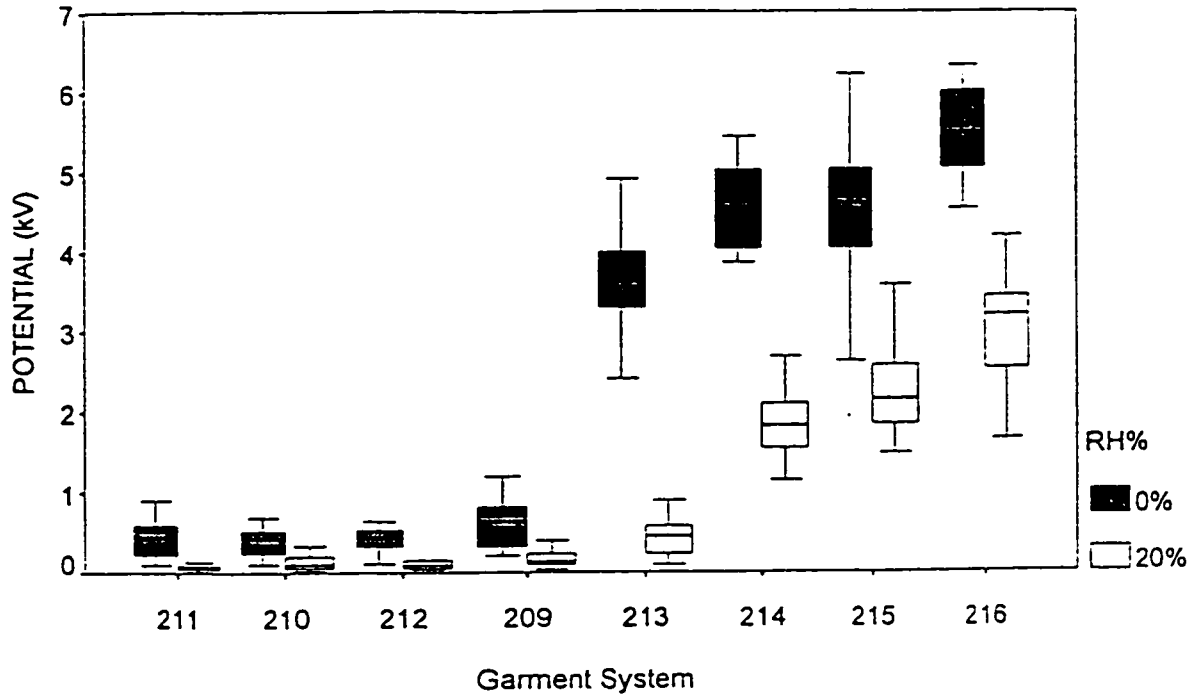


Fig. 3 Discharge potentials showing minimum and maximum values, and interquartile ranges at different relative humidity levels: experiment 2

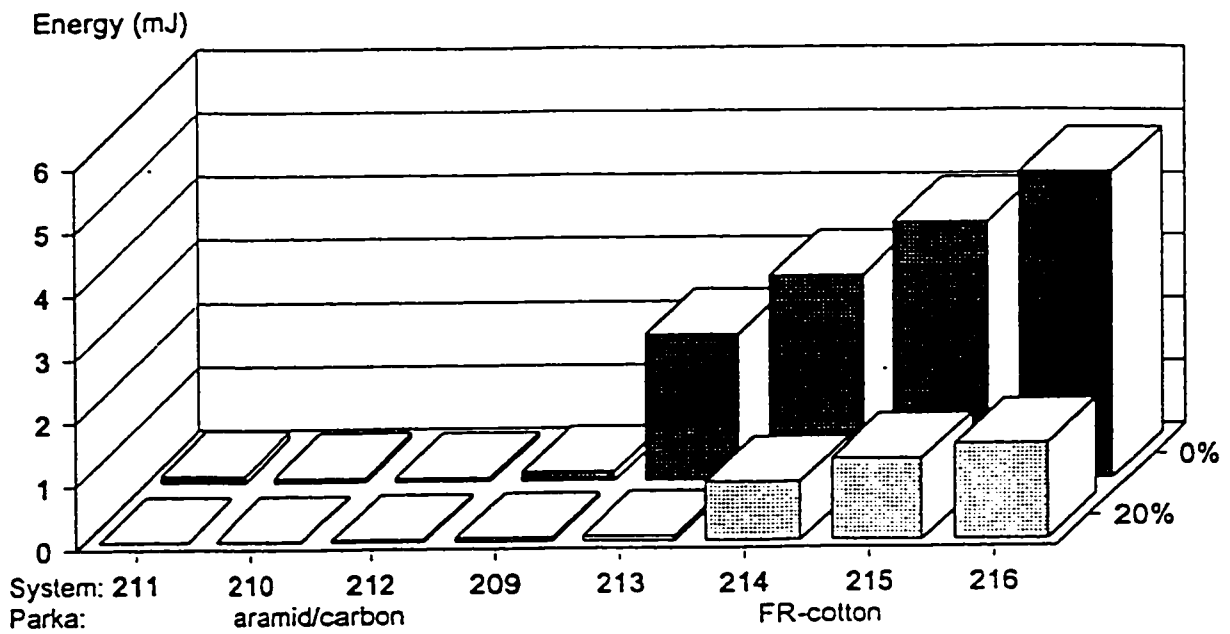


Fig.4 Maximum body-discharge energies at different relative humidity levels: experiment 2

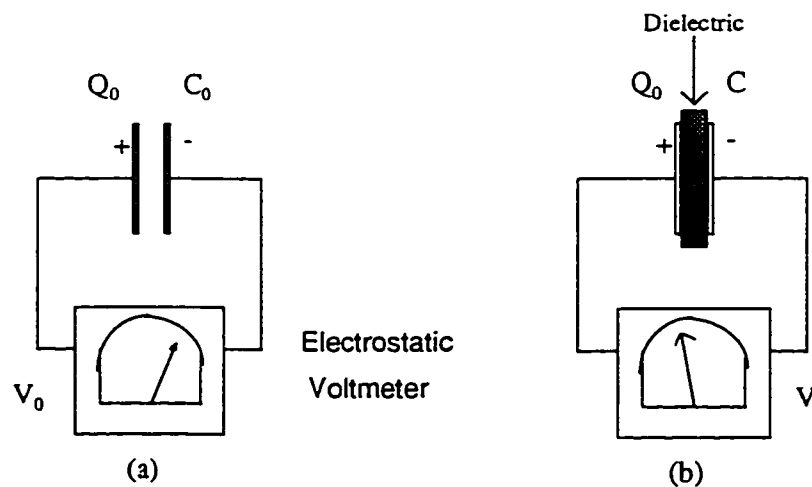
Appendix 3. Method to Determine the Dielectric Constant

A dielectric is a non-conducting material, such as rubber, glass, waxed paper, or fabric. When a dielectric material is inserted between the plates of a capacitor, the capacitance increases. If the dielectric completely fills the space between the plates, the capacitance increases by a dimensionless factor K , called the **dielectric constant** or **relative permittivity**.

The set up shown below was used to determine the dielectric constant of textile materials. The parallel-plate capacitor is charged to a charge Q_0 and has a capacitance of C_0 in the absence of a dielectric. The potential difference across the capacitor as measured by the electrostatic voltmeter is $V_0 = Q_0 / C_0$.

Then, a textile material, as a dielectric, is inserted between the plates filling the space between plates. A new reading of the potential difference with the electrostatic voltmeter is done. The potential difference decreases by a factor K to a value V , where:

$$V = \frac{V_0}{K}$$



Set up to determine the dielectric constant of textile materials using a parallel-plate capacitor and an electrostatic voltmeter

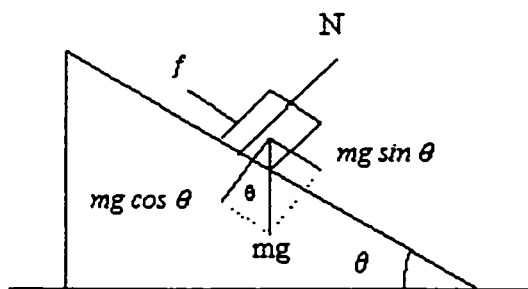
Appendix 4. Method to Determine the Coefficient of Static Friction μ_s

A simple method of measuring the coefficient of static friction (μ_s) between a fabric surface and a rough surface (vinyl in this case) was used to obtain the values shown below. A block covered with the fabric is placed on an inclined plane with respect to the horizontal as shown in the figure. The angle of the inclined plane is increased until the block slips. By measuring the angle θ_c at which the slipping occurs, the coefficient of static friction is obtained according to the following equation:

$$\mu_s = \tan \theta_c$$

Static friction coefficients (μ_s) between thermal protective fabrics and vinyl

Fabric	μ_s at 0% RH	μ_s at 20% RH
FR cotton	25.5	24.2
100% cotton	26.9	25.3
aramid/FR viscose	22.6	23.0
aramid/PBI	23.4	23.2
aramid/carbon	23.1	22.8



Set up to determine the static friction coefficient using an inclined plane

Appendix 5. Average Resistance and Surface Resistivity of fabrics at 0 and 20% RH^a

	100% Cotton				FR Cotton			
	0% RH		20% RH		0% RH		20% RH	
	weft	warp	weft	warp	weft	warp	weft	warp
Resistance (Ohms)	7.15E+15	7.60E+15	3.70E+14	2.60E+14	5.17E+15	5.44E+15	4.50E+14	3.90E+14
Surface Resistivity (log of Ohms per square)	16.3402	16.3667	15.0544	14.9002	16.1940	16.2215	15.1430	15.0764

	Kermel				Nomex/PBI			
	0% RH		20% RH		0% RH		20% RH	
	weft	warp	weft	warp	weft	warp	weft	warp
Resistance (Ohms)	3.50E+15	2.85E+15	1.39E+14	9.30E+13	8.20E13 ^b	4.01E+15	5.90E13 ^c	7.80E+13
Surface Resistivity (log of Ohms per square)	16.0300	15.9407	14.6302	14.4562	15.4015 ^b	16.0892	14.2597 ^c	14.3769

^a reported averages are of 10 specimens

^b reported averages are of only 3 specimens

^c reported averages are of only 5 specimens

Appendix 6. Results of Testing Following the Proposed and Modified ASTM Methods with Vinyl Rubbing Wheel at Various Humidities and Temperatures

Table 1. Mean values for peak potentials (kV) following the proposed ASTM Method

Fabric System	0% RH			30% RH		
	4 °C	22 °C	30 °C	22 °C	22 °C	22 °C
Nomex IIIA	-0.745	0.590	-0.486	0.721	-0.549	-1.251
Nomex/PBI	-1.275	1.770	-1.771	0.989	1.764	13.00
Kermel	15.94	14.99	3.70	12.14	11.16	
100% non-FR cotton	25.90	23.70	22.67	16.10		
FR cotton - FR cotton	25.82	25.41	20.67	14.18		

Table 2. Mean values for charge decay (%) following the proposed ASTM Method

Fabric System	0% RH			30% RH		
	4 °C	22 °C	30 °C	22 °C	22 °C	22 °C
Nomex/PBI	55.64	8.96	22.21	34.16	66.94	77.91
Kermel	7.60	4.03	27.79	26.09	51.61	45.52
100% non-FR cotton	15.80	2.79	4.24	9.24	5.78	
FR cotton	13.17	2.17	5.17	6.74		
Nomex IIIA	10.19	4.81	14.05	6.07		

Table 3. Mean values for peak discharge potential (V) following a modified ASTM Method

Fabric System	0% RH		20% RH		30% RH	
	22 °C	22 °C	22 °C	22 °C	22 °C	22 °C
Nomex IIIA	73.20	70.09	73.20	70.09	73.20	70.09
Nomex/PBI	104.10	83.65	104.10	83.65	104.10	83.65
Kermel	210.90	96.00	210.90	96.00	210.90	96.00
FR cotton	323.40	212.00	323.40	212.00	323.40	212.00
100% non-FR cotton	547.70	221.60	547.70	221.60	547.70	221.60

Table 4. Mean values for peak potentials (kV) following the proposed ASTM Method

Fabric System	0% RH			20% RH			30% RH		
	4 °C	22 °C	30 °C	22 °C	30 °C	22 °C	30 °C	22 °C	30 °C
Nomex/PBI - Nomex IIIA	0.480	0.827	-0.462	0.641	-1.404	0.641	-1.404	0.641	-1.404
Nomex IIIA - Nomex IIIA	0.385	1.166	-0.279	0.793	-0.415	0.793	-0.415	0.793	-0.415
Nomex IIIA - 100% non-FR cotton	0.456	1.379	-0.643	0.874	-0.317	0.874	-0.317	0.874	-0.317
Kermel - Nomex IIIA	1.026	2.006	0.492	1.538	-0.159	1.538	-0.159	1.538	-0.159
Nomex/PBI - 100% non-FR cotton	-2.066	2.489	-2.166	0.690	-1.166	0.690	-1.166	0.690	-1.166
Kermel - 100% non-FR cotton	10.940	19.030	1.859	15.320	-0.267	15.320	-0.267	15.320	-0.267
FR cotton - 100% non-FR cotton	28.640	23.080	17.69	19.960	5.940	19.960	5.940	19.960	5.940
FR cotton - FR cotton	25.120	23.470	17.985	19.340	7.230	19.340	7.230	19.340	7.230

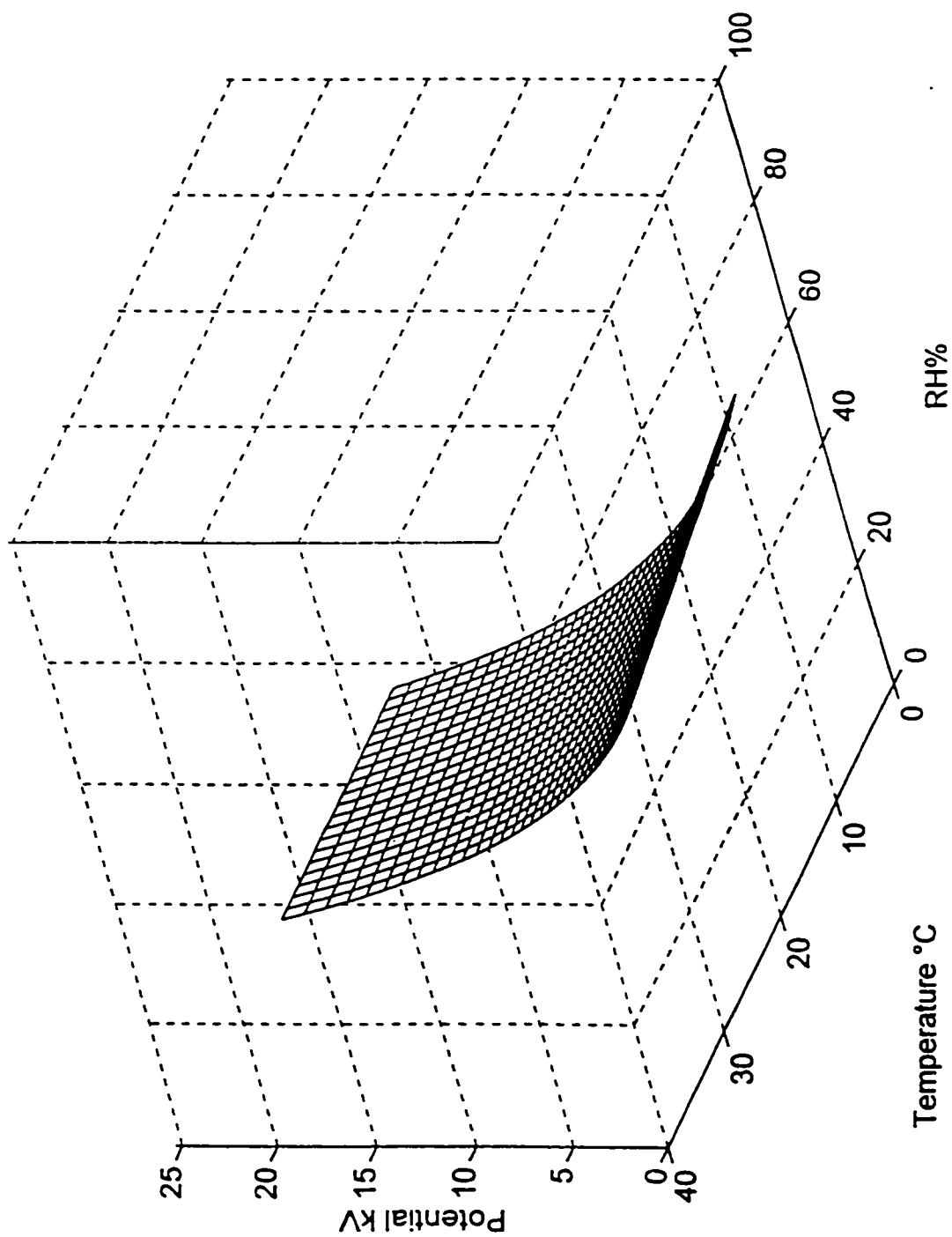
Table 5. Mean values for charge decay (%) following the proposed ASTM Method

Fabric System	0% RH			20% RH		30% RH	
	4 °C	22 °C	30 °C	22 °C	22 °C	22 °C	22 °C
Nomex/PBI - 100% non-FR cotton	44.30	8.83	18.68	36.03	72.86		
Kermel - 100% non-FR cotton	24.84	2.63	9.82	32.99	25.24		
FR cotton - 100% non-FR cotton	10.93	2.30	4.72	12.96	83.12		
Kermel - Nomex IIIA	27.06	3.32	10.33	12.49	10.79		
FR cotton - FR cotton	22.92	2.07	4.62	10.24	76.76		
Nomex/PBI - Nomex IIIA	16.23	7.44	8.01	9.20	25.69		
Nomex IIIA - 100% non-FR cotton	15.98	5.00	10.00	8.91	9.48		
Nomex IIIA - Nomex IIIA	7.44	3.41	5.16	6.63	8.17		

Table 6. Mean values for peak discharge potential (V) following a modified ASTM Method

Fabric System	0% RH		20% RH		30% RH	
	22 °C	22 °C	22 °C	22 °C	22 °C	22 °C
Nomex/PBI - 100% non-FR cotton	67.40	67.40	28.87	28.87	12.31	12.31
Nomex/PBI - Nomex IIIA	71.68	71.68	9.33	9.33	28.64	28.64
Nomex IIIA - 100% non-FR cotton	88.20	88.20	51.95	51.95	2.13	2.13
Nomex IIIA - Nomex IIIA	88.80	88.80	20.88	20.88	10.53	10.53
Kermel - Nomex IIIA	89.70	89.70	58.45	58.45	3.56	3.56
Kermel - 100% non-FR cotton	262.70	262.70	117.68	117.68	2.35	2.35
FR cotton - 100% non-FR cotton	268.40	268.40	258.20	258.20	36.60	36.60
FR cotton - FR cotton	458.40	458.40	194.68	194.68	44.83	44.83

Appendix 7a. Modeling the Humidity and Temperature Effect on 100% Cotton



Appendix 7a. Cont'd...

**Mathematical Model: Humidity and Temperature Effect on Peak Potential, Following the Proposed ASTM Method F23.20.05
Fabric: 100% cotton**

$V_p = V_o \exp [b \exp (cT) H]$

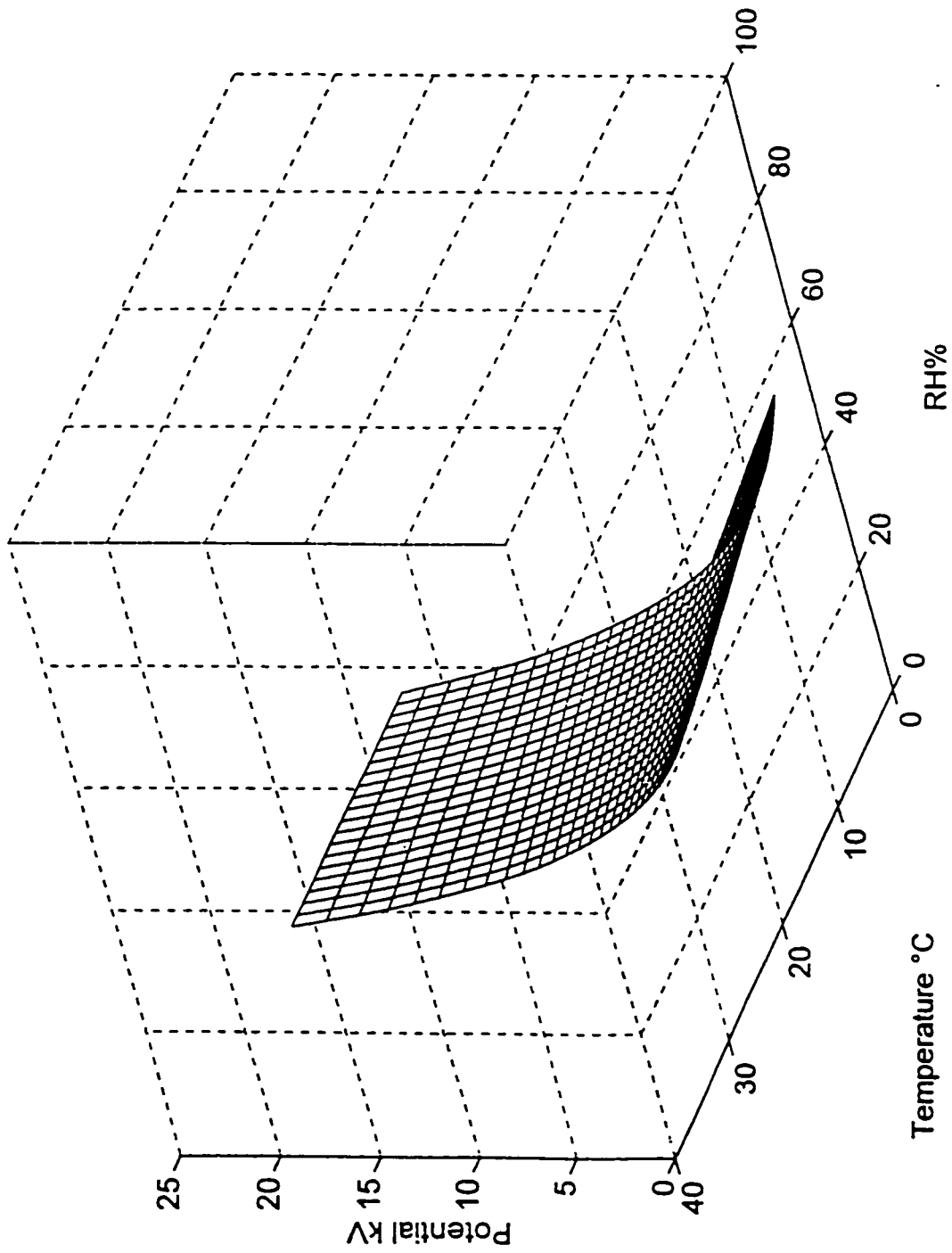
Where: $V_o = 25.90$ kV; $b = -0.02066$; $c = 0.00509$; $T =$ temperature °C; $H =$ relative humidity %

	1%	3%	5%	7%	9%	11%	13%	15%	17%	19%	21%
0	25.3704	24.3435	23.3581	22.4126	21.5054	20.6349	19.7996	18.9982	18.2292	17.4913	16.7833
2	25.3650	24.3280	23.3334	22.3795	21.4645	20.5870	19.7453	18.9380	18.1638	17.4212	16.7089
4	25.3596	24.3124	23.3085	22.3460	21.4233	20.5387	19.6905	18.8775	18.0980	17.3506	16.6342
6	25.3541	24.2967	23.2834	22.3123	21.3817	20.4900	19.6354	18.8165	18.0317	17.2797	16.5590
8	25.3486	24.2808	23.2580	22.2783	21.3398	20.4409	19.5798	18.7551	17.9650	17.2082	16.4834
10	25.3430	24.2648	23.2324	22.2440	21.2976	20.3915	19.5239	18.6932	17.8979	17.1364	16.4073
12	25.3374	24.2486	23.2066	22.2094	21.2550	20.3416	19.4675	18.6310	17.8303	17.0641	16.3309
14	25.3317	24.2323	23.1805	22.1745	21.2120	20.2914	19.4107	18.5683	17.7624	16.9914	16.2540
16	25.3260	24.2158	23.1542	22.1393	21.1688	20.2408	19.3535	18.5051	17.6939	16.9183	16.1767
18	25.3202	24.1991	23.1277	22.1037	21.1251	20.1898	19.2959	18.4416	17.6251	16.8448	16.0990
20	25.3143	24.1823	23.1009	22.0679	21.0811	20.1384	19.2379	18.3776	17.5558	16.7708	16.0208
22	25.3084	24.1653	23.0739	22.0318	21.0367	20.0866	19.1794	18.3132	17.4861	16.6964	15.9423
24	25.3024	24.1482	23.0467	21.9954	20.9920	20.0345	19.1206	18.2484	17.4160	16.6215	15.8633
26	25.2963	24.1309	23.0191	21.9586	20.9470	19.9819	19.0613	18.1831	17.3454	16.5463	15.7839
28	25.2902	24.1134	22.9914	21.9216	20.9015	19.9289	19.0016	18.1174	17.2744	16.4706	15.7042
30	25.2841	24.0958	22.9634	21.8842	20.8557	19.8756	18.9415	18.0513	17.2029	16.3945	15.6240
32	25.2778	24.0780	22.9351	21.8465	20.8095	19.8218	18.8809	17.9847	17.1311	16.3179	15.5434
34	25.2716	24.0600	22.9066	21.8085	20.7630	19.7676	18.8200	17.9177	17.0588	16.2410	15.4624
36	25.2652	24.0419	22.8778	21.7701	20.7161	19.7130	18.7586	17.8503	16.9860	16.1636	15.3810
38	25.2588	24.0236	22.8488	21.7315	20.6688	19.6581	18.6968	17.7825	16.9129	16.0858	15.2992
40	25.2523	24.0051	22.8195	21.6925	20.6211	19.6027	18.6345	17.7142	16.8393	16.0076	15.2170

Appendix 7a. Cont'd...

	23%	25%	27%	29%	31%	33%	35%	37%	39%	41%	43%
0	16.1039	15.4521	14.8266	14.2265	13.6506	13.0980	12.5679	12.0591	11.5710	11.1026	10.6532
2	16.0258	15.3706	14.7422	14.1395	13.5614	13.0070	12.4752	11.9652	11.4760	11.0068	10.5568
4	15.9473	15.2888	14.6575	14.0522	13.4719	12.9156	12.3823	11.8710	11.3808	10.9109	10.4603
6	15.8684	15.2065	14.5723	13.9646	13.3821	12.8240	12.2892	11.7766	11.2855	10.8148	10.3637
8	15.7890	15.1239	14.4868	13.8766	13.2920	12.7321	12.1958	11.6820	11.1900	10.7186	10.2671
10	15.7093	15.0409	14.4010	13.7883	13.2016	12.6399	12.1022	11.5873	11.0943	10.6223	10.1703
12	15.6291	14.9575	14.3147	13.6996	13.1109	12.5475	12.0083	11.4923	10.9984	10.5258	10.0735
14	15.5485	14.8737	14.2281	13.6106	13.0199	12.4548	11.9142	11.3971	10.9025	10.4293	9.9766
16	15.4676	14.7895	14.1412	13.5213	12.9286	12.3619	11.8200	11.3018	10.8064	10.3327	9.8797
18	15.3862	14.7050	14.0539	13.4317	12.8370	12.2687	11.7255	11.2063	10.7102	10.2360	9.7828
20	15.3044	14.6200	13.9663	13.3417	12.7451	12.1752	11.6308	11.1107	10.6138	10.1392	9.6858
22	15.2223	14.5348	13.8783	13.2515	12.6530	12.0815	11.5359	11.0149	10.5174	10.0424	9.5888
24	15.1397	14.4491	13.7900	13.1609	12.5606	11.9876	11.4408	10.9189	10.4209	9.9455	9.4918
26	15.0568	14.3631	13.7013	13.0701	12.4679	11.8935	11.3456	10.8229	10.3242	9.8486	9.3948
28	14.9734	14.2767	13.6124	12.9790	12.3750	11.7992	11.2501	10.7267	10.2275	9.7516	9.2979
30	14.8897	14.1899	13.5231	12.8875	12.2819	11.7046	11.1546	10.6303	10.1308	9.6546	9.2009
32	14.8056	14.1028	13.4334	12.7958	12.1884	11.6099	11.0588	10.5339	10.0339	9.5577	9.1040
34	14.7211	14.0154	13.3435	12.7038	12.0948	11.5150	10.9630	10.4374	9.9370	9.4607	9.0071
36	14.6363	13.9276	13.2533	12.6116	12.0009	11.4199	10.8669	10.3408	9.8401	9.3637	8.9103
38	14.5511	13.8395	13.1627	12.5190	11.9068	11.3246	10.7708	10.2441	9.7431	9.2667	8.8135
40	14.4655	13.7510	13.0719	12.4263	11.8125	11.2291	10.6745	10.1473	9.6462	9.1698	8.7169

Appendix 7b. Modeling the Humidity and Temperature Effect on FR Cotton



Appendix 7b. Cont'd...

Mathematical Model: Humidity and Temperature Effect on Peak Potential, Following the Proposed ASTM Method F23.20.05
Fabric: FR cotton

$V_p = V_o \exp [b \exp (cT) H]$

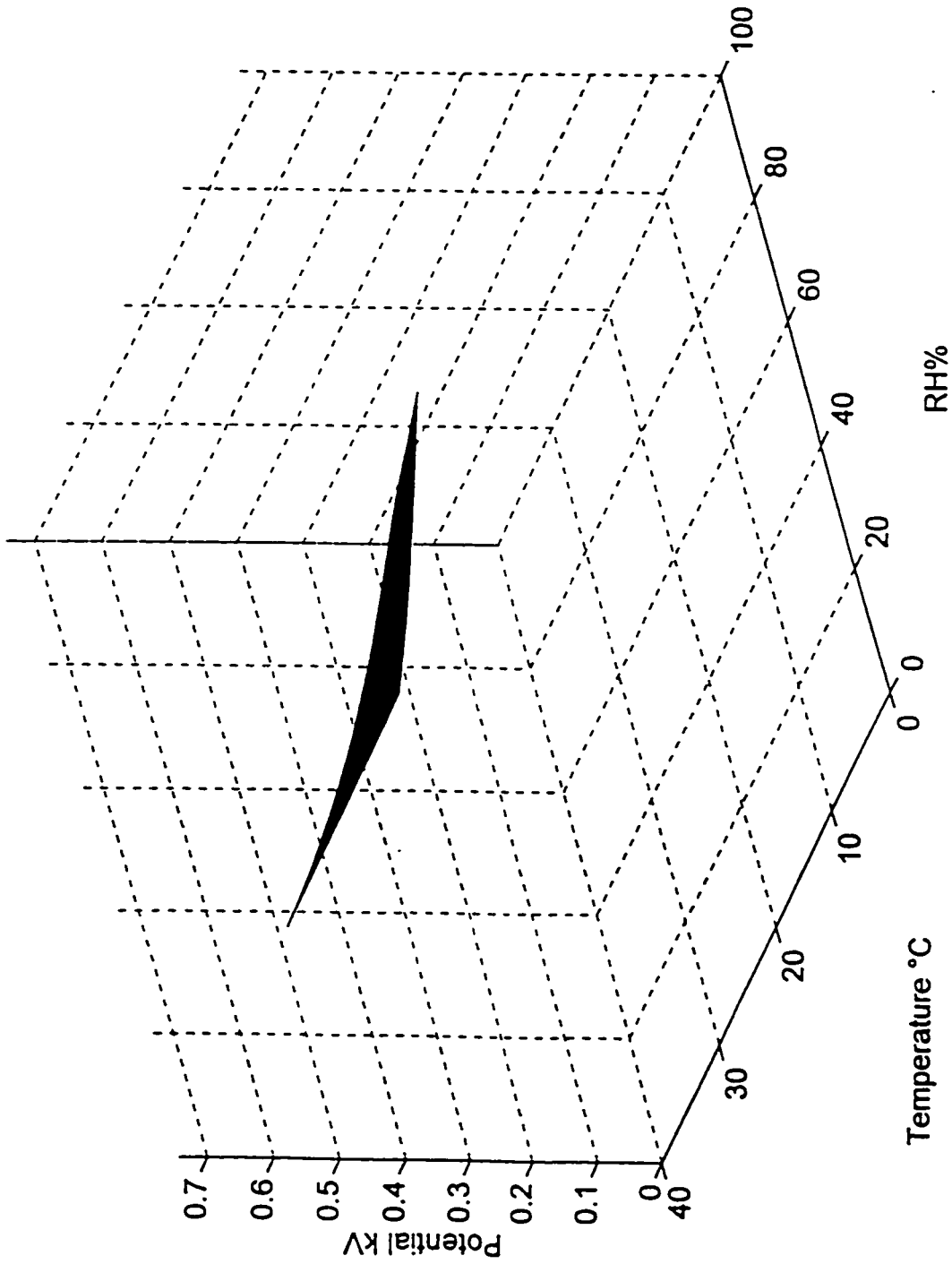
Where: $V_o = 25.82$ kV; $b = -0.02867$; $c = 0.007259$; $T =$ temperature °C; $H =$ relative humidity %

	1%	3%	5%	7%	9%	11%	13%	15%	17%	19%	21%
0	25.0903	23.6920	22.3718	21.1250	19.9478	18.8362	17.7865	16.7953	15.8594	14.9756	14.1410
2	25.0797	23.6623	22.3249	21.0631	19.8727	18.7495	17.6898	16.6900	15.7467	14.8567	14.0171
4	25.0691	23.6321	22.2775	21.0005	19.7967	18.6620	17.5923	16.5839	15.6333	14.7371	13.8924
6	25.0582	23.6015	22.2294	20.9372	19.7200	18.5736	17.4938	16.4768	15.5190	14.6168	13.7670
8	25.0473	23.5705	22.1808	20.8731	19.6424	18.4843	17.3945	16.3689	15.4039	14.4957	13.6410
10	25.0362	23.5391	22.1316	20.8082	19.5640	18.3942	17.2943	16.2602	15.2879	14.3738	13.5143
12	25.0249	23.5073	22.0818	20.7427	19.4848	18.3032	17.1933	16.1506	15.1712	14.2512	13.3870
14	25.0134	23.4751	22.0313	20.6764	19.4048	18.2113	17.0913	16.0402	15.0537	14.1279	13.2590
16	25.0018	23.4424	21.9803	20.6093	19.3239	18.1186	16.9885	15.9289	14.9354	14.0038	13.1304
18	24.9900	23.4093	21.9286	20.5415	19.2421	18.0250	16.8848	15.8168	14.8163	13.8791	13.0012
20	24.9781	23.3758	21.8762	20.4729	19.1596	17.9305	16.7803	15.7038	14.6964	13.7537	12.8714
22	24.9660	23.3418	21.8233	20.4035	19.0762	17.8351	16.6749	15.5901	14.5758	13.6276	12.7410
24	24.9537	23.3074	21.7697	20.3334	18.9919	17.7389	16.5686	15.4755	14.4545	13.5008	12.6101
26	24.9413	23.2725	21.7154	20.2625	18.9068	17.6418	16.4614	15.3600	14.3323	13.3734	12.4786
28	24.9286	23.2372	21.6605	20.1908	18.8208	17.5438	16.3534	15.2438	14.2095	13.2454	12.3466
30	24.9158	23.2014	21.6049	20.1183	18.7340	17.4449	16.2446	15.1268	14.0859	13.1167	12.2141
32	24.9029	23.1652	21.5487	20.0451	18.6463	17.3452	16.1349	15.0090	13.9617	12.9874	12.0812
34	24.8897	23.1284	21.4918	19.9710	18.5578	17.2446	16.0243	14.8904	13.8367	12.8576	11.9477
36	24.8763	23.0912	21.4342	19.8961	18.4684	17.1431	15.9129	14.7710	13.7110	12.7271	11.8138
38	24.8628	23.0535	21.3759	19.8204	18.3781	17.0407	15.8007	14.6509	13.5847	12.5962	11.6795
40	24.8491	23.0154	21.3170	19.7439	18.2869	16.9375	15.6876	14.5299	13.4577	12.4646	11.5448

Appendix 7b. Cont'd...

	23%	25%	27%	29%	31%	33%	35%	37%	39%	41%	43%
0	13.3530	12.6089	11.9062	11.2427	10.6162	10.0246	9.4659	8.9384	8.4403	7.9700	7.5258
2	13.2248	12.4774	11.7722	11.1068	10.4791	9.8868	9.3280	8.8008	8.3034	7.8341	7.3914
4	13.0961	12.3454	11.6377	10.9707	10.3418	9.7490	9.1902	8.6634	8.1668	7.6987	7.2574
6	12.9667	12.2129	11.5029	10.8342	10.2044	9.6111	9.0524	8.5261	8.0305	7.5636	7.1239
8	12.8368	12.0799	11.3677	10.6975	10.0668	9.4732	8.9147	8.3891	7.8945	7.4290	6.9910
10	12.7062	11.9465	11.2321	10.5605	9.9290	9.3353	8.7771	8.2523	7.7589	7.2949	6.8587
12	12.5752	11.8126	11.0962	10.4233	9.7912	9.1975	8.6397	8.1158	7.6236	7.1613	6.7270
14	12.4436	11.6783	10.9600	10.2860	9.6534	9.0597	8.5025	7.9796	7.4888	7.0283	6.5960
16	12.3114	11.5435	10.8236	10.1485	9.5155	8.9220	8.3655	7.8437	7.3545	6.8958	6.4657
18	12.1788	11.4084	10.6868	10.0108	9.3776	8.7844	8.2288	7.7083	7.2207	6.7639	6.3361
20	12.0457	11.2730	10.5498	9.8731	9.2397	8.6470	8.0923	7.5732	7.0874	6.6327	6.2072
22	11.9121	11.1372	10.4126	9.7352	9.1019	8.5098	7.9562	7.4386	6.9546	6.5022	6.0792
24	11.7781	11.0011	10.2753	9.5974	8.9642	8.3728	7.8204	7.3044	6.8225	6.3724	5.9520
26	11.6437	10.8647	10.1377	9.4595	8.8266	8.2360	7.6849	7.1708	6.6910	6.2433	5.8256
28	11.5089	10.7280	10.0001	9.3216	8.6891	8.0995	7.5499	7.0377	6.5602	6.1150	5.7001
30	11.3737	10.5911	9.8623	9.1837	8.5518	7.9634	7.4154	6.9052	6.4300	5.9876	5.5756
32	11.2382	10.4540	9.7245	9.0459	8.4147	7.8275	7.2813	6.7732	6.3006	5.8610	5.4520
34	11.1023	10.3166	9.5866	8.9082	8.2779	7.6921	7.1478	6.6420	6.1720	5.7352	5.3294
36	10.9661	10.1792	9.4487	8.7707	8.1413	7.5571	7.0148	6.5114	6.0442	5.6104	5.2078
38	10.8296	10.0415	9.3108	8.6333	8.0050	7.4225	6.8824	6.3815	5.9172	5.4866	5.0873
40	10.6929	9.9038	9.1730	8.4961	7.8691	7.2884	6.7506	6.2524	5.7910	5.3637	4.9679

Appendix 7c. Modeling the Humidity and Temperature Effect on Aramid/Carbon



Appendix 7c. Cont'd...

Mathematical Model: Humidity and Temperature Effect on Peak Potential, Following the Proposed ASTM Method F23.20.05
Fabric: Aramid/carbon

$V_p = V_o \exp [b \exp (cT) H]$

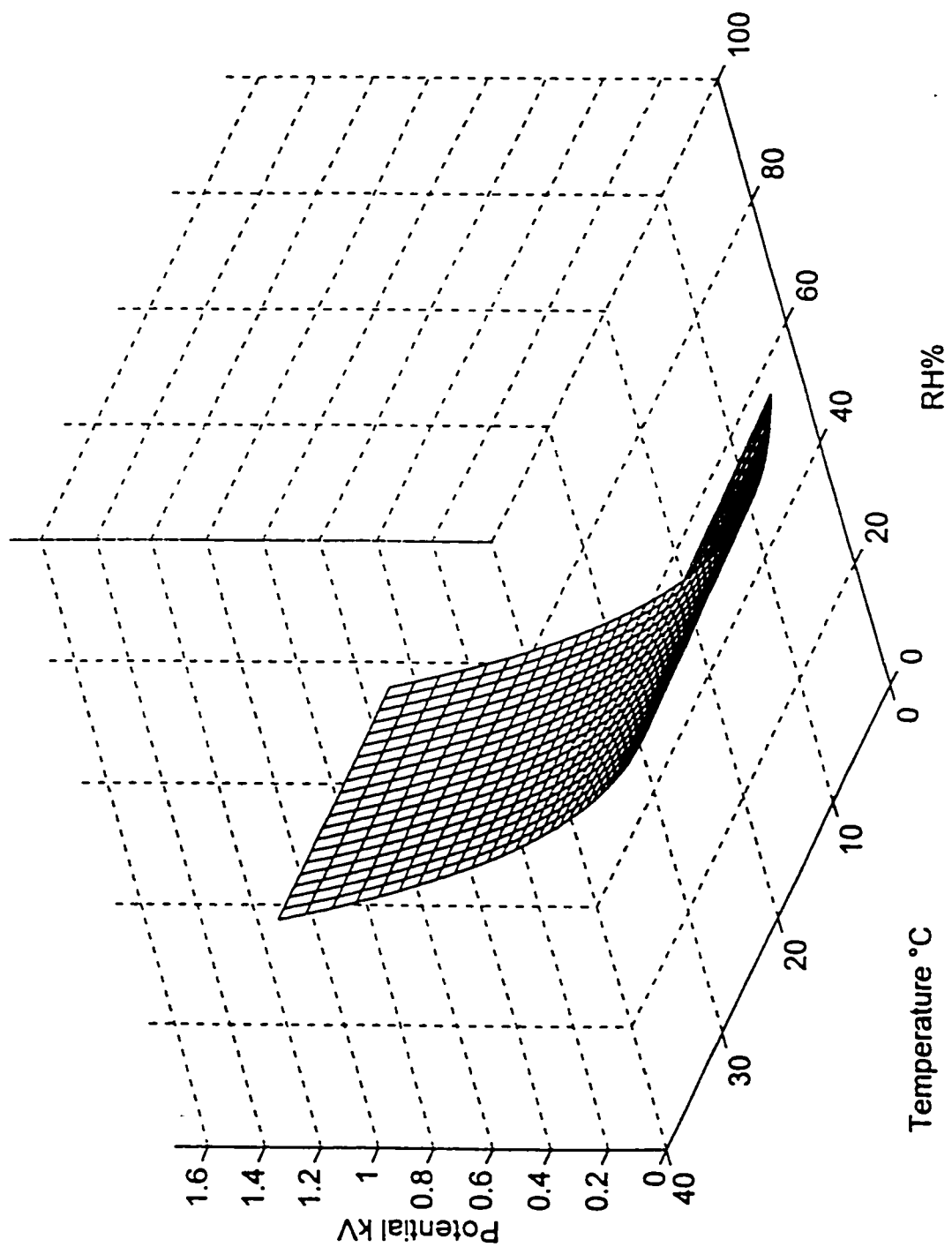
Where: $V_o = 0.745$ kV; $b = -0.00237$; $c = 0.01584$; $T =$ temperature °C; $H =$ relative humidity %

	1%	3%	5%	7%	9%	11%	13%	15%	17%	19%	21%
0	0.7432	0.7397	0.7362	0.7327	0.7293	0.7258	0.7224	0.7190	0.7156	0.7122	0.7088
2	0.7432	0.7396	0.7359	0.7323	0.7288	0.7252	0.7217	0.7181	0.7146	0.7112	0.7077
4	0.7431	0.7394	0.7356	0.7319	0.7283	0.7246	0.7209	0.7173	0.7137	0.7101	0.7065
6	0.7431	0.7392	0.7354	0.7315	0.7277	0.7239	0.7202	0.7164	0.7127	0.7090	0.7053
8	0.7430	0.7390	0.7350	0.7311	0.7272	0.7233	0.7194	0.7155	0.7117	0.7079	0.7041
10	0.7429	0.7388	0.7347	0.7307	0.7266	0.7226	0.7186	0.7146	0.7106	0.7067	0.7028
12	0.7429	0.7386	0.7344	0.7302	0.7260	0.7219	0.7177	0.7136	0.7096	0.7055	0.7015
14	0.7428	0.7384	0.7341	0.7297	0.7254	0.7211	0.7169	0.7126	0.7084	0.7043	0.7001
16	0.7427	0.7382	0.7337	0.7292	0.7248	0.7204	0.7160	0.7116	0.7073	0.7030	0.6987
18	0.7427	0.7380	0.7333	0.7287	0.7242	0.7196	0.7151	0.7106	0.7061	0.7017	0.6973
20	0.7426	0.7378	0.7330	0.7282	0.7235	0.7188	0.7141	0.7095	0.7049	0.7003	0.6958
22	0.7425	0.7375	0.7326	0.7277	0.7228	0.7180	0.7132	0.7084	0.7036	0.6989	0.6942 *
24	0.7424	0.7373	0.7322	0.7271	0.7221	0.7171	0.7122	0.7072	0.7023	0.6975	0.6927
26	0.7423	0.7370	0.7318	0.7266	0.7214	0.7162	0.7111	0.7061	0.7010	0.6960	0.6911
28	0.7423	0.7368	0.7314	0.7260	0.7206	0.7153	0.7101	0.7048	0.6996	0.6945	0.6894
30	0.7422	0.7365	0.7309	0.7254	0.7199	0.7144	0.7090	0.7036	0.6982	0.6929	0.6877
32	0.7421	0.7363	0.7305	0.7248	0.7191	0.7134	0.7078	0.7023	0.6968	0.6913	0.6859
34	0.7420	0.7360	0.7300	0.7241	0.7182	0.7124	0.7067	0.7010	0.6953	0.6897	0.6841
36	0.7419	0.7357	0.7295	0.7234	0.7174	0.7114	0.7055	0.6996	0.6937	0.6879	0.6822
38	0.7418	0.7354	0.7290	0.7228	0.7165	0.7104	0.7042	0.6982	0.6921	0.6862	0.6803
40	0.7417	0.7351	0.7285	0.7221	0.7156	0.7093	0.7030	0.6967	0.6905	0.6844	0.6783

Appendix 7c. Cont'd...

	23%	25%	27%	29%	31%	33%	35%	37%	39%	41%	43%
0	0.7055	0.7021	0.6988	0.6955	0.6922	0.6889	0.6857	0.6824	0.6792	0.6760	0.6728
2	0.7042	0.7008	0.6974	0.6940	0.6906	0.6872	0.6838	0.6805	0.6772	0.6739	0.6706
4	0.7029	0.6994	0.6959	0.6924	0.6889	0.6854	0.6820	0.6785	0.6751	0.6717	0.6683
6	0.7016	0.6980	0.6944	0.6907	0.6872	0.6836	0.6800	0.6765	0.6730	0.6695	0.6660
8	0.7003	0.6965	0.6928	0.6891	0.6854	0.6817	0.6780	0.6744	0.6708	0.6672	0.6636
10	0.6989	0.6950	0.6912	0.6873	0.6835	0.6797	0.6760	0.6722	0.6685	0.6648	0.6611
12	0.6975	0.6935	0.6895	0.6856	0.6816	0.6777	0.6739	0.6700	0.6662	0.6624	0.6586
14	0.6960	0.6919	0.6878	0.6837	0.6797	0.6757	0.6717	0.6677	0.6638	0.6599	0.6560
16	0.6944	0.6902	0.6860	0.6818	0.6777	0.6736	0.6695	0.6654	0.6613	0.6573	0.6533
18	0.6929	0.6885	0.6842	0.6799	0.6756	0.6714	0.6672	0.6630	0.6588	0.6546	0.6505
20	0.6913	0.6868	0.6823	0.6779	0.6735	0.6691	0.6648	0.6605	0.6562	0.6519	0.6477
22	0.6896	0.6850	0.6804	0.6758	0.6713	0.6668	0.6624	0.6579	0.6535	0.6491	0.6448
24	0.6879	0.6831	0.6784	0.6737	0.6691	0.6644	0.6598	0.6553	0.6508	0.6463	0.6418
26	0.6861	0.6812	0.6764	0.6715	0.6668	0.6620	0.6573	0.6526	0.6479	0.6433	0.6387
28	0.6843	0.6793	0.6743	0.6693	0.6644	0.6595	0.6546	0.6498	0.6450	0.6403	0.6356
30	0.6824	0.6773	0.6721	0.6670	0.6619	0.6569	0.6519	0.6470	0.6420	0.6372	0.6323
32	0.6805	0.6752	0.6699	0.6646	0.6594	0.6542	0.6491	0.6440	0.6390	0.6340	0.6290
34	0.6785	0.6730	0.6676	0.6622	0.6568	0.6515	0.6462	0.6410	0.6358	0.6307	0.6256
36	0.6765	0.6708	0.6652	0.6597	0.6542	0.6487	0.6433	0.6379	0.6326	0.6273	0.6221
38	0.6744	0.6686	0.6628	0.6571	0.6514	0.6458	0.6403	0.6347	0.6293	0.6238	0.6185
40	0.6722	0.6663	0.6603	0.6545	0.6486	0.6429	0.6371	0.6315	0.6259	0.6203	0.6148

Appendix 7d. Modeling the Humidity and Temperature Effect on Aramid/PBI



Appendix 7d. Cont'd...

Mathematical Model: Humidity and Temperature Effect on Peak Potential, Following the Proposed ASTM Method F23.20.05
Fabric: Aramid/PBI

$$V_p = V_o \exp [b \exp (cT) H]$$

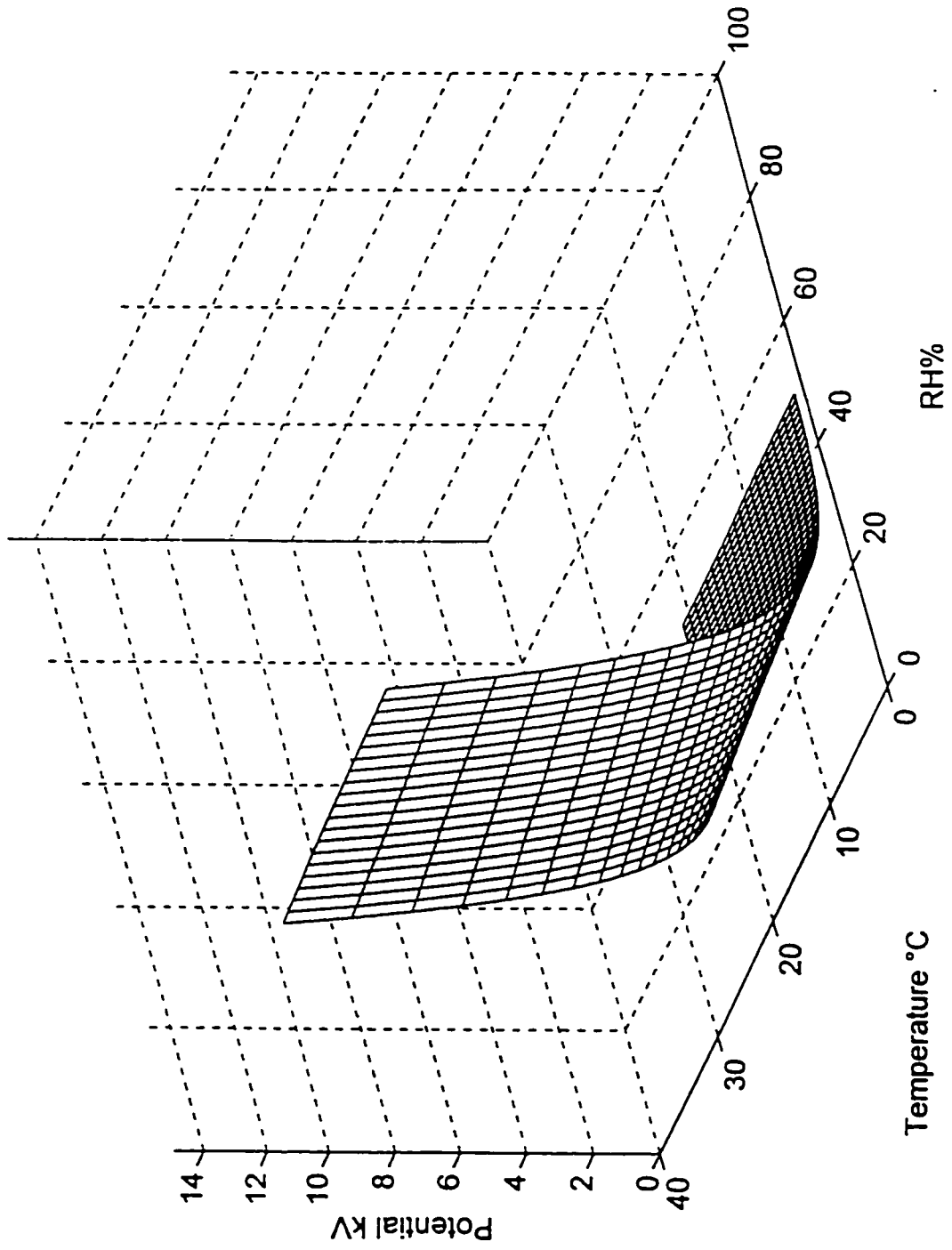
Where: $V_o = 1.775$ kV; $b = -0.02970$; $c = 0.00098$; $T =$ temperature °C; $H =$ relative humidity %

	1%	3%	5%	7%	9%	11%	13%	15%	17%	19%	21%
0	1.7231'	1.6237	1.5301	1.4418	1.3587	1.2803	1.2065	1.1369	1.0713	1.0095	0.9513
2	1.7230	1.6234	1.5296	1.4412	1.3579	1.2795	1.2056	1.1359	1.0703	1.0084	0.9502
4	1.7229	1.6231	1.5292	1.4406	1.3572	1.2787	1.2046	1.1349	1.0692	1.0073	0.9490
6	1.7228	1.6228	1.5287	1.4400	1.3565	1.2778	1.2037	1.1339	1.0681	1.0062	0.9478
8	1.7227	1.6226	1.5283	1.4395	1.3558	1.2770	1.2028	1.1329	1.0671	1.0051	0.9467
10	1.7226	1.6223	1.5278	1.4389	1.3551	1.2762	1.2019	1.1319	1.0660	1.0040	0.9455
12	1.7225	1.6220	1.5274	1.4383	1.3544	1.2754	1.2010	1.1309	1.0649	1.0028	0.9443
14	1.7224	1.6217	1.5269	1.4377	1.3537	1.2745	1.2001	1.1299	1.0639	1.0017	0.9432
16	1.7222	1.6214	1.5265	1.4371	1.3529	1.2737	1.1991	1.1289	1.0628	1.0006	0.9420
18	1.7221	1.6211	1.5260	1.4365	1.3522	1.2729	1.1982	1.1279	1.0617	0.9995	0.9408
20	1.7220	1.6208	1.5256	1.4359	1.3515	1.2721	1.1973	1.1269	1.0607	0.9983	0.9397
22	1.7219	1.6205	1.5251	1.4353	1.3508	1.2712	1.1964	1.1259	1.0596	0.9972	0.9385
24	1.7218	1.6202	1.5247	1.4347	1.3500	1.2704	1.1954	1.1249	1.0585	0.9961	0.9373
26	1.7217	1.6200	1.5242	1.4341	1.3493	1.2696	1.1945	1.1239	1.0575	0.9950	0.9361
28	1.7216	1.6197	1.5237	1.4335	1.3486	1.2687	1.1936	1.1229	1.0564	0.9938	0.9350
30	1.7215	1.6194	1.5233	1.4329	1.3479	1.2679	1.1927	1.1219	1.0553	0.9927	0.9338
32	1.7214	1.6191	1.5228	1.4323	1.3471	1.2671	1.1917	1.1209	1.0542	0.9916	0.9326
34	1.7213	1.6188	1.5224	1.4317	1.3464	1.2662	1.1908	1.1199	1.0532	0.9904	0.9314
36	1.7212	1.6185	1.5219	1.4311	1.3457	1.2654	1.1899	1.1189	1.0521	0.9893	0.9303
38	1.7211	1.6182	1.5215	1.4305	1.3450	1.2645	1.1889	1.1178	1.0510	0.9882	0.9291
40	1.7210	1.6179	1.5210	1.4299	1.3442	1.2637	1.1880	1.1168	1.0499	0.9870	0.9279

Appendix 7d. Cont'd...

	23%	25%	27%	29%	31%	33%	35%	37%	39%	41%	43%
0	0.8965	0.8448	0.7960	0.7501	0.7069	0.6661	0.6277	0.5915	0.5574	0.5252	0.4949
2	0.8953	0.8435	0.7948	0.7489	0.7056	0.6648	0.6264	0.5902	0.5561	0.5240	0.4937
4	0.8941	0.8423	0.7935	0.7476	0.7043	0.6636	0.6251	0.5889	0.5549	0.5227	0.4925
6	0.8929	0.8411	0.7923	0.7463	0.7030	0.6623	0.6239	0.5877	0.5536	0.5215	0.4912
8	0.8917	0.8398	0.7910	0.7451	0.7018	0.6610	0.6226	0.5864	0.5523	0.5202	0.4900
10	0.8905	0.8386	0.7898	0.7438	0.7005	0.6597	0.6213	0.5851	0.5511	0.5190	0.4888
12	0.8892	0.8374	0.7885	0.7425	0.6992	0.6584	0.6200	0.5839	0.5498	0.5177	0.4875
14	0.8880	0.8361	0.7873	0.7413	0.6979	0.6572	0.6187	0.5826	0.5485	0.5165	0.4863
16	0.8868	0.8349	0.7860	0.7400	0.6967	0.6559	0.6175	0.5813	0.5473	0.5152	0.4851
18	0.8856	0.8337	0.7848	0.7387	0.6954	0.6546	0.6162	0.5800	0.5460	0.5140	0.4838
20	0.8844	0.8324	0.7835	0.7375	0.6941	0.6533	0.6149	0.5788	0.5448	0.5127	0.4826
22	0.8832	0.8312	0.7823	0.7362	0.6928	0.6520	0.6136	0.5775	0.5435	0.5115	0.4814
24	0.8820	0.8300	0.7810	0.7349	0.6916	0.6508	0.6124	0.5762	0.5422	0.5102	0.4801
26	0.8808	0.8287	0.7797	0.7336	0.6903	0.6495	0.6111	0.5750	0.5410	0.5090	0.4789
28	0.8796	0.8275	0.7785	0.7324	0.6890	0.6482	0.6098	0.5737	0.5397	0.5077	0.4777
30	0.8784	0.8263	0.7772	0.7311	0.6877	0.6469	0.6085	0.5724	0.5385	0.5065	0.4764
32	0.8772	0.8250	0.7760	0.7298	0.6864	0.6456	0.6072	0.5711	0.5372	0.5053	0.4752
34	0.8760	0.8238	0.7747	0.7286	0.6852	0.6444	0.6060	0.5699	0.5359	0.5040	0.4740
36	0.8747	0.8225	0.7734	0.7273	0.6839	0.6431	0.6047	0.5686	0.5347	0.5028	0.4728
38	0.8735	0.8213	0.7722	0.7260	0.6826	0.6418	0.6034	0.5673	0.5334	0.5015	0.4715
40	0.8723	0.8201	0.7709	0.7247	0.6813	0.6405	0.6021	0.5661	0.5322	0.5003	0.4703

Appendix 7e. Modeling the Humidity and Temperature Effect on Aramid/FR Viscose



Appendix 7e. Cont'd...

Mathematical Model: Humidity and Temperature Effect on Peak Potential, Following the Proposed ASTM Method F23.20.05
Fabric: Aramid/FR viscose

$V_p = V_o \exp [b \exp (cT) H]$

Where: $V_o = 15.94 \text{ kV}$; $b = -0.06555$; $c = 0.00542$; $T = \text{temperature } ^\circ\text{C}$; $H = \text{relative humidity } \%$

	1%	3%	5%	7%	9%	11%	13%	15%	17%	19%	21%
0	14.9286	13.0944	11.4855	10.0742	8.8364	7.7507	6.7984	5.9630	5.2304	4.5877	4.0240
2	14.9180	13.0663	11.4445	10.0240	8.7798	7.6900	6.7355	5.8995	5.1673	4.5259	3.9641
4	14.9072	13.0381	11.4033	9.9735	8.7229	7.6292	6.6726	5.8360	5.1042	4.4642	3.9045
6	14.8963	13.0096	11.3617	9.9227	8.6658	7.5682	6.6096	5.7724	5.0413	4.4027	3.8451
8	14.8854	12.9808	11.3199	9.8715	8.6085	7.5070	6.5465	5.7089	4.9785	4.3415	3.7860
10	14.8743	12.9518	11.2778	9.8201	8.5509	7.4457	6.4834	5.6454	4.9157	4.2804	3.7271
12	14.8631	12.9225	11.2353	9.7685	8.4931	7.3842	6.4201	5.5819	4.8531	4.2195	3.6686
14	14.8517	12.8930	11.1926	9.7165	8.4350	7.3226	6.3568	5.5185	4.7907	4.1588	3.6104
16	14.8403	12.8632	11.1496	9.6642	8.3767	7.2608	6.2935	5.4551	4.7283	4.0984	3.5524
18	14.8287	12.8332	11.1062	9.6117	8.3182	7.1988	6.2301	5.3917	4.6661	4.0382	3.4948
20	14.8171	12.8029	11.0626	9.5588	8.2595	7.1368	6.1666	5.3284	4.6041	3.9782	3.4375
22	14.8053	12.7724	11.0187	9.5057	8.2005	7.0745	6.1032	5.2652	4.5422	3.9185	3.3805
24	14.7934	12.7416	10.9744	9.4524	8.1414	7.0122	6.0397	5.2020	4.4805	3.8591	3.3239
26	14.7813	12.7106	10.9299	9.3987	8.0820	6.9498	5.9761	5.1389	4.4190	3.7999	3.2676
28	14.7692	12.6793	10.8851	9.3448	8.0224	6.8872	5.9126	5.0759	4.3577	3.7410	3.2116
30	14.7569	12.6477	10.8399	9.2905	7.9626	6.8245	5.8491	5.0130	4.2965	3.6824	3.1561
32	14.7445	12.6158	10.7945	9.2361	7.9026	6.7617	5.7855	4.9503	4.2356	3.6241	3.1009
34	14.7320	12.5837	10.7487	9.1813	7.8425	6.6988	5.7220	4.8876	4.1749	3.5661	3.0461
36	14.7194	12.5514	10.7027	9.1263	7.7821	6.6359	5.6585	4.8250	4.1144	3.5084	2.9916
38	14.7066	12.5187	10.6563	9.0710	7.7215	6.5728	5.5950	4.7626	4.0541	3.4510	2.9376
40	14.6937	12.4858	10.6097	9.0155	7.6608	6.5097	5.5315	4.7004	3.9941	3.3939	2.8840

Appendix 7e. Cont'd...

	23%	25%	27%	29%	31%	33%	35%	37%	39%	41%	43%
0	3.5296	3.0959	2.7155	2.3819	2.0892	1.8325	1.6073	1.4098	1.2366	1.0847	0.9514
2	3.4721	3.0411	2.6637	2.3330	2.0435	1.7898	1.5677	1.3731	1.2027	1.0534	0.9226
4	3.4149	2.9867	2.6122	2.2847	1.9982	1.7477	1.5285	1.3369	1.1693	1.0227	0.8944
6	3.3581	2.9327	2.5613	2.2369	1.9535	1.7061	1.4900	1.3013	1.1365	0.9925	0.8668
8	3.3016	2.8791	2.5108	2.1895	1.9094	1.6651	1.4520	1.2662	1.1042	0.9629	0.8397
10	3.2454	2.8260	2.4607	2.1427	1.8657	1.6246	1.4146	1.2318	1.0726	0.9339	0.8132
12	3.1896	2.7732	2.4111	2.0963	1.8226	1.5847	1.3778	1.1979	1.0415	0.9055	0.7873
14	3.1342	2.7208	2.3620	2.0505	1.7801	1.5453	1.3415	1.1646	1.0110	0.8777	0.7619
16	3.0792	2.6689	2.3134	2.0052	1.7381	1.5065	1.3058	1.1318	0.9811	0.8504	0.7371
18	3.0245	2.6175	2.2652	1.9604	1.6966	1.4683	1.2707	1.0997	0.9517	0.8236	0.7128
20	2.9702	2.5665	2.2176	1.9162	1.6557	1.4306	1.2362	1.0681	0.9229	0.7975	0.6891
22	2.9163	2.5159	2.1705	1.8724	1.6153*	1.3935	1.2022	1.0371	0.8947	0.7719	0.6659
24	2.8629	2.4658	2.1238	1.8293	1.5755	1.3570	1.1688	1.0067	0.8671	0.7468	0.6432
26	2.8098	2.4162	2.0777	1.7866	1.5363	1.3211	1.1360	0.9769	0.8400	0.7223	0.6211
28	2.7572	2.3670	2.0321	1.7445	1.4977	1.2857	1.1038	0.9476	0.8135	0.6984	0.5996
30	2.7050	2.3183	1.9870	1.7030	1.4596	1.2509	1.0721	0.9189	0.7876	0.6750	0.5785
32	2.6532	2.2701	1.9424	1.6620	1.4220	1.2167	1.0411	0.8908	0.7622	0.6521	0.5580
34	2.6019	2.2225	1.8984	1.6215	1.3851	1.1831	1.0106	0.8632	0.7373	0.6298	0.5380
36	2.5510	2.1753	1.8549	1.5817	1.3487	1.1501	0.9807	0.8362	0.7131	0.6080	0.5185
38	2.5006	2.1286	1.8119	1.5423	1.3129	1.1176	0.9513	0.8098	0.6893	0.5868	0.4995
40	2.4506	2.0824	1.7695	1.5036	1.2777	1.0857	0.9225	0.7839	0.6661	0.5660	0.4810

Appendix 8: Triboelectric Series

Apparatus

The equipment used included a triboelectric test device and vinyl rubbing wheel, described in the ASTM Method draft F23.20.05, a Simco static eliminator model 300, an Electro-Tech System electrometer model 105, and a Tektronix digital oscilloscope model TDS 320.

Fabrics

Four 200 mm by 200 mm specimens were prepared according to standard sampling procedures, of the following fabrics: 100% non-FR cotton, FR cotton, aramid/FR viscose, aramid, aramid/carbon, aramid/PBI, nylon 6, orlon, polyester, rayon, silk, triacetate, wool, vinyl. Each test specimen was washed and conditioned at 0% RH according to standard procedures.

Procedure

For this experiment, the proposed ASTM Method was used with some modifications. Each fabric was used as the cover of the rubbing wheel with every other fabric rubbed against it. The test specimen was rubbed for ten seconds at 200 RPM; then, the peak potential and polarity generated on the surface of the test specimen was recorded. The placement of each fabric in a triboelectric series was determined by comparing the magnitude and polarity of charge of the wheel cover 1 - specimen 2 combination with the wheel cover 2 - specimen 1 combination. If the charge on specimen 1 was greater than that on specimen 2, then the fabric 1 was placed above the fabric 2 in the series. These comparisons were done for each combination of fabrics.

Developed triboelectric series by frictional charging

+VE

NYLON 6
 ARAMID
 WOOL
 SILK
 100% NON-FR COTTON
 FR COTTON
 RAYON
 TRIACETATE
 ARAMID/FR VISCOSE
 POLYESTER
 ARAMID/CARBON
 ARAMID/PBI
 ORLON
 VINYL

-VE

CURRICULUM VITAE

Jose Alberto Gonzalez

Home Address

31 Bantry Place
Winnipeg, MB
R2N 1H3
Phone: (204) 254-6814

Business Address

Department of Clothing and Textiles
University of Manitoba
Winnipeg, MB R3T 2N2
Telephone: (204) 474-8065
Fax: (204) 474-7592
E-mail: gonzale0@ms.umanitoba.ca

Education

- | | |
|------------------|--|
| Jan-95 to Jun-98 | Graduated with a Doctor in Philosophy degree in Clothing and Textiles from the University of Alberta |
| Jan-93 to Dec-94 | Graduated with a Master of Science degree in Clothing and Textiles from the University of Alberta |
| Apr-91 to May-91 | Northern Alberta Institute of Technology
Edmonton, Alberta
Automotive Mechanic Apprentice Course |
| Oct-90 to Mar-91 | Alberta Vocational College
Edmonton, Alberta
Trade Occupational English Program |
| Sep-73 to Aug-77 | Graduated with a Bachelor of Science degree in Textile Engineering from the Superior School of Textile Engineering of National Polytechnic Institute, Mexico City. Major in Spinning and Weaving |

Professional Experience

- | | |
|-------------------|--|
| Aug-97 to Present | Department of Clothing and Textiles, University of Manitoba Winnipeg, MB
Assistant Professor
* Teach Textile Science Courses to undergraduate and graduate students
* Co-ordinate Textile Science laboratory activities
* Develop Textile Science research projects
* Assist undergraduate and graduate students in academic matters |
|-------------------|--|

- Dec-92 to Jul-97
 Department of Human Ecology, University of Alberta,
 Edmonton, Alberta
Research Assistant
 * Assisted in research on static propensity of
 protective clothing
 * Processed research data in computer
 * Co-ordinated electrostatic tests for commercial
 testing carried out in our facilities
- Jul-92 to Oct-92
 Boardwalk Realty Ltd.
 Edmonton, AB
Maintenance Administrator
 * Attended tenants maintenance complaints
 * Supervised and controlled maintenance work
 * Processed maintenance data in computer
- Jan-89 to Feb-90
 Shotgun Delivery Services
 Burlingame, CA
Courier Driver
 * Picked up and delivered packages and documents
- Nov-77 to Dec-88
 Minerva-Molins and Co.
 San Salvador, El Salvador
Production Manager
 * Planned production and oversaw maintenance in a
 textile plant with approximately 600 employees.
 Produced cotton yarns and fabrics.
 * Supervised all facets of quality control
 * As a member of the management team, negotiated
 union contracts and resolved employee conflicts
 * Planned and directed modernization of spinning
 plant, from ring spinning to open-end rotor spinning
 * Developed and implemented a new plant of textile
 medical products
 * Developed and implemented a new plant for
 production of towels
- * Provided technical consultation and problem solving in areas ranging from
 mechanical difficulties to methods for improving production and product quality
 in spinning and weaving for several companies in the San Salvador area.

Contributions to Research and Development

Published Articles in Refereed Journal Publications

Rizvi, S.A.H., Crown, E.M., Osei-Ntiri, K., Smy, P.R., & Gonzalez, J.A. (1995). Electrostatic characteristics of thermal-protective garments at low humidity. Journal of The Textile Institute, 86, 549-558.

Articles Accepted for Publication in Refereed Journals

Rizvi, S.A.H., Crown, E.M., Gonzalez, J.A., & Smy, P.R. (in press). Electrostatic characteristics of thermal-protective garment systems at various low humidities. Journal of The Textile Institute.

Other Refereed Contributions

Gonzalez, J.A., Crown, E.M., Rizvi, S.A., & Smy, P.R. (1997). Electrostatic modeling of protective clothing systems. Proceedings of the 19th Annual Electrical Overstress/ Electrostatic Discharge Symposium (pp. 153-161), September 1997. Santa Clara, CA.

Gonzalez, J.A., Rizvi, S.A., Crown, E.M., & Smy, P.R. (1997). A modified version of proposed ASTM F23.20.05: Correlation with human body experiments on static propensity. In J.O. Stull and A.D. Schwobe (Eds.), Performance of Protective Clothing: 6th Volume, ASTM STP 1273 (pp. 47-61). Philadelphia, PA: American Society for Testing and Materials.

Gonzalez, J.A., Rizvi, S.A., Crown, E.M., & Smy, P.R. (1996). Modeling the static propensity of protective clothing systems. Proceedings of the 1996 International Textiles and Apparel Association Meeting (p. 57). Banff, AB.

Gonzalez, J.A., Crown, E.M., Rizvi, S.A., & Smy, P.R. (1994). Development of a laboratory protocol to predict the electrostatic propensity of textile systems. Proceedings of the 24th Canadian Textile Seminar International, Hightex 1994. Montreal, PQ (May 29-31).

Non-Refereed Contributions

Gonzalez, J.A., Rizvi, S.A., & Crown, E.M. (1997, February). Electrostatic hazards in protective clothing systems. Paper presented at Research Revelations'97, University of Alberta, Edmonton, AB.

Gonzalez, J.A., Rizvi, S.A., & Crown, E.M. (1996, May). Assessment of static propensity on clothing systems. Paper presented at the DuPont Canada Flame Resistant Workwear 5th Seminar. Calgary and Edmonton, AB.

Gonzalez, J.A. (1995). Development of a laboratory protocol to predict the electrostatic propensity of clothing systems. Unpublished master's thesis. University of Alberta, Edmonton, AB.

Participation in Industrially Relevant R&D Activities

Development of a device for measuring peak discharge potential and total discharge energy from a resistance/capacitor unit of electrostatic discharges generated by tribo-electrification.

Based on previous development, a modification to the proposed ASTM Test Method for Evaluating Triboelectric (Static) Charge Generation on Protective Clothing Materials (F23.20.05) has been proposed by the applicant.

Different mathematical models and numerical techniques based on empirical and theoretical knowledge have been developed for explaining the electrostatic phenomenon and predicting the static propensity of protective clothing systems.

Participation in Conferences, Symposiums, & Seminars

Attended and presented a poster at the Research Revelations'97 of the University of Alberta, Edmonton, AB, February 1997.

Attended and presented a poster at the Canadian Reflections Conference '96 of the International Textile and Apparel Association, Banff, AB, August 1996.

Presented a paper and attended the Sixth International ASTM Symposium on Performance of Protective Clothing, Orlando, FL, June 1996.

Attended and presented a poster at the Research Revelations'95 of the University of Alberta, Edmonton, AB, March 1995.

Attended and presented a poster at the 24th Canadian Textile Seminar International, Montreal, May 1994.

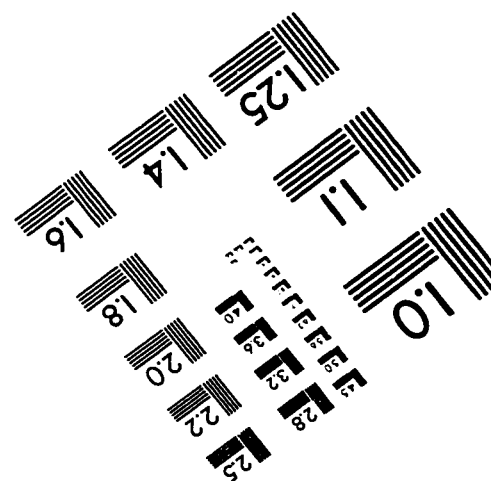
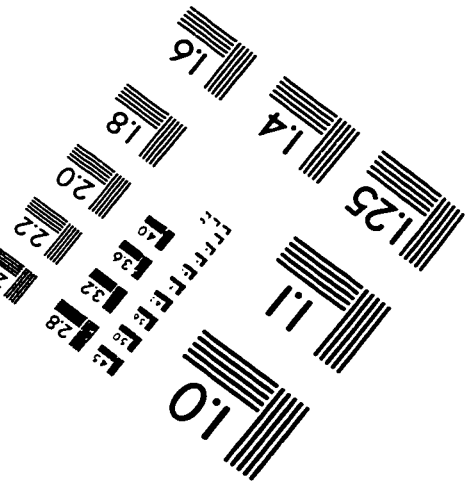
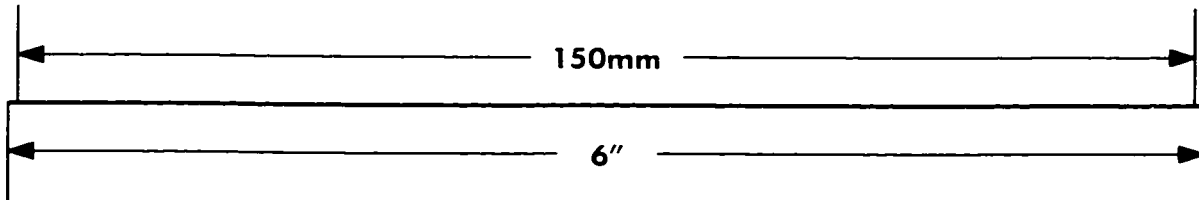
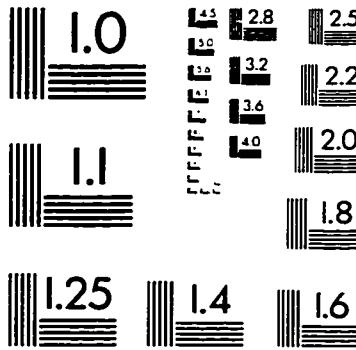
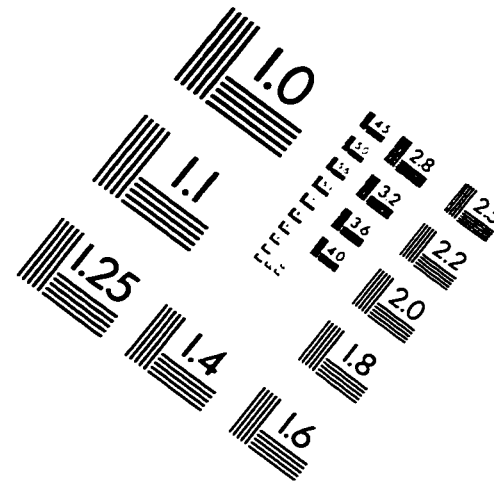
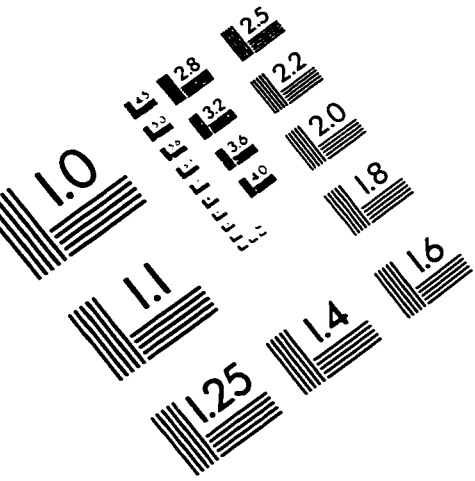
Attended and presented a poster at the Research Revelations'94 of the University of Alberta, Edmonton, AB, March 1994.

Attended and delivered a presentation at the Sixth National Congress of Engineering, San Salvador, El Salvador, CA, September 1988.

Awards and Honors

- * Mary Louise Imrie Graduate Student Award (1996)
- * Walter Johns Scholarship from University of Alberta (1995-1997)
- * Natural Sciences and Engineering Research Council of Canada PGS-B Scholarship (1995-1997)
- * Mary Louise Imrie Graduate Student Award (1994)
- * Walter Johns Scholarship from University of Alberta (1993-1995)
- * Natural Sciences and Engineering Research Council of Canada PGS-A Scholarship (1993-1995)
- * Received "Best Student of Mexico, 1977" Award upon graduation

IMAGE EVALUATION TEST TARGET (QA-3)



APPLIED IMAGE, Inc
 1653 East Main Street
 Rochester, NY 14609 USA
 Phone: 716/482-0300
 Fax: 716/288-5989

© 1993, Applied Image, Inc., All Rights Reserved